OXFORD BROOKES UNIVERSITY

Computer Vision in Vehicle and Driver Performance

Submitted to requirements of the award M.Sc. By Research

Director of Studies:

PROF. DENISE MORREY

Co-Director of Studies

DR. PETER BALL

Secondary Supervisors:

ANDREW BRADLEY

Author:

CHRIS HOLMES

Acknowledgements

The opportunity to further myself study towards my MSc by Research has provided me with a very rewarding experience not only to manage my own research project but also to inspire my ideas and fulfil areas of personal interest with industrial relevance. I would like to thank Andrew Bradley for playing a significant role in the successful completion of this study, your help and guidance is very much appreciated.

I'd like to also thank Professor Denise Morrey for your patience and willingness to support me further with my ideas and career growth. I am also thankful to Dr. Peter Ball for his guidance with hardware development.

I'd further like to thank Sam Kamperis, Nick Tonkin, Tim Murdoch and Giuseppe Naselli. I am grateful for your support with experimental and data analysis work and I'd like to thanks John and Ian for their assistance with experimental and logistical support for this research.

Lastly I'd like to give a big Thank you to my parents and to Brett and Jen for your continued support and guidance. You've provided much strength and support throughout all of university study and I am deeply grateful.

Abstract

Understanding the driving task for on-road driving has been a complex problem for a long time, conventional method of data acquisition have proven to aid in portraying events and furthering understanding in relation to driver and vehicle performance.

This study identifies they key aspects required to measure driver performance and statistical analysis is performed on a number of participants conducting driving events around a specified route around Oxford, England. Steering, throttle and braking parameters are measured, analysed and characteristic behaviours are resulted. For each participant a professional driving assessor provided by the RDAC, scores drivers on their performance.

Data acquisition and video capture devices have been developed with the video capture device development undertaken in collaboration with Goldstar Onboard Ltd. Device validation and development measures have been conducted to ensure device performance is suitable for the desired measurements.

Computer vision techniques have been applied to help identify and support results gathered by the data acquisition system. A method to identify external influencing factors is proposed allowing for identification and explanations of performance characteristics that cannot be explained using conventional forms of data acquisition.

Results have suggested benchmarking methods for steering, braking and throttle use for a given driver and how computer vision techniques can be used to support and further increase the accuracy of portraying and understanding driver behaviour for the on-road driving task.

TABLE OF CONTENTS

Acknowledgements..2

Abstract..3

List of Figures..7

List of Tables..10

Introduction..11

1.1 Background..11

1.2 Research Motivation..12

Aims and objectives..15

Review of Literature..16

2.1 Driver Behaviour..16

2.1.1 Driver analysis using conventional forms of data acquisition..16

2.1.2 Driver Modelling..18

2.2 Chassis Behaviour - Ride and Handling..20

2.2.1 Ride..20

2.2.2 Handling..23

2.2.3 Limitations of Characterising Driver and Chassis Behaviour..24

2.3 Conventional Data Acquisition Techniques..25

2.3.1 Physical Measurement..25

2.3.2 Sensor Selection..27

2.3.3 Measurement Limitations..28

2.4 Computer Vision..29

2.4.1 Definition..29

2.4.2 Digital Image Creation....29
2.4.3 Feature Detection....30
2.4.4 Computer Vision Limitations....32
2.5 Previous Studies in On-road Driver Behaviour....35
2.6 Chapter Summary....37
Video and Data Acquisition System Development....38
3.1 Data Acquisition Device (DAQ)....40
3.1.1 Configuration....40
3.1.2 Schematic....41
3.2 Video Device....42
3.2.1 Requirements....42
3.2.2 Initial Device Configuration Concepts....42
....44
....44
....44
3.2.3 Device Concepts – Cameras....45
3.2.4 Device Concepts - Processors....47
3.2.5 Selection Matrix and Concept Evaluation....50
3.2.6 Final Device....51
3.3 Chapter Summary....52
Result Analysis....53
4.1 Video and Data Acquisition Development Analysis....53
4.1.1 Data Acquisition System – Limitations....53
4.1.2 Video System Analysis....57
4.2 Data Acquisition Result Analysis....69
4.2.1 Testing Outline....69
4.2.2 Steering....70
4.2.3 Braking....81
4.2.4 Throttle....86
Application of Computer Vision....93
5.1 Definition....93
5.2 Lane Detection....94

5.2.1 Colour Space and Region of Interest 94
5.2.2 Detecting Edges 95
5.2.3 Probabilistic Hough Transforms 96
5.3 Combined DAQ and Video Data Analysis 97
Conclusions 103
Further Work 104
References 106
Appendix A – Capture Data Tables 109
Goldstar Onboard Dual Camera 109
Pandaboard 109
Ez Storage Device 110
Appendix B – Video Capture Device Procedure 112

List of Figures

Figure 1 - Formula 3 Sample Data, Snetterton 17
Figure 2 - Formula 3 Sample Data, Snetterton Enlarged 17
Figure 3 - Snetterton Circuit Map 18
Figure 4 – 7 Degree of Freedom Vehicle Model (Crolla, 1992) 20
Figure 5 – 2 Degree of Freedom or Quarter Vehicle Model (Crolla, 1992) 21
Figure 6 – Road Profile Frequency Content (Blundell & Harty, 2004) 21
Figure 7 – Sinusoidal Road Surface Approximation (Balkwill, 2013) 22
Figure 8 – Simple 2 Degree of Freedom Handling Model (Crolla, 1992) 23
Figure 9 – Coordinate System (Blundell & Harty, 2004) 23
Figure 10 – Recovered waveform and recorded signal with 4 times per cycle sampling (Larminie & Martin, 2009) 25
Figure 11 – Recovered waveform and recorded signal with 10 times per cycle sampling. (Larminie & Martin, 2009) 26
Figure 12 – Characteristics of Chebyshev and Butterworth Filters (Larminie & Martin, 2009) 27
Figure 13 – Linear Sensor Output (Larminie & Martin, 2009) 27
Figure 14 – RGB Colour Space Model 30
Figure 15 - (a) ($\boldsymbol{\rho}$,$\boldsymbol{\theta}$) parameterization of line in the xy-plane. (b) Sinusoidal curves in the $\boldsymbol{\rho\theta}$-plane; the point of intersection ($\boldsymbol{\rho', \theta'}$) corresponds to the line passing through points (x_i, y_i) and (x_j, y_j) in the xy-plane. (c) Division of the $\boldsymbol{\rho\theta}$-plane into accumulator cells. (Gonzalez & Woods, 2008) 33
Figure 16 – On-road Driving Assessment Criteria (Lee, et al., 2003) 36
Figure 17 – Top level System Layout 39
Figure 18 – Data Acquisition Device Image 40
Figure 19 – Data Acquisition Schematic 41
Figure 20 – Raspberry Pi Camera 45
Figure 21 – Tsact Camera 45
Figure 22 – Semtech Serial Receiver 45
Figure 23 – Raptor 1 Camera 46
Figure 24 – Raspberry Pi 47
Figure 25 – Beaglebone Black 48
Figure 26 - Pandaboard 49

Figure 27 - Final Video Capture Device Layout ... 51
Figure 28 – Video Device System Front View ... 52
Figure 29 – Video Device Internal Image ... 52
Figure 30 – DAQ and GPS Time Samples ... 54
Figure 31 – Data point Delta Histogram ... 54
Figure 32 – Data acquistion programme layout ... 55
Figure 33 – Video capture File Time Differences ... 57
Figure 34 - Ez Storage Frame Capture 1 – M40 – 1 Camera – 30 fps – 1.5 Mbps ... 59
Figure 35 - Histogram of Fig. 34 ... 59
Figure 36 - Pandaboard Frame Capture 1 – M40 – 1 Camera – 30 fps – 1.5 Mbps ... 60
Figure 37 - Histogram of Fig. 36 ... 60
Figure 38 - Goldstar Onboard Frame Capture 1 – M40 – 1 Camera – 30 fps – 1.5 Mbps ... 61
Figure 39 - Histogram of Fig. 38 ... 61
Figure 40 - Ez Storage Frame Capture 2 – Wheatley Village – 1 Camera – 30 fps – 1.5 Mbps ... 62
Figure 41 - Histogram of Fig. 40 ... 62
Figure 42 - Pandaboard Frame Capture 2 – Wheatley Village – 1 Camera – 30 fps – 1.5 Mbps ... 63
Figure 43 - Histogram of Fig. 42 ... 63
Figure 44 - Goldstar Onboard Frame Capture 2 – Wheatley Village – 1 Camera – 30 fps – 1.5 Mbps ... 64
Figure 45 - Histogram of Fig. 44 ... 64
Figure 46 – Pandaboard – Wheatley Village – 1 Camera – 30 fps - 10Mbps ... 65
Figure 47 - Pandaboard - Wheatley Village – 1 Camera – 30 fps - 4Mbps ... 66
Figure 48 – Pandaboard - 4 Mbps ... 66
Figure 49 – Pandaboard - 10 Mbps ... 66
Figure 50 - Device Capture Rates ... 67
Figure 51 - Data Transfer Rates ... 67
Figure 52 – Testing Driving Route ... 69
Figure 53 – Testing Driving Route – Close up ... 69
Figure 54 – Steering Displacement and Velocity with Driving Assessor Score ... 71
Figure 55 – GPS Coordinates – Section F ... 72
Figure 56 – Driving Route Sections ... 73
Figure 57 – Steering Displacement – Sector F ... 74
Figure 58 – Steering Velocity Section Standard Deviation ... 75
Figure 59 – Steering Displacement Section Standard Deviation ... 76
Figure 60 – Steering Displacement, Velocity and Driving Assessor Scores Section 1(A) ... 76
Figure 61 - Steering Displacement, Velocity and Driving Assessor Scores Section 2(B) ... 77
Figure 62 - Steering Displacement, Velocity and Driving Assessor Scores Section 4(C) ... 77
Figure 63 - Steering Displacement, Velocity and Driving Assessor Scores Section 5(D) ... 78
Figure 64 - Steering Displacement, Velocity and Driving Assessor Scores Section 6(E) ... 78
Figure 65 - Steering Displacement, Velocity and Driving Assessor Scores Section 7(F) ... 79
Figure 66 - Steering Displacement, Velocity and Driving Assessor Scores Section 8(G) ... 79
Figure 67 – Emergency Stop Reaction Times ... 82
Figure 68 – Brake Reactions and Maximum Input Time Differences ... 83
Figure 69 – Brake Response Times ... 84

Figure 70 – Maximum Throttle Velocities 86
Figure 71 – Maximum Throttle Velocities Sections A, B and C 87
Figure 72 - Maximum Throttle Velocities Sections A, B and C 88
Figure 73 - Maximum Throttle Velocities Sections D, E, F and G 88
Figure 74 – Mean Throttle Pedal Velocities Sections A, B and C 89
Figure 75 – Mean Throttle Pedal Velocities Section D, E, F and G 89
Figure 76 – Maximum Thorttle use Variations 90
Figure 77 – Mean Throttle use Variations 90
Figure 78 – Original Capture – Section 8 - Frame 0 94
Figure 79 – Capture after grayscale conversion and image crop – Section 8 – Frame 0 95
Figure 80 – Edges detected within the image – Section 1 – Frame 6508 95
Figure 81 – Probabilistic Hough Transform 96
Figure 82 – GPS Coordinates – Section 5 – Participant 6 97
Figure 83 – Section 5 Steering Trace Participant 6 98
Figure 84 – Section 5- Frame 33 98
Figure 85 – Section 5 Steering Trace with Markers 99
Figure 86 – frame 128 – Section 5 99
Figure 87 – frame 281 – Section 5 100
Figure 88 – frame 377 – Section 5 100
Figure 89 – Frame 1492 – Section 1 101
Figure 90 – Frame 1492 – Section 1 – Edge Detection Results 102

List of Tables

Table 1 – Video Device Concept Selection Matrix 50
Table 2 – Steering Displacement and Velocity Standard Deviation with Driving Assessor Scores 70
Table 3 – 5 point assessment scale 71
Table 4 – Figure 60 Averages and Standard Deviations 76
Table 5 – Figure 61 Averages and Standard Deviations 77
Table 6 – Figure 62 Averages and Standard Deviations 77
Table 7 – Figure 64 Averages and Standard Deviations 78
Table 8 – Figure 63 Averages and Standard Deviations 78
Table 9 – Figure 65 Averages and Standard Deviations 79
Table 10 – Figure 66 Averages and Standard Deviations 79
Table 11 – Driving Assessor Steering Results 81
Table 12 – Emergency Stop Reaction Times 81
Table 13 – Maximum Brake Input Time 82
Table 14 – Brake Response Times 83
Table 15 – Braking Driving Assessor Results 85
Table 16 – Brake Reaction Times 85
Table 17 – Throttle Pedal Velocity 86
Table 18 – Driving Assessor Throttle use Scores 92
Table 19 – Frames with lanes detected percentages 101

Chapter 1

Introduction

This study is an investigation of methods to assess driver and vehicle performance using data acquisition and high definition multi-camera video capture systems both developed to aid in research for quantifying performance measures. Work has been done in collaboration with the Regional Driving Assessment Centre (RDAC), the centre have provided a road going vehicle to allow for physical measurements with volunteering participants from the general public. This introductory chapter will present the background and motivation for undertaking the research followed by an outline of aims and objectives of the study.

1.1 Background

Assessment of driver performance on public roads typically utilise a professional driving assessor, where a given number of manoeuvres are required and performed and scored by the assessor. A score is given for the nature of how manoeuvres have been undertaken, and these scores will ultimately determine whether the overall drive has been deemed good or poor. The RDAC, an accredited member of the Forum of Mobility Centres conduct driving assessments to help people gain independent mobility for the first time or as returning drivers. Recent work at Oxford Brookes University has investigated the measurement of driver performance using an in house simulator alongside a number of projects to theoretically model ideal and real drivers for motorsport applications. Work undertaken with the RDAC is part of a larger collaboration with the Movement Science Department at Oxford Brookes, where analysis of cognitive functions during driving are recorded to help quantify behaviour for participants that maybe considered to have restricted mobility.

The development of the video capture system has been undertaken in collaboration with Goldstar Onboard Ltd.

1.2 Research Motivation

Early 1962 member companies of MIRA (Motor Industry Research Association) set up a committee to review British engineering methods to enhance vehicle stability and control. The following 3 outcomes were made based on agreed recommendations for research:-

1 – Terminology definitions should be standardized for general industry use

2 – MIRA should develop improved methods and facilities for the practical measurement of steady state vehicle characteristics

3 – MIRA should carry out theoretical and practical studies of vehicle transient behaviour to further understanding in this area.

Standardisations of coordinate systems and definitions have been generally accepted and most literature adopts the SAE defined vehicle axes, the SAE Vehicle Axis System was first proposed in 1956 in a publication by L. Segel, it is a vehicle fixed system and is heavily adopted in vehicle dynamics work today. (Milliken & Milliken, 1995) (Segel, 1956).

The further two recommendations highlight the necessity to undertake a more theoretical and practical study for steady state and transient approaches to aid in the understanding of vehicle behaviour. Since these outcomes were delivered there has been a great deal of literature published in both driver and vehicle beahviour. Observing and measuring the behaviour of a driven vehicle can generally be categorised by the following:-

1 – Vehicle Functionality

2 – Driver Behaviour

3 – Chassis Behaviour

Vehicle functionality tends toward assessing areas such as engine, power-train and cooling performance. Typical driver behaviour investigates inputs given by the driver to the vehicle, sensors on the vehicle are used to assess driver requests and vehicle response, and this can then be used to determine if driver requests can be improved. Chassis behaviour looks at the dynamics of the vehicle, in general terms sensors are used to assess vehicle suspension and mass behaviour for given driving scenarios. All 3 categories are interrelated and should perform together in a harmonious fashion for optimum vehicle performance. This study concerns the 2 latter aspects, driver and chassis behaviour.

Driver performance has been under scrutiny for some time to help improve quality of on road driving safety, road and infrastructure development, more intensely in the motorsport arena it is to help in competitive gains and technological advancements. Gathering accurate data to understand the relationship between the driver, vehicle and operating environments such as public roads or race circuits plays a large role in the development of solutions to help such aspects as safety, traffic volumes and performance gains. Addressing these problems has yielded in a great deal of work in increasing the fidelity at which real world events are recorded and sampled, though there is less work investigating the breadth of such measurements, for example external environmental influences. Evaluation of performance parameters commonly looks into driver inputs and vehicle response, for motorsport applications the nature of the vehicle response if crucial for maximising vehicle power and aerodynamic forces etc. Whereas for public road applications vehicle response isn't as crucial as long as a driving hazard isn't caused, the main factors influencing behaviour are external, i.e. other road users, weather conditions and traffic control systems. These add cognitive load that a good driver needs to be prepared to deal with at any time whilst driving, such events are significantly harder to measure compared to driver input controls.

To expect a driver to driver around a populated area more than say 3 times and to drive the same route, with the same road positing, steering behaviour, brake behaviour etc. is very difficult, mostly due to the dynamic nature of other road users. For motorsport applications, driving as close to an ideal line as possible is significantly easier due to the nature of the race circuit, race etiquette and performance motivations. It is much easier to understand why a driver brakes earlier or more aggressively than deemed ideal. For on road driving, little to no known data on the environment means accurate performance portrayals are hard to accomplish. With the addition of cameras, external and environmental influences can begin to be recorded and understood revealing answers as to why a given driver reacted in such a way, for example, observation of lane discipline, nature of driven corners and the effects of weather conditions can be scrutinised for analysis. This will allow for correlations between gathered data and driver assessment scorings to be drawn.

Recent literature on vehicle and driver performance investigates behaviour and performance using driving simulators in controlled environments to help characterise typical driver traits for given driving scenarios. Simulators allow for safe and cost effective testing, where measurements for theoretical models can be easily validated compared to on road measurements. Such theories range from researching driver performance characteristics to understanding human biomechanics and neuromuscular control. Though simulators do provide an invaluable resource there are many aspects of on road driving that professional driving assessors will critique for effective measurement of performance that cannot be accurately portrayed using simulators. For example, road and traffic awareness, driving confidence, effective vehicle control while checking aspects such as blind spots. On the contrary using driving assessors solely for evaluation can yield a variation in comparable results. If a given participant was to replicate their driving run exactly but with two different assessors the results may not be the same due to individual professional opinions on poor and good behaviour, also it is not quantifiably guaranteed two participants may receive the same score if a given corner was to be replicated exactly under the same conditions. So there is a need to apply objective methods to help validate assessor scorings and introduce standards that can be agreed upon, similarly there is also a need to measure real world interaction accurately to aid in increasing fidelity between on road and simulator driving analysis. For these reasons this study will present a method to measure driving performance using developed data acquisition devices alongside assessments conducted with a professional driving assessor.

Aims and objectives

The overall aim of this research is to investigate methods of assessing driver and vehicle performance from on road driving using conventional forms of data acquisition with the addition of computer vision techniques and a professional driving assessor.

- To identify system and analysis requirements
  - *Research the required hardware and software components using methods and technology currently available*
  - *Work with Goldstar to develop a required system specification*

- To identify existing technology
  - *Identify methods of capturing digital images meeting an agreed specification with Goldstar*

- To investigate hardware concepts
  - *Conceptualise techniques to capture digital images to meet specification*
  - *Develop physical bench top systems*

- To develop synchronised video and data acquisition devices
  - *Further develop final chosen method for image capture*
  - *Design and build a data acquisition system*
  - *Investigate the need to design and produce further integrated circuitry*

- To investigate computer vision techniques applicable to vehicle behaviour analysis
  - *Research methods of computer vision available that would aid in the understanding of vehicle behaviour and performance.*

- To apply simple vision and image processing techniques to captured video
  - *Use available methods of computer vision to aid in quantifying vehicle and driver performance*

- To demonstrate use of combined data capture technology for analysis of driving situations
  - *Use parameters gained from video and data acquisition for performance and behaviour validation.*

- Investigate the potential for exploitation in the form of research paper or journal article

Chapter 2

Review of Literature

2.1 Driver Behaviour

2.1.1 Driver analysis using conventional forms of data acquisition

Conventionally driver behaviour is assessed using vehicle sensors to record inputs or requests made by the driver. For example, velocity control can be outlined using throttle and brake data where recorded signals on pedal displacement can be used to find input timings for reaction and response behaviour. Further analysis can be undertaken to find the rate of change for a given displacement to describe the nature of the input, i.e. erratic or smooth usage. Motorsport applications will tend to start with these techniques alongside further recorded data to generate initial understanding of driver performance for a given driven distance.

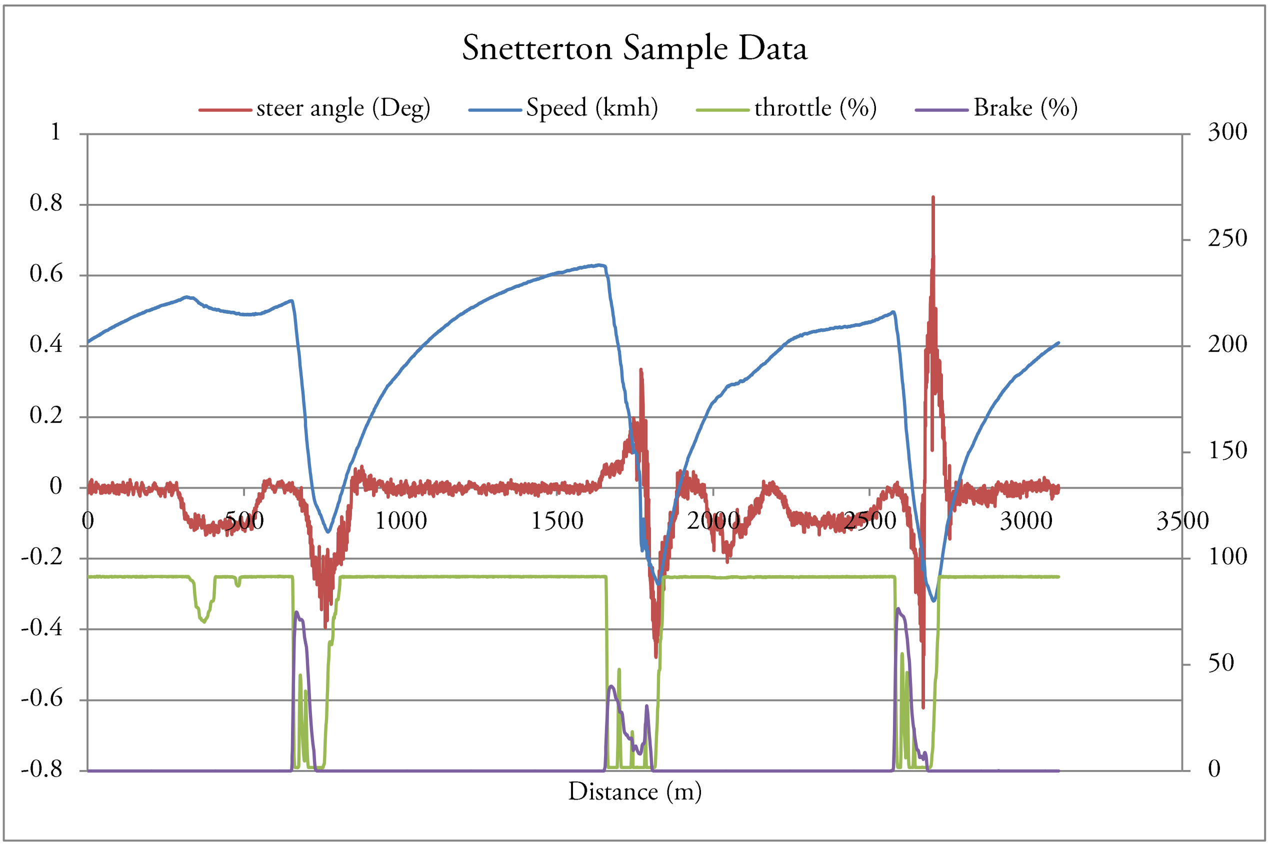

Figure 1 - Formula 3 Sample Data, Snetterton

Figure 1 shows sample data taken from a lap in a Formula 3 car around the Snetterton circuit. Using speed, steer angle and relative throttle/brake positioning a basic performance portrayal can be made.

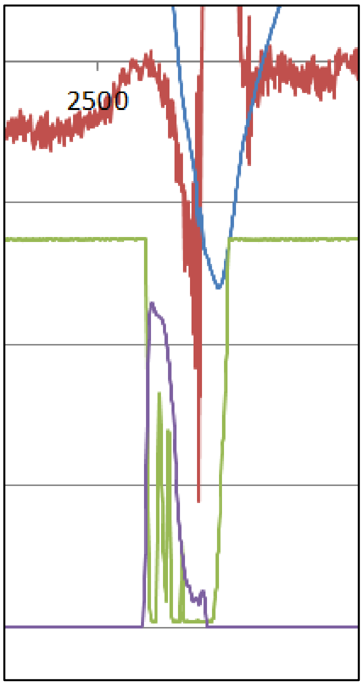

Figure 2 - Formula 3 Sample Data, Snetterton Enlarged

The data can be scrutinised in closer detail for specific behaviour around a desired sector of the circuit. Figure 8 shows the driver navigating the penultimate corner, Russell Bend before exiting onto Senna Straight. Analysis is generally undertaken in this manner to assess the efficiency of transition between throttle and brake behaviour when entering and exiting the corner, alongside the responsiveness and nature of steering control.

On this occasion the driver has demonstrated a good blend of throttle and brake use entering the corner, with a slight delay on the exit. This delay may be considered negligible but if deeper analysis is deemed necessary the only reliable source would be to ask the driver.

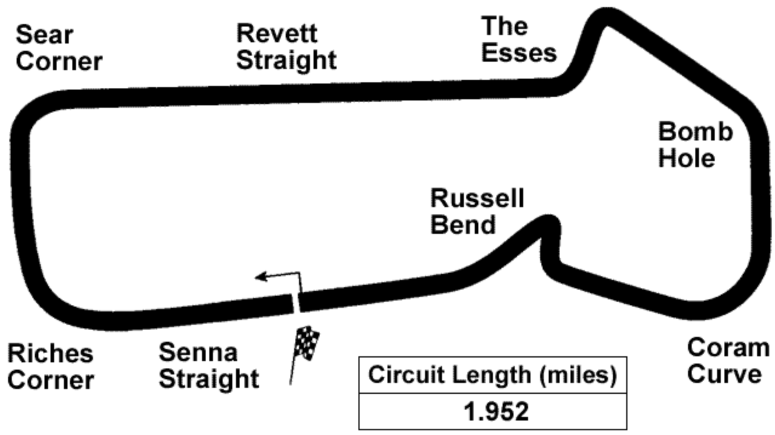

Figure 3 - Snetterton Circuit Map

This approach is a very useful and effective way to assess behaviour and performance, but based on observing vehicle response, the approach is limited in its abilities to find a deeper understanding on why certain driver responses are undertaken, i.e. cognitive and environmental influences. To begin understanding driver – real world interaction with the desire to recognize behavioural characteristics, anticipate future actions, a different approach must be made.

2.1.2 Driver Modelling

"The variety of models of the driving task is almost as numerous as the number of authors who have contributed to the models"

(Carsten, 2007)

Literature on attempts to derive methods for the driving task begun in 1938 when Gibson and Crook investigated the connection between a driver's behaviour and objects within the road infrastructure

(Oppenheim, 2010). Since then extensive literature has pursued and many advancements have been made in the area and as Carsten outlines, many authors. Carsten also outlines due to the complex nature of the driving task and the numerous tasks a driver will execute simultaneously, a general consensus toward a modelling approach is hard to standardise. There are two main approaches identified, descriptive and motivational.

The descriptive approach attempts to describe the actions expected from a driver and what the driver is required to do. This approach tends toward being more analytical than predictive and doesn't consider cognitive influences. Motivational or functional models attempt to explain and predict the performance of a driver in a given driving situation depicting risk and task difficulty (Carsten, 2007) (Oppenheim, 2010). This approach helps to understand these influences behind a made decision, gear selection for example, and is a more apt solution for assessing external and cognitive influences. It seems although defined as separate taxonomies they are deeply interrelated, though descriptive methods may be assessed individually, accurate motivational techniques rely on accurate portrayals of response expectations from the driver.

2.2 Chassis Behaviour - Ride and Handling

2.2.1 Ride

"Figuring the suspension of a car is almost entirely a matter of making useful approximations. It is not an exact science. But neither is it a blind application of rule-of-thumb principles"

Maurice Olley

Chassis and dynamic vehicle behaviour can be broken down into ride and handling. The simplest and most common method to describe full vehicle behaviour is the seven degree of freedom model.

copyrighted image removed

Figure 4 – 7 Degree of Freedom Vehicle Model (Crolla, 1992)

Freedom of movement is given in heave, pitch and roll conditions, while each wheel has freedom of movement in the vertical direction. The rear configuration may either be declared independent left to right or rigid with heave and roll motions of the rear axle. The vehicle body is assumed rigid throughout.

Heave motion can be defined as all wheels in contact with a given surface vertically moving at the same rate and displacement, in phase. While pitching will occur from a phase difference front to rear and a phase difference left to right produces rolling characteristics. There is a further motion known as warp where a phase difference diagonally is present (Balkwill, 2013).

Crolla justifies reasoning to reduce to 4 and 2 degrees of freedom. Figure 2 represents a 2 degree of freedom system, otherwise known as a quarter vehicle model (Crolla, 1992).

copyrighted image removed

Figure 5 – 2 Degree of Freedom or Quarter Vehicle Model **(Crolla, 1992)**

Equations of motions are used to assess vehicle response characteristics from given road inputs. Though there is not a common standardised method for replicating road profiles mainly due to the measurement of which isn't easy. Blundell and Harty present an expression to approximate the frequencies experienced by the vehicle (Blundell & Harty, 2004).

$$u(\omega) = \frac{K(2\pi V)^{R-1}}{\omega^R}$$

copyrighted image removed

Figure 6 – Road Profile Frequency Content **(Blundell & Harty, 2004)**

Figure 3 shows road profile amplitudes generally decrease linearly with an increase in frequency. So a frequency sweep input approximation can be used for assessment of vertical vehicle response for a range of road profiles.

copyrighted image removed

Figure 7 – Sinusoidal Road Surface Approximation **(Balkwill, 2013)**

Equations of motion can be applied to the 2 degree of freedom system allowing for the motion calculations of the sprung and un-sprung masses.

$$M_w z_1 = K_t(x_o - z_1) - K_s(z_1 - z_2) - C_s(\dot{z}_1 - \dot{z}_2)$$

$$M_b z_2 = K_s(z_1 - z_2) + C_s(\dot{z}_1 - \dot{z}_2)$$

(Crolla, 1992)

K_s = Spring Stiffness Coefficient C_s = Damping Coefficient

Though the above method does not offer a high fidelity representation of vehicle behaviour, Crolla provides reliable foundations for which to increase complexity. We now have a method to assess vertical response, ride. An area that hasn't been discussed is the motions and forces imposed laterally typically from cornering conditions. Crolla also proposes a simple handling approach again with 2 degrees of freedom allowing for lateral and yawing motion.

2.2.2 Handling

copyrighted image removed

Figure 8 – Simple 2 Degree of Freedom Handling Model **(Crolla, 1992)**

We can calculate these freedoms of motion as follows.

$$m(\dot{v} + Ur) = F_{yf} + F_{yr}$$

$$I\dot{r} = aF_{yf} - bF_{yr}$$

copyrighted image removed

Figure 9 – Coordinate System **(Blundell & Harty, 2004)**

To maintain an axes convention throughout the study a coordinate system the generally agreed SAE coordinate system will be applied, as shown in Figure 6.

2.2.3 Limitations of Characterising Driver and Chassis Behaviour

As motivational techniques to model driver behaviour fundamentally require some form of descriptive platform from gathered data, an empirical approach to begin outlining key behavioural aspects is a logical place to start. Further analysis into understanding external influences should then be considered, this ensures any modelling approaches are based on real findings. Applying these techniques and the theoretical frameworks outlined for ride and handling in a motorsport environment where ideal characteristic behaviour can be predictably calculated far easier than on-road offers a very good platform to develop such modelling techniques. The complexity of this predictability increases somewhat when considering the on-road driving case, ultimately reducing the effectiveness and accuracy of the model. Empirical methods to measure characteristic behaviour in real traffic scenarios, the relationship between the driver, road infrastructure and further environmental and external influences should be investigated before the application of modelling techniques can yield accurate and consistent results.

2.3 Conventional Data Acquisition Techniques

2.3.1 Physical Measurement

Measurement of real world events will commonly use analogue or digital sensors to relay physical events into electrical signals to be translated into numerical values for processing, analysis and storage. The key identifier for system quality is the ability to maintain signal accuracy and integrity (Texas Instruments Incorporated, 1994).

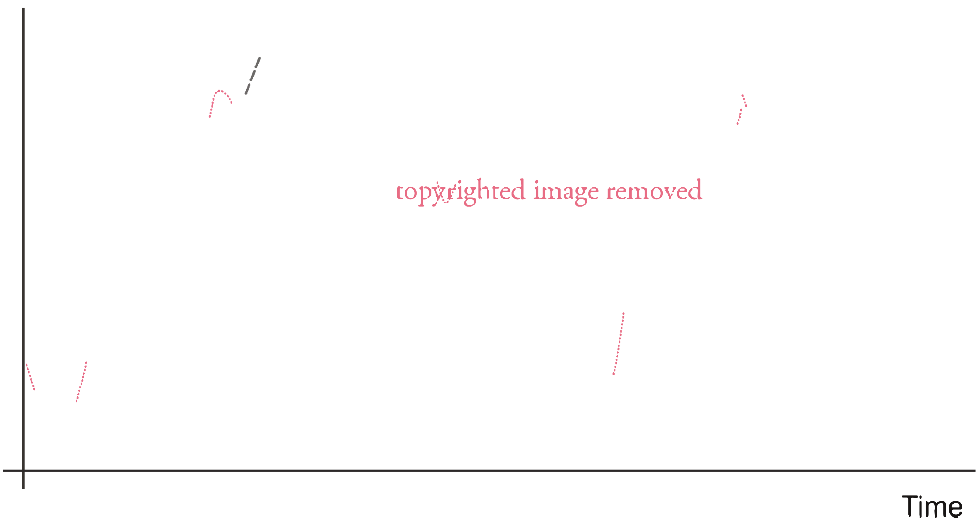

Figure 10 – Recovered waveform and recorded signal with 4 times per cycle sampling **(Larminie & Martin, 2009)**

Signals are sampled at rates based on the required resolution to record the physical event. A rate that is too high can incur data anomalies and surpass memory capabilities, rates that are too low can lead to important data loss. Spectral ranges of frequencies expected from the event being measured can be used to identify suitable sample rates. The Nyquist Sampling Theorem states the maximum frequency a signal can be recorded is half that of the sampling frequency, so the sampling frequency should be at a minimum of twice the recorded signal frequency. Figure 10 (Larminie & Martin, 2009) shows an analogue signal sampled 4 times per cycle, twice that of the signal frequency, it exhibits some loss of data throughout some sections, though variance and amplitudes have been deemed acceptable. This accuracy can be improved by increasing the sample to signal relationship, Figure 11 shows a signal sampled at ten times that of the signal frequency, a clear increase in correlation can be noticed. (Larminie & Martin, 2009).

copyrighted image removed

Figure 11 – Recovered waveform and recorded signal with 10 times per cycle sampling. **(Larminie & Martin, 2009)**

Recorded signals commonly also incur noise or unwanted data points throughout the data set, this noise can be filtered out using either hardware filters or post process software techniques. It can be hard to identify the most suitably accurate filter for a given measurement configuration, digital filtering algorithms are becoming more popular than hardware filters due to their cost effectiveness and flexibility. Probably the simplest form of filter is a moving average filter, a five-point moving average filter can be expressed by the following equation:-

$$y_n = \frac{X_n + X_{n-1} + x_{n-2} + x_{n-3} + x_{n-4}}{5}$$

The number of points can be increased to give a high resolution of filter, though this sacrifices processing time taken. Two common filters, not as computationally dominant as the moving average method, that have derived from hardware configurations are the Butterworth and Chebyshev filters.

copyrighted image removed

Figure 12 – Characteristics of Chebyshev and Butterworth Filters **(Larminie & Martin, 2009)**

It is desirable for a filter to instantaneously stop at the critical frequency, though in reality this is very hard to achieve. Figure 12 shows the drop off characteristics of both filters for a low pass.

2.3.2 Sensor Selection

Driver inputs are to be measured from the pedals and steering wheel. Linear potentiometers will be used to measure pedal and steering displacements. Larminie outlines the importance of measuring analogue sensor linearity (Larminie & Martin, 2009).

copyrighted image removed

Figure 13 – Linear Sensor Output **(Larminie & Martin, 2009)**

It is important to understand and include these characteristics when processing the measured data to ensure accuracy in representation of the occurred event. The sensitivity of the sensor can be found from the gradient of voltage output vs measure plot ($\frac{\Delta Y}{\Delta X}$). The zero offset should also be found. The following equation can then be used to find the desired measurement quantity, typically for displacement this will be in mm or m.

$$Measurand = \frac{Voltage - Zero\ Offset}{Sensitivity}$$

*It should be noted this applies to the linear range of sensors, polynomial equations should be for no linear sensors.

Measurement of velocity will be undertaken using a Global Positioning System (GPS), this allows for positioning at any point on the globe to be established based on triangulation of orbiting satellites. Longitude, Latitude, height and time are the 4 values communicated between the transmitter and receiver. These can then be used to find velocity and direction of travel (course), (Zogg, 2007). 28 satellites orbiting the globe every 11 hours 58 minutes inclined at 55° to the equator at a height of 20,180 km on 6 different orbital planes allow for positioning for a given receiver from a minimum number of 4 satellites, (Zogg, 2007). Velocity can be calculated by dividing the distance taken from two different positions by the time taken to travel between them.

2.3.3 Measurement Limitations

Data acquisition systems will commonly take measurements from digital or analogue sensors converting voltages into a binary format. Analogue signals like our potentiometers require an analogue to digital converter (ADC), ADC's will have a fixed resolution, for example for a 0-5V input signal with an 8 bit ADC 5V converts to a binary number of 255 or 11111111. Acquisition accuracy can then be calculated as,

$$\frac{5}{255} = 0.0196\, V$$

Resolution and sampling rates can result in poor event measurement if not considered appropriately, acquisition systems also suffer from a phenomenon known at as *aliasing*, relating to signal and sampling rates. A different signal is presented to the recorded one, Larminie suggests this can result from an input with a greater frequency than that or the Nyquist sample frequency (Larminie & Martin, 2009). Filters such as Butterworth or Chebyshev can be applied as a solution to help remove frequencies above that of the Nyquist.

2.4 Computer Vision

2.4.1 Definition

Assessing the presence of an object within an image against a given background is commonly defined in text as an occluding contour. Such contours separate the background from the area of interest in the image, so detecting them accurately is important (Forsyth & Ponce, 2012). They hold important information about the shape, size and behaviour of the object in question, consistency throughout a given number of frames is crucial and has been noted as one of the most challenging aspects in computer vision to date (Szeliski, 2010).

2.4.2 Digital Image Creation

Digital images are commonly generated using two colour models. RGB or CMYK, it is not within the scope of this study to assess the most appropriate colour model, nor is it important for the resulting image analysis. The RGB colour scheme will be used for all analysis.

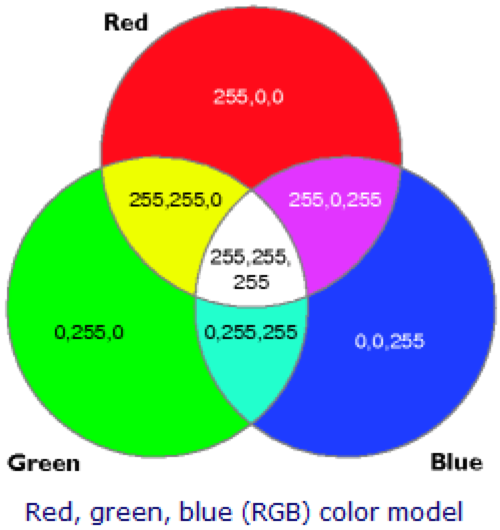

Figure 14 – RGB Colour Space Model

2.4.3 Feature Detection

In order to identify and apply accurate real world dimensions to objects captured from the real world, accurate and reliable methods of recognizing features for a large numbers of frames is necessary. Taking the case of the a vehicle mounted camera poised in the heading direction of the vehicle the most noticeable and easily tracked features can become occluded, causing detection methods to drift from the original region of interest.

Feature detection is typically taken in two forms, tracking and matching. Feature tracking is more useful for images that have a small amount of motion and change in appearance in a frame sequence. Feature positions are identified in one frame and then searches are made for the same positions and features in corresponding frames. This suits images with high gradients and stable feature positioning. For features that tend to move around the frame more and further searching is required, more efficient matching methods are usually used. Matching will detect features in the range of frames under consideration and preliminary common components established. A matching strategy will then be applied to determine areas for further processing (Szeliski, 2010).

Shi and Tomasi (1994) proposed a feature selection criterion focused more on the techniques of tracking. Affine registration is made between the feature region of the current frame and region of the first frame the feature was detected. Translation methods are used to compare regions in neighbouring frames and feature locations estimated before registration can be made. Features are detected infrequently when the tracking has failed and the area surrounding the current region of interest is searched with an incremental registration algorithm (Szeliski, 2010). By focusing on the quality of detection and the method to affine changes within images, the author provides a much more stable approach than focusing on attempting to simply follow a feature of interest. The method also monitors feature dissimilarity allowing for the errors in tracking to be clearly identified from occlusions or further problems. Since this paper has been published there has been further interest in its methods and applications.

Dependant on the region of interest and the nature of the parameter being estimated two initial problems are encountered, rigid and deforming features. If for example the behaviour of a tyre was the subject for analysis, deformation is a very important aspect to understand as it has an important role on the contact area to the road surface which governs the forces that can be produced for cornering, braking and accelerating. For this type of detection matching methods may be more efficient.

Non-Deforming/Rigid Features

Fischler and Bolles (1981) developed what is known as the RANSAC estimator (Random Sample Consensus). When identifying features from image sequences it is important to ensure measurement errors do not occur. Measurement errors are the incorrect feature identification with a change in frame in the sequence, so if we were to analyse the corner of a simple 2-D box we need to be able to ensure the exact point of the box is identified again if it is displaced. This is perhaps one of the most important factors when attempting to quantify real world parameters using video capture. The main focus of the RANSAC paradigm is to smooth data from positively recognized features to reduce such errors. The consensus initially uses the minimum amount of data points necessary and increases this with only consistent data when required. When a competent amount of points exist a smoothing technique will be applied to improve the computed estimate. Error deviations can be recorded and tolerances applied. There are two main errors with this approach, occlusions and lighting variances can yield high errors and are not taken into consideration. The second is when the amount of points required for assessment is increased, the computational power required to solve increased considerably due to the resources required to computer error deviations and validate tolerances. This method indicates suitability for measurement of displacements of rigid bodies such as vehicle wheel and body movement.

Edge detection methods are possibly the most common techniques of feature and boundary detection for rigid bodies. Edge points can be used for curved and straight contours. Canny (1986) developed one of the most popular edge detection techniques used today and is considered one of the most powerful, the approach is based on 3 main objectives:

1– Low error rate

2– Edge points should be well localised

3 – Single edge point response

(Canny, 1986)

A 2-D circular Gaussian function is initially applied to the image, the image gradient is then calculated and the magnitude used to locate edges within the image. A suppression technique is applied to the gradient to help highlight edges, edges can typically be found around the local maxima (Ovren, et al., 2013), both high and low thresholds are then applied before edges are detected and linked (Gonzalez & Woods, 2008).

2.4.4 Computer Vision Limitations

The main limitation with using digital imagery is the frame rate. High definition cameras are available with frames rates in the region on 25600 fps but currently aren't cost effective and have inappropriate packaging size for most automotive applications. Bullet style cameras offer frames rates generally at 30 to 60 fps and often give a trade-off with image resolution, where lower frame rates can give higher resolution images. This is not only due to sensor prices but also due to hardware and processing capabilities to transfer the high amount of data efficiently and cost effectively.

Video analytics are by their nature are computationally demanding and real time applications suffer because of this. Driving situations also have a high variance in objects exposed to the camera and developing a consistent reliable solution is not only harder than using conventional sensors but also less cost effective. For example distance approximation can accurately be done using radar and proximity sensor technology that has proven reliability, though the shortfalls in measuring events other than the sole purpose of the sensor are easily recognizable.

Hough Transforms

Sometimes detecting lines and curves is hard because they can be broken up or disconnected. Connecting such lines can not only be computationally resource heavy but also inaccurate for a large frame sequences. The Hough transform uses a voting method, votes are made based on the amount of other feature points along a given line.

For a given point on a 2-D image with (x,y) coordinates the Hough transform will calculate an infinite number of lines that satisfy (equation 1)

Equation 1

$$\rho = x\cos\theta + y\sin\theta$$

Where ρ is the normal distance from point(i) to the origin and θ is the clockwise angle between the projection of ρ and the horizontal axis.

copyrighted image removed

Figure 15 - (a) ($\boldsymbol{\rho}$,$\boldsymbol{\theta}$) parameterization of line in the xy-plane. (b) Sinusoidal curves in the $\boldsymbol{\rho\theta}$-plane; the point of intersection ($\boldsymbol{\rho}', \boldsymbol{\theta}'$) corresponds to the line passing through points (x_i, y_i) and (x_j, y_j) in the xy-plane. (c) Division of the $\boldsymbol{\rho\theta}$-plane into accumulator cells. **(Gonzalez & Woods, 2008)**

Points from the xy-plane are then transposed to sinusoids in the $\rho\theta$-plane, intersections in the sinusoids outline a line has been calculated at the point. This plane is then split into intervals known as accumulator cells. Peaks from discreet ρ, θ curves highlight where lines are found within the image.

Deforming Features

Pilet, Lepetit and Fua (2006) developed a real-time method for deformable objects by creating recognizer algorithms that are able to search for matching features anywhere in an image. A calibration or training image is first introduced where a baseline point matching technique is applied to outline the feature before its deformation. A set will be matched between the calibration image and a given input image, this set include erroneous and non-erroneous matches. The transformation from the un-deformed image to the deformed image is mapped as a 2-D hexagonally connected mesh. Occlusions and outliers are weighted using a 'radius of confidence' and a 'ridge of confidence', the result will be true or false based on the sum matches falling within the 'ridge of confidence'.

The author's algorithm performs at 8-10 frames per second on a 2.3 GHz processor for 2-D image. Thought the method is robust and efficient for outlining a feature and matching it, it is unclear whether the points correlate 100% to the same parts of the feature before and after deformation. This is important when applying dimensions and measuring real world quantities. The method also inherits some self-occlusions from some surface textures.

2.5 Previous Studies in On-road Driver Behaviour

Davis (2006) proposed a method to evaluate older driver performance from the development and implementation of a system to measure vehicle dynamics parameters. The study was undertaken at The University of Florida with the National Older Driver Research and Training Centre (NODTRC), who received funding from the Centers for Disease Control (CDC). The Federal Highway Administration (FHWA) and The Florida Department of Transportation (FDOT). The study evaluated the effects of road intersection improvement recommendation from the FHWA to aid in making their negotiation easier. The study focused on evaluating older drivers as they were thought to benefit more from the recommended improvements compared to younger drivers. Results indicated the improvements benefited both age ranges but were more helpful for the older age range. The study used a fully instrumented vehicle using accelerometers, string potentiometers, laser tachometer, event triggers from brake and turn signals, GPS and 4 digital pinhole cameras. The GPS, vehicle sensors and video captures device all begin recording at different times and time corrections are made in a post process manner. Dynamic characteristics of the vehicle were found using accelerometers with the following manoeuvres:-

- Normal Acceleration manoeuvre
- Aggressive Acceleration manoeuvre
- Normal Deceleration manoeuvre
- Aggressive Deceleration manoeuvre
- Normal Right and Left turn manoeuvre
- Aggressive Right and Left turn manoeuvre

To investigate driver improvements statistics standard deviations are found for maximum combined accelerations, maximum longitudinal and lateral accelerations and maximum yaw and speed. These are then analysed for significant differences between older and younger age groups. The video captures were used as an aid to ensure evaluation errors were consistent between drivers and were not technically analysed to aid in vehicle dynamic evaluation.

Most recent and previous literature on assessment of driver performance using instrumented on road vehicles concerns older drivers. A current study conducted by The Massachusetts Institute of Technology, AgeLab has identified for older individuals the loss of driving independence is ranked one of the highest personal concerns with declining overall cognitive functionality (Massachusetts Institute of Technology, 2014). (Lee, et al., 2003) published a study with collaborations from The School of Occupational

Therapy, Driving Assessment and Consultancy Centre, The Occupational Therapy Research Centre and the Department of Epidemiology and Biostatistics all at the Curtin University of Technology, to validate a previous study published earlier that year that assessed 129 older volunteering drivers ages 60 or more for the development of an appropriate assessment criteria of older driver performance (Lee, et al., 2003). The second publication addressing the assessment of on-road driving versus simulated driving conducted on-road assessments in participants along a predetermined route. The assessment criteria consisted of 11 elements (Table..) measured by the principle investigator assessing the drive (Lee, et al., 2003).

copyrighted image removed

Figure 16 – On-road Driving Assessment Criteria **(Lee, et al., 2003)**

Methods used for on-road driver performance are descriptive, where the principle investigator of the study conducted the assessment on the participant driving their own car along prescribed route. The study goes on to correlate simulated driving with on-road driving using principle component analysis and statistical analysis methods to identify correlations between results of both simulated and real driving methods. Results highlighted the use of simulators for on-road resemblance with further development and the use of simulators for initial screening techniques.

2.6 Chapter Summary

Considering the 3 outcomes delivered by MIRA outlined in the research motivation and literature published there seems to be a clear focus on early theoretical definitions especially for vehicle behaviour that has been taken forward into more simulation focused work more recently. Less published work on driver performance is available, this may relate to types of analysis being heavily related to high end sports where literature on analysis methods typically isn't a done thing, due to competitive advantages etc. There has been a great amount of work conducted in mathematical approaches to understanding human behaviour, mainly cognitive functions that aren't necessarily relative to an automotive application, again these are mainly theoretical. Though the 3 outcomes relate heavily to vehicle characteristics, empirical work in driver behaviour should be under as much observation, not only to help understand their behaviour but also to aid in furthering vehicle dynamic behaviour. Though theoretical methods offer scope to portray in depth relationships, as much focus should be paid to empirical approaches not only to validate theories but more to gather real data that allows analysis of actual behaviour and begin outlining characteristics based on real world measurements. Descriptive techniques of driver performance are of initial interest to this study due to their analytical relevance. It is hoped with the use of camera acquisition we can begin to answer the question *'why'* a driver responded in a given way allowing for deeper analysis for both vehicle and driver behaviour.

To achieve a good foundation to analyse behaviour for on road driving scenarios identification of parameters required for measurement need clearly outlining. The main and key aspect of assessment should be based around how well the car is controlled and the nature of vehicle response for a given driver request. When driving on the road there are typically 2 main top level driver inputs of interest, velocity and steering control. The following two sections will review methods of measuring such parameters with relevant literature in context with the objectives of this study.

Chapter 3

Video and Data Acquisition System Development

Data and video acquisition systems have both been developed for this study. Data validation and processing has been validated in a post process manner but further development would need to be implemented to further this into an on vehicle solution. Results have been gathered in conjunction with The Movement Science Group at Oxford Brookes as well as the Regional Driving Assessment Centre (RDAC) for validation of results from the data acquisition and video capture systems. Both RDAC and Movement Science Group are looking to quantify human driving behaviour through the use of an EEG system. This has given a good opportunity to gather results with public participants driving on the road while being assessed by a professional assessor provided by the RDAC.

The following diagram shows a top level view of system interaction and connectivity.

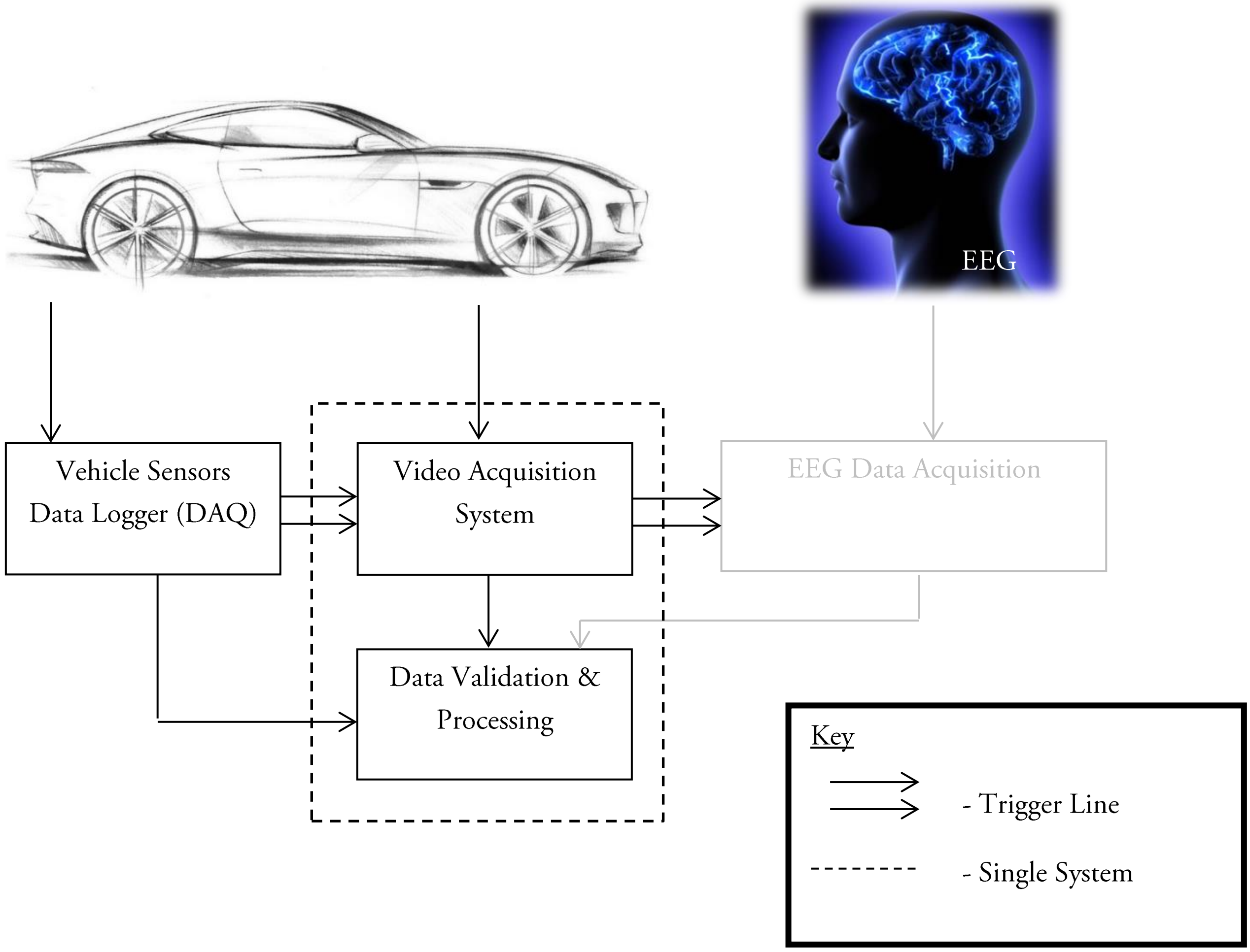

Figure 17 – Top level System Layout

Each of these elements will now be described in turn, it should be noted the EEG system does not play a role in this study but the developed data acquisition systems acts a central trigger also for the EEG system.

3.1 Data Acquisition Device (DAQ)

3.1.1 Configuration

The designed data acquisition system comprises of the following configuration:-

- Up to 15 Analogue Inputs (3 used)
- 6 axis Inertial Measurement Unit (IMU)
- GPS
- SD Card Storage
- 3 Digital Inputs (1x Start/Stop Button, 2x User Data Trigger Button)
- Synchronisation Triggers
    - EEG System
    - Camera System

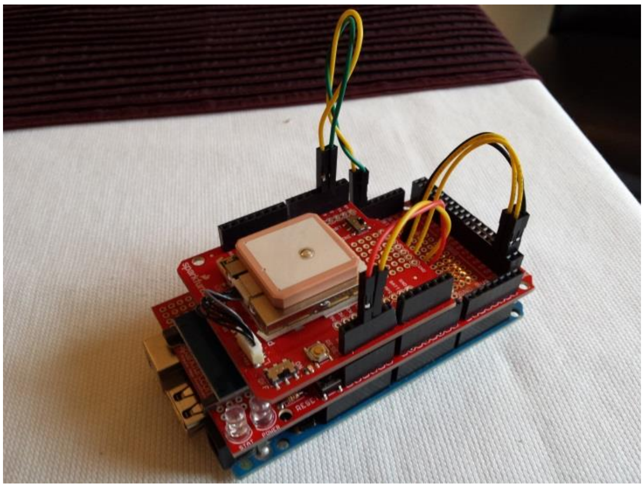

Figure 18 – Data Acquisition Device Image

The three analogue inputs use 3 potentiometers connected to the throttle, brake and steering inputs. The IMU is mounted on the data acquisition system, the system will be place near the CoG of the vehicle. There digital inputs allow for the system to start and stop when required on a button, with a further button that allows for areas of drive with specific interest to be flagged, a third button is used by the driving assessor for indication of the emergency stop event.

The storage card contains 2 files, where one files logs the analogue sensors and digital inputs, the second file holds the GPS data. The reason for 2 files is that this allows for the slower GPS logging rate not impinging on the faster rate of the other sensors. The following schematic outlines the system connectivity for the data acquisition device.

3.1.2 Schematic

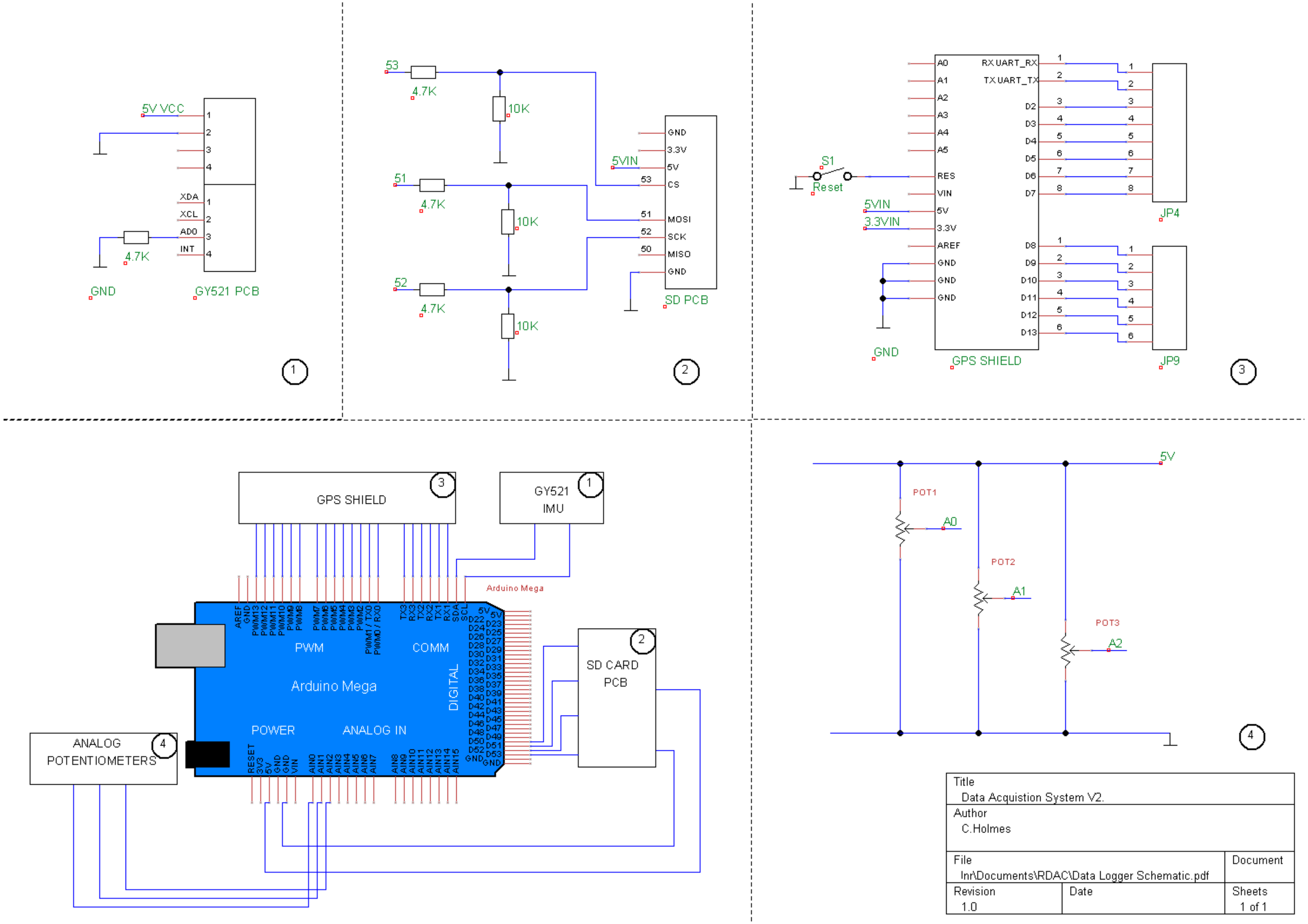

Figure 19 – Data Acquisition Schematic

3.2 Video Device

3.2.1 Requirements

In agreement with the specification supplied by Goldstar Onboard Ltd the video device should have the following top level configuration:-

- Resolution – 1280 x 720 or 1920 x 1080
- Frame Rate – 30 or 60 fps
- Storage – A single solid state device (memory card or USB storage device)
- Cable length 3m

Further functionality can be found in the design specification. The following concepts have been generated based on the required hardware specification.

3.2.2 Initial Device Configuration Concepts

A

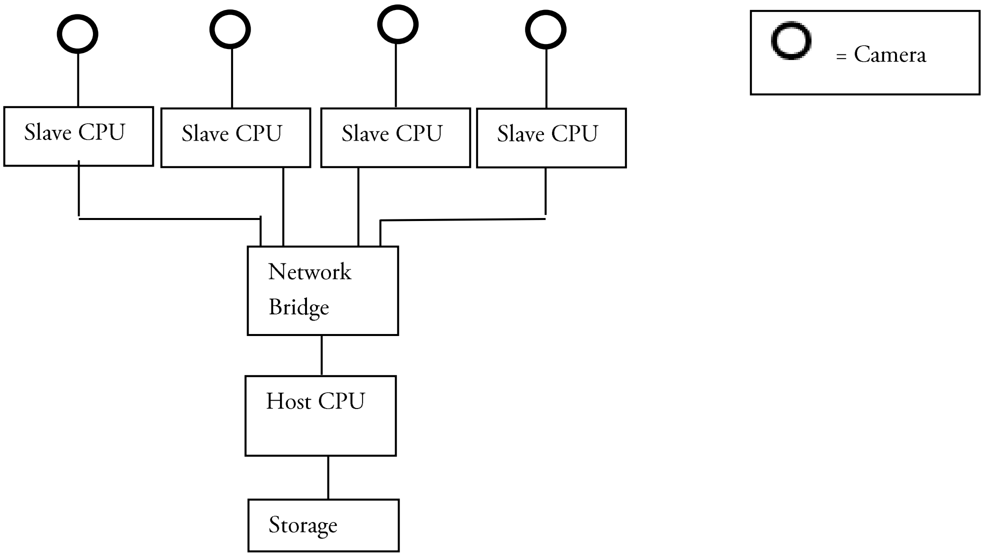

Concept A uses a static wired Ethernet network constituting of multiple slave devices capturing the video and a single host device to transfer multiple video captures to a single storage device.

Raspberry Pi computers were used for both host and slaves devices. A single camera is connected using a CSI (Camera Serial Interface) communicating raw video captures to the Raspberry Pi for encoding. The slave devices are then connected via a network bridge to the host device. A storage medium connected to the host device is mounted via a network directory. This directory is then made available to the slave devices to allow for storage of the encoded video captures to the storage device connected to the host.

A delay was experienced when communicating encoded video streams to the storage medium, causing a slower than real time solution, this was due to the processor capabilities of the host device. This could be overcome by mounting the camera to the slave CPU but due to large packaging another method was required.

B

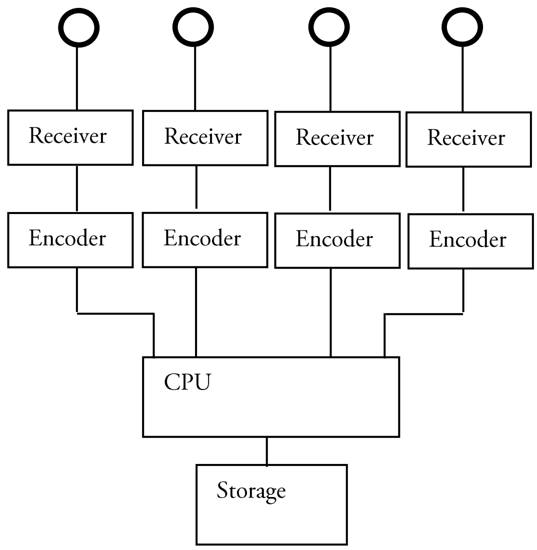

Concept B allows for capture via a HD-SDI *(High Definition – Serial Digital Interface)* communication protocol, this transmits a raw video stream from the camera to a receiver for conversion to a parallel type protocol for encoding. Once encoded the compressed streams are sent to the processor to then be stored.

This concept allows for a single processor to be implemented with camera devoted video encoders that accept and convert the raw video stream to a decoded format for viewing. This is transferred over a USB interface to the host CPU for storage.

The main problems encountered with concepts A and B relate to the transfer of raw uncompressed data from the camera sensors. Both configurations rely on encoders that would be implemented on the recording and storage hardware rather than the capture hardware. This creates two problems, the first is finding a suitable protocol to transfer high data rates at approximately 1.5 Gbit/s for raw high definition video. The second is the reliability of the transfer. The agreed specification expects cable lengths from the cameras to the host processor to be around 3m. This means any noise or reliability problems that occur will have an effect on the quality of raw data to be processed, giving a significant decrease in encoding efficiency and quality of video compared to that of such effects on already encoded video streams. The Beaglebone Black and Semtech devices were used. For sufficient transfer of data, isochronous USB support is required, the Bealgebone does not support this protocol, The Pandaboard provides this support and is used for Concept C.

C

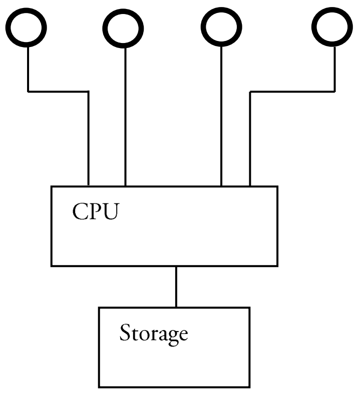

To overcome the problems encountered in concepts A and B, concept C uses sourced cameras with on-board encoders. Encoded video captures are then streamed to a processor to store the multiple captures to a single storage device. The reduction in transfer rates from raw video at around 1.5 Gbit/s to encoded data at a range between approximately 1 Mbit/s and 10 Mbit/s, dependant on the desired capture characteristics, allows for the captures to be encoded much more efficiently and also transferred much faster. Transferring encoded data over longer lengths than the raw data offers an increase in capture reliability and quality.

3.2.3 Device Concepts – Cameras

Raspberry Pi Camera – Concept A

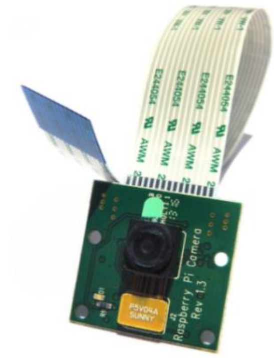

Figure 20 – Raspberry Pi Camera

Resolution – 1280 x 720 or 1920 x 1080 ** Frame rate – 30 fps ** Sensor – CMOS ** Interface – CSI - Ethernet

HD-SDI Camera (Tsact TBT-HD760) – Concept B

Figure 21 – Tsact Camera

Resolution – 1280 x 720 or 1920 x 1080 ** Frame rate – 30 fps@1080, 60 fps@720 ** Sensor – CMOS ** Interface – HD-SDI – parallel – USB

Semtech Serial receiver – Conversion of raw HD-SDI format camera data to a parallel format for encoding

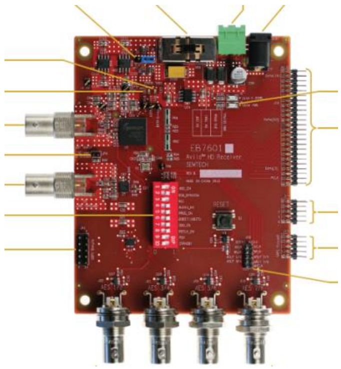

Figure 22 – Semtech Serial Receiver

Geo Semi. Camera (Raptor 1 & Raptor 2) – Concept C

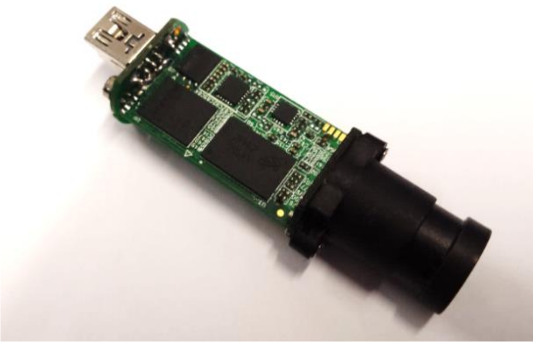

Figure 23 – Raptor 1 Camera

Resolution – 1280 x 720 or 1920 x 1080 ** Frame rate – Raptor 1,(720@30) Raptor 2, (1080@60) ** Sensor – CMOS ** Interface - USB

The raptor 1 camera is used for this study with the raptor camera offering increased resolution and frame rates currently in development.

3.2.4 Device Concepts - Processors

Raspberry Pi

Raspberry Pi can capture 1920 x 1080 resolutions at 30 fps using a Camera Serial Interface (CSI), the board configuration allows for a single camera to be connected. A network file system (NFS) was created with multiple boards and cameras connected via Ethernet. The capture of 2 devices was successful to a single host directory.

Figure 24 – Raspberry Pi

Rapsberry Pi Model B Configuration

O.S – Debian(Supported), SD ** CPU – 700 MHz(x1) Broadcom BCM2835 ARM1176 ** RAM – 512 MB DDR3 ** USB – 1.0(x2) ** Ethernet – (10/100)

Beaglebone Black

The beaglebone was sourced due to its increased power capabilities compared to the Raspberry Pi, the board also has further I/O functionality with an on-board ADC. The manufacture files are freely available as well as the ability to source processor chip individually.

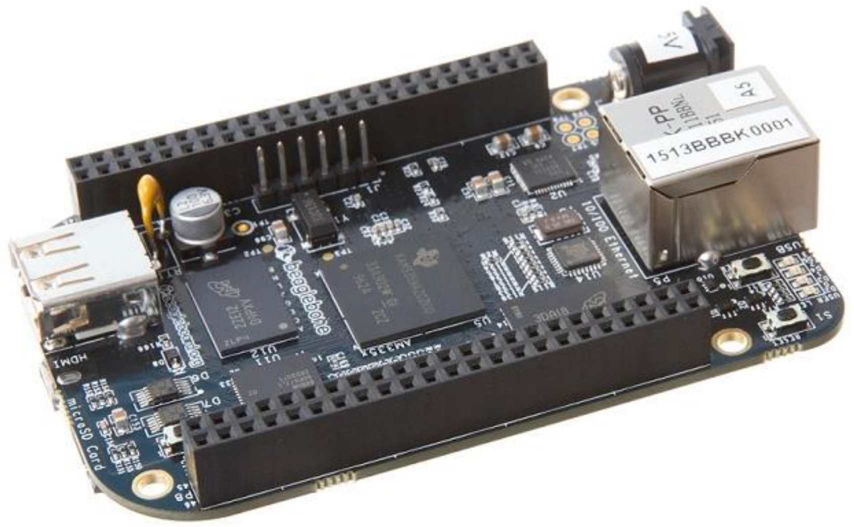

Figure 25 – Beaglebone Black

Beaglebone Black Configuration

O.S – Debian(Supported), SD ** CPU – 1 GHz(x1) T.I Arm Cortex-A8 ** RAM – 512 MB DDR3 ** eMMC – 2 GB ** USB – 2.0(x1) ** Ethernet – (10/100)

Pandaboard ES

Pandaboard ES offers isochronous USB support, along with further processing capabilities and GPU.

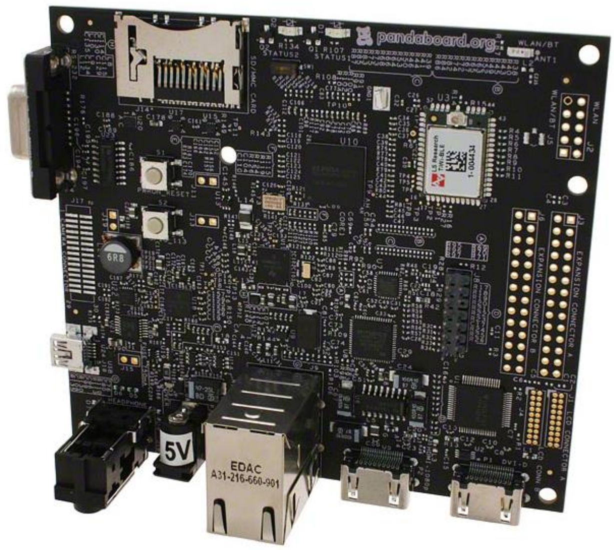

Figure 26 - Pandaboard

Pandaboard ES Configuration

O.S – Debian, Android (Supported), SD ** CPU – Dual-core 1.2 GHz (each) OMAP Cortex-A9 ** RAM – 1 GB DDR3 ** USB – 2.0(x3) ** Bluetooth ** GPU – Imagination technologies POWERVR SGX540 ** Ethernet – (10/100)

3.2.5 Selection Matrix and Concept Evaluation

Concept	Configuration Complexity	Cost	Transfer rate efficiency	Storage	Ease of maintenance	Ease of adding further cameras	Total
A	15	15	10	5	10	15	70
B	20	20	20	5	10	5	80
C	5	5	5	5	5	5	30

Table 1 – Video Device Concept Selection Matrix

1 – Good, 4 – Bad

Identified in table (1) are the key aspects considered when investigating the functional characteristics of the three outlined concepts. Scores generated on key parameters from the hardware specification have been multiplied by a weighting factor of 5. The lowest total score yields the most desirable concept. The results show concept C with the lowest score.

3.2.5.1 Configuration Complexity

Concepts A, B and C comprise of 11, 14 and 5 major components respectively, the higher number of components increase the complexity of the device and the necessity to rely on the combination of more components for system functionality. Device costing will inevitably relate to the complexity, when considering manufacturing intent to be more than 100 units the number of components, manufacturing complexity and component cost can have a much larger affect at larger unit numbers.

3.2.5.2 Transfer Rate Efficiency

The efficiency at which the device handles raw and encoded data streams is considered. As the final intent should deliver a solution that as is close to real time as possible, the time to transfer raw images to the storage medium is crucial. Considering uncompressed data rates can be approximately 1185 Mbps and compressed rates can range from 1 Mbps up to 10 Mbps, to conserve image quality bandwidth considerations should allow for a solution that transfers the larger uncompressed data over the shortest distance. This not only reduces the risk of noise affecting large amounts of raw data but also allows for increased encoding efficiency where the encoded data can be transmitted over the desired distance for a camera location. Concept A requires encoding on the storage device requiring raw data to be transmitted over longer distances. Concept B has the ability to encode raw data close to the camera but due to the hardware required (raw data receiver and encoder) means a large packaging solution would be required.

Concept C utilises encoding on the camera with a small favourable packaging solution, this encoded data is then transmitted over a serial protocol for storage.

3.2.6 Final Device

Concept C has been deemed the chosen concept to pursue development with the Geo Semi. Raptor Camera 1 and the Pandaboard board for storage and user functionality.

A file will be created per camera on the USB storage along with a log file (.txt) per capture. Please note, once capture has been stopped, further video files will not append, they will overwrite. To overcome this, please power down the device and remove the storage medium, clear the files and insert the USB again before powering back up.

The device is only fused through the externally connected power filter, this can be removed and has been tested with the accompanying battery but should be used for any further power inputs. A single power input is divided up inside the device and the input should not exceed 12V 5A.

The following diagram shows the final video capture device layout.

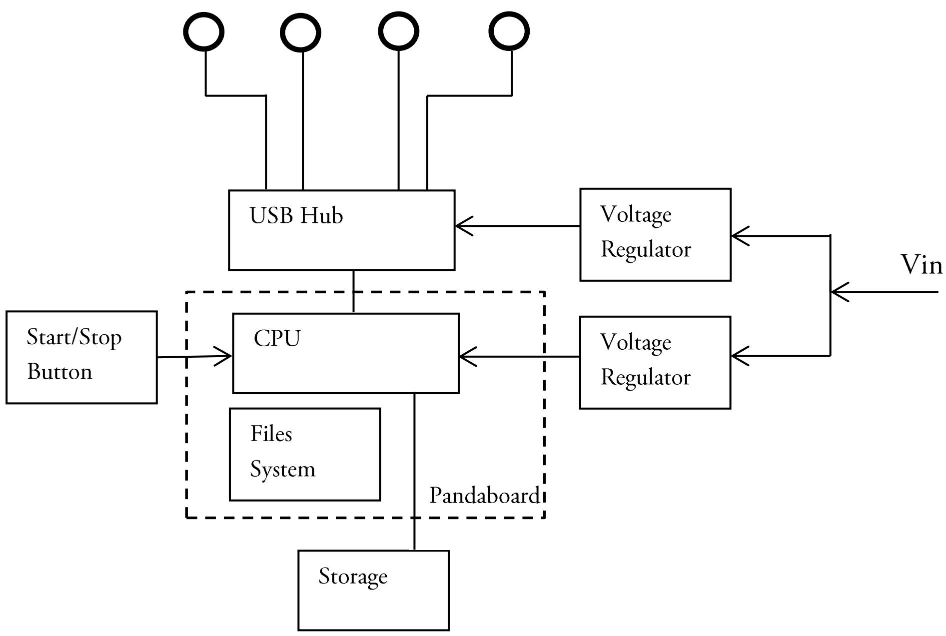

Figure 27 - Final Video Capture Device Layout

Figure 28 – Video Device System Front View

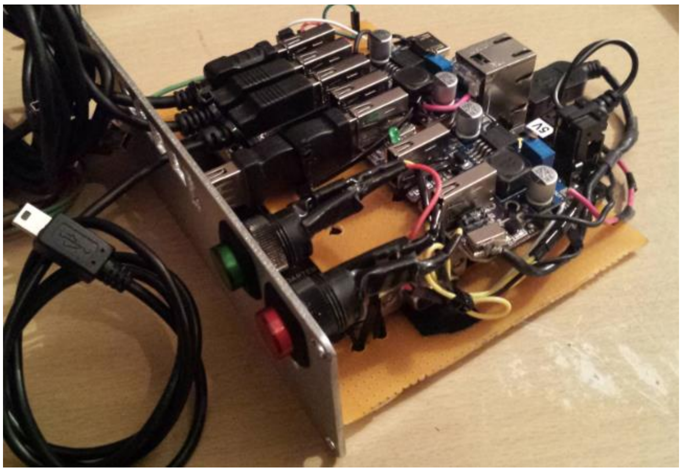

Figure 29 – Video Device Internal Image

3.3 Chapter Summary

Both data acquisition and video capture system configurations have been outlined. Sensors used in the data acquisition system have been specified based on key aspects to be measured outlined in the literature review. The video capture system has been configured based on requirements outlined by the design specification. Both systems will need to be assessed for their performance characteristic s. Analysis of results captured by the data acquisition system and results provided by the driving assessor will be scrutinised for correlation and identification of key aspects that will be of most benefit by the application of computer vision techniques.

Chapter 4

Result Analysis

4.1 Video and Data Acquisition Development Analysis

4.1.1 Data Acquisition System – Limitations

When considering the effectiveness of gathering data sampling rates of acquisition will first be investigated. The GPS and DAQ have been developed to measure data at different rates. As the GPS is limited by a rate of approximately 1 sample per second, an increased rate needs to be established to ensure measurement of driver inputs. The DAQ has been programmed to gather data at approximately 40 Hz. Figure (30) shows the time data points for both DAQ and GPS.

Assessment of logging rates are made for logging stability.

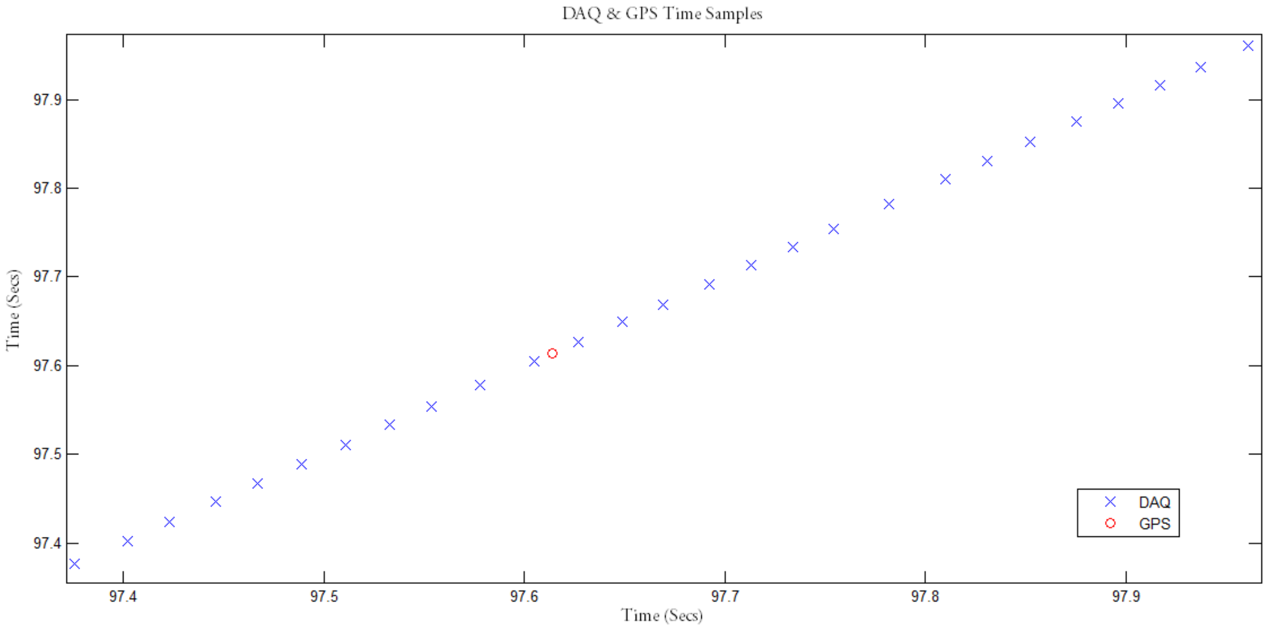

Figure 30 – DAQ and GPS Time Samples

The following histogram in figure(31) shows the density of time differences for a given run. It shows some deviation, 0.06 Secs (16.67 Hz) being the longest difference between 2 time points. It now needs to be established if this variation still offers a reliable method to portray events with sufficient accuracy.

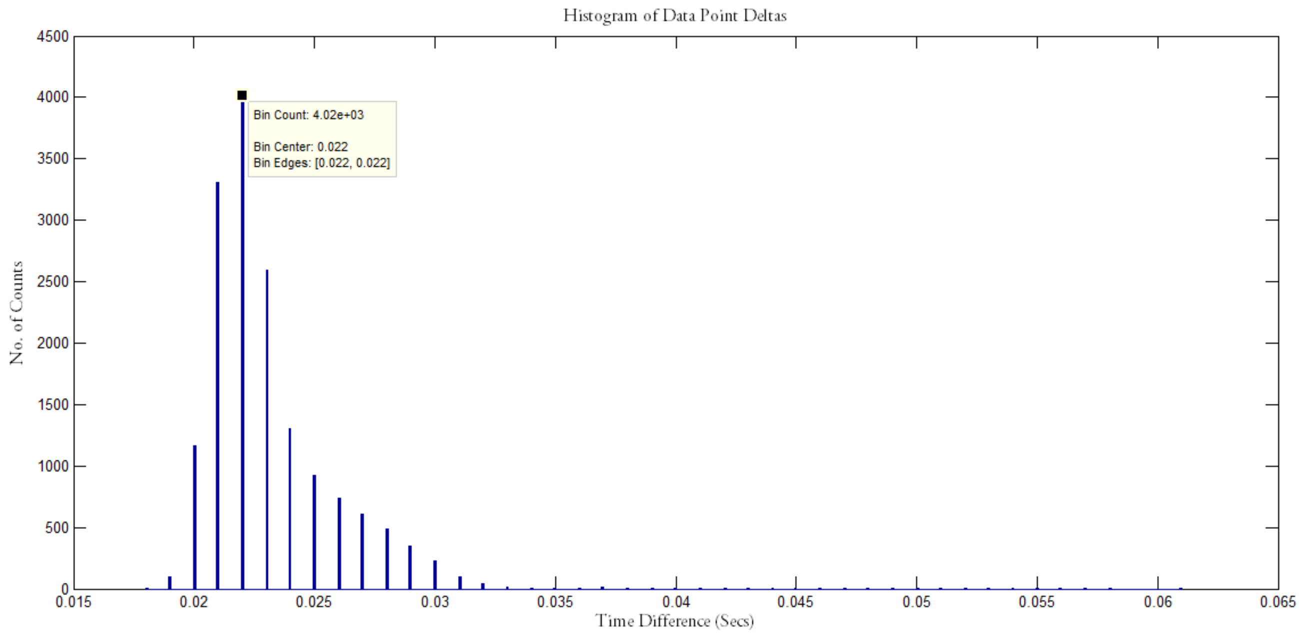

Figure 31 – Data point Delta Histogram

19.24% of our values are larger than 0.025 Secs, with a maximum difference of 0.06 Secs (16.67 Hz). 80.76% of our values are below or equal to 0.025 Secs with a minimum difference of 0.018 Secs (55.56 Hz). It now needs to be established if this variance is suitable for the events being measured.

An emergency brake event has been outlined in the testing procedure by the RDAC where the driving assessor will request the driver to stop in the fastest time possible, the assessor will press a button when he has requested the driver to react, this allows the data acquisition device to log the difference between the request made and the time at which the driver reacted. Remaining with the same data set the driver reaction time has been calculated as 0.473 Secs. (Elliott & Louttit, 1937) have measured braking reactions no faster than 0.1 Secs. So as long as the sampling rate is faster than 0.1 samples per seconds the events under consideration should be captured successfully. This variation has been deemed acceptable as our slowest data point gap is faster than the fastest event in question.

The causes behind this variation in logging rate will be now assessed. The following diagram shows how the design of the acquisition system has been programmed to measure and log the defined values.

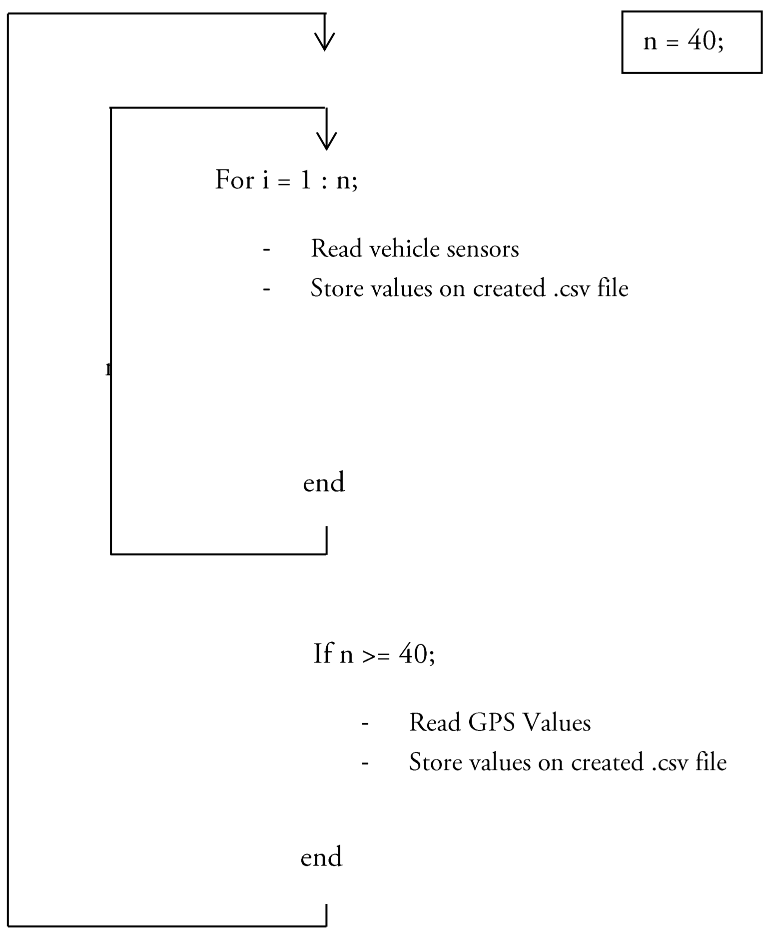

Figure 32 – Data acquistion programme layout

Considering reading just the vehicle sensors, 40 values throughout the loop are stored in a buffer. The buffer size in the Arduino Mega 2560 is 8 KB. 4 analogue inputs, 6 values from the IMU and a timestamp gives approximately 24 Bytes of data. At 40 Hz this is around 0.96 KB/Sec. The buffer will require flushing approximately every 8 samples. The time taken to flush the buffer has been measured at 14 ms, giving an increased time delta of 0.04 Secs. SD cards also inherently suffer from varying latency, specifications outline latencies ranging in regions 0.025 – 2.5 Secs (Association, 2010), this doesn't state the minimum latency to be 0.025 Secs, the latencies range from card classes, sizes and quality of components. A card latency of 0.025 Secs explains our varying time deltas up to around 0.06 Secs. This doesn't explain why rates faster than 40 Hz have been observed. As the data logger has been programmed to log at 40 Hz, a faster frequency is indicative of poor time maintenance from the microcontroller. The instability of a clock or oscillator is known at clock jitter, its affects mean values may be recorded slightly out of synchronisation from the desired frequency, jitter will usually have more effect on demanding higher frequencies. When converting analogue signals to digital the ADC timing must be as accurate as the microcontroller oscillator. An external dedicated ADC should be further implemented to investigate its causes.

4.1.2 Video System Analysis

All devices were tested under the same conditions at the same time. One camera from each system was used on a windscreen mount positioned toward the heading direction of the vehicle. Each system comprised of the following camera arrangement;

Goldstar Onboard Dual Cam – 2 cameras available, 1 used

Ez Storage Device – 4 cameras available, 3 used

Pandaboard – 1 Camera available, 1 used

Both the Goldstar Onboard and Pandaboard devices created a single file that lasted until a user input ceased capture. The Ez storage device creates a new file after approximately every 5 minutes of recording time.

Figure 33 show the time delays between the average 5 minutes long files over the total range of files created. It should be noted camera 1 was used throughout the entirety of the testing whilst cameras 2 and 3 were only used for part of the testing period.

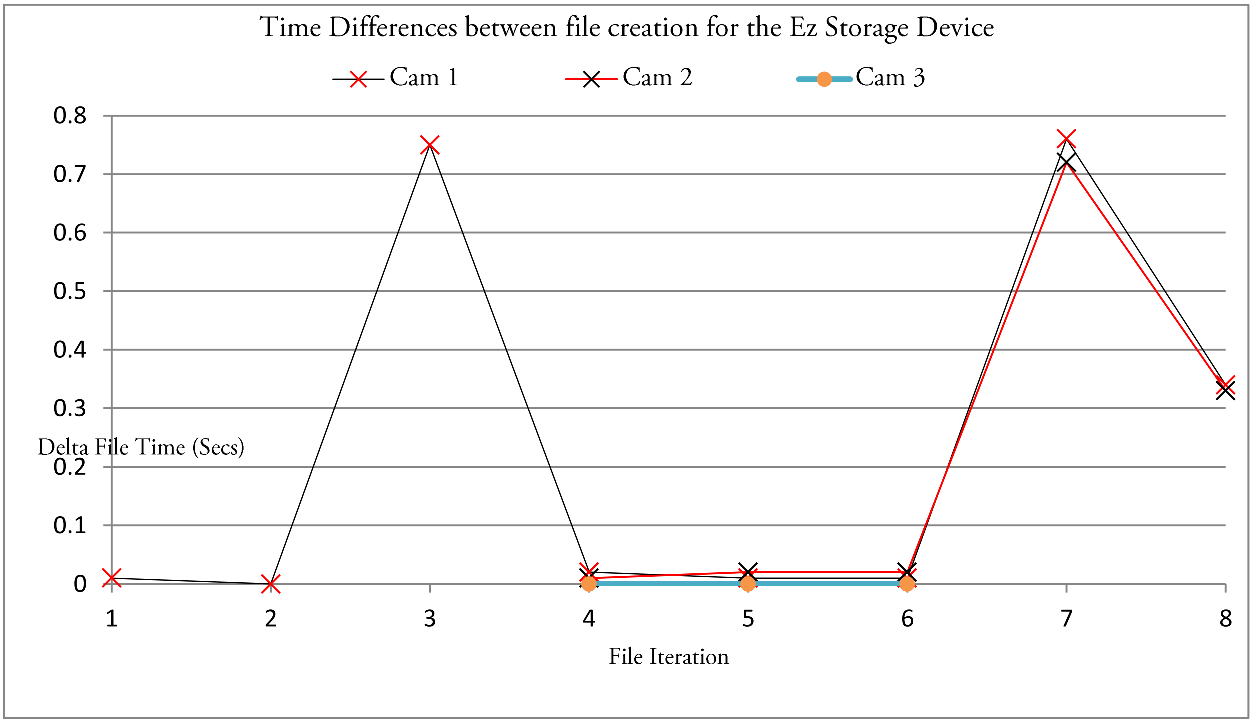

Figure 33 – Video capture File Time Differences

File iterations consist of the following camera configuration

1 – 3, 1 camera | 4 – 6, 3 cameras | 6 – 8, 2 cameras

The longer time delay at file 3 is related to the addition of more cameras to the system, similarly with 7 as this is the first transition after the third camera was removed. Delta values during stable operation range from 0.01 seconds to 0.02 seconds.

There was also no noticeable change in image quality as more devices were introduced and removed on the Ez Storage device.

4.1.2.1 On-road Device Comparisons

Figure 34 - Ez Storage Frame Capture 1 – M40 – 1 Camera – 30 fps – 1.5 Mbps

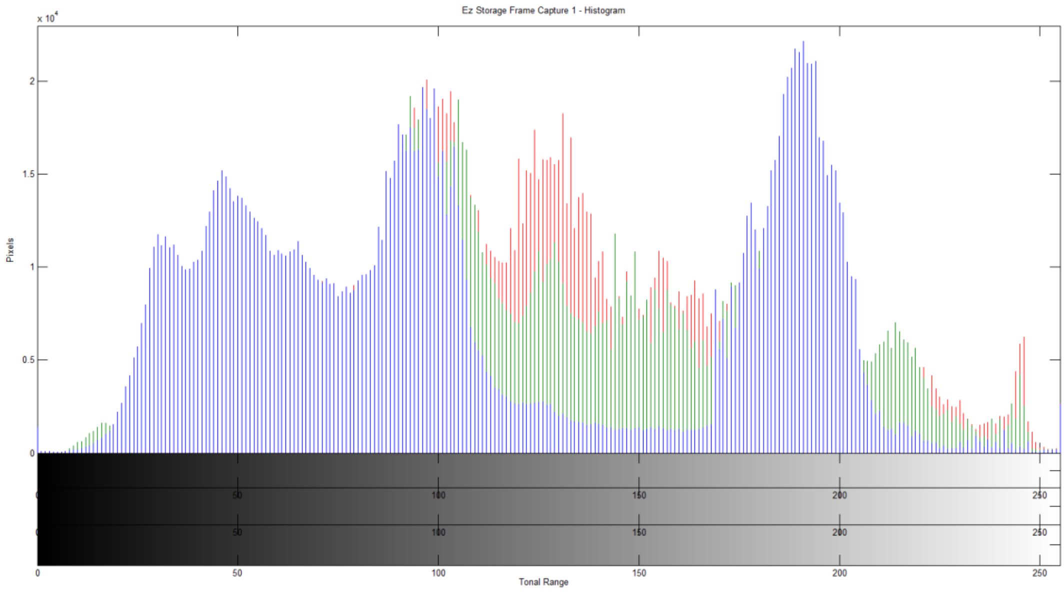

Figure 35 - Histogram of Fig. 34

Figure 36 - Pandaboard Frame Capture 1 – M40 – 1 Camera – 30 fps – 1.5 Mbps

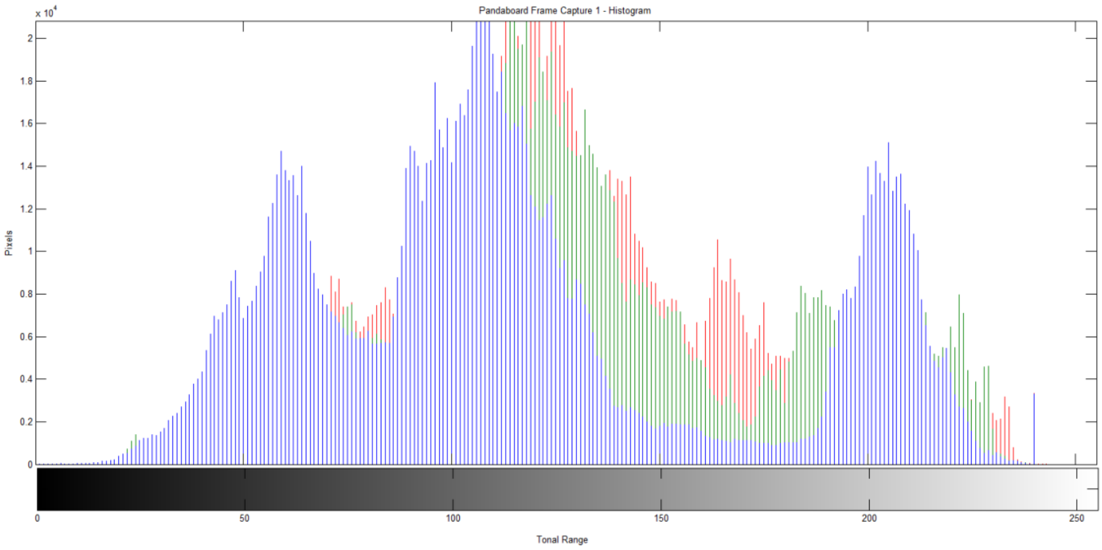

Figure 37 - Histogram of Fig. 36

Figure 38 - Goldstar Onboard Frame Capture 1 – M40 – 1 Camera – 30 fps – 1.5 Mbps

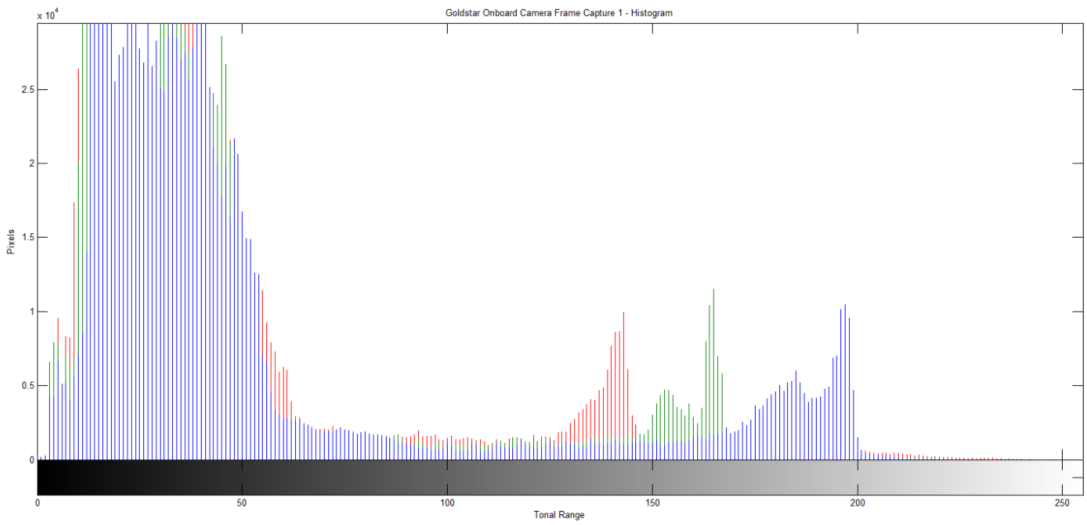

Figure 39 - Histogram of Fig. 38

The motorway (M40) setting shown in the first frame captures attempts to represent a scenario close to a race track environment, where the background doesn't subject the camera to large changes in composition.

Initial observations show a noticeable difference in colour definition between all three devices. The Goldstar device shows a much larger difference. Colour calibration should be investigated.

Barrel distortion can be noticed more evidently in the Ez storage device and Pandboard, further investigations into the effects of changing focal lengths are required. Though this distortion may offer increased angle of view. Further analysis into methods the sensor uses to locate a focus point within the screen should also be assessed, it is unclear whether the camera uses the centre of the image to locate this point or whether it can find such a point anywhere in the frame. Quick observations show a clear difference between the definition of the dash areas in all 3 devices.

Figure 40 - Ez Storage Frame Capture 2 – Wheatley Village – 1 Camera – 30 fps – 1.5 Mbps

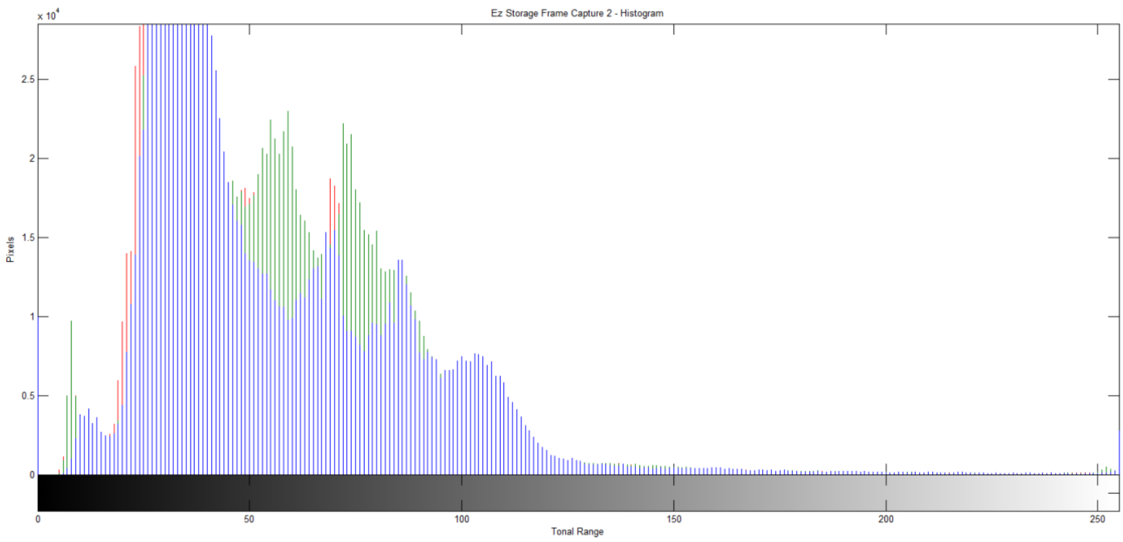

Figure 41 - Histogram of Fig. 40

Figure 42 - Pandaboard Frame Capture 2 – Wheatley Village – 1 Camera – 30 fps – 1.5 Mbps

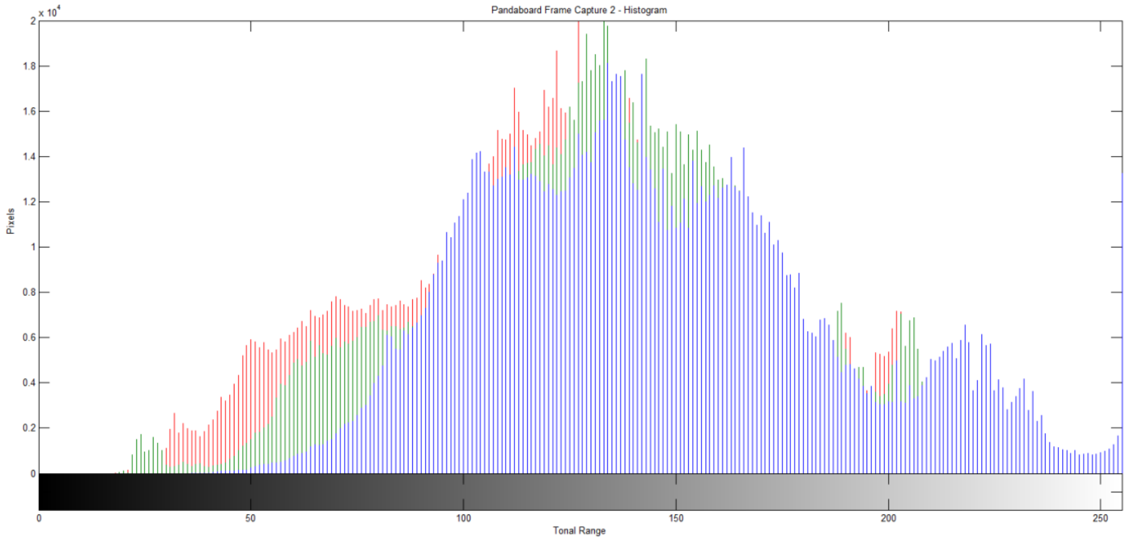

Figure 43 - Histogram of Fig. 42

Figure 44 - Goldstar Onboard Frame Capture 2 – Wheatley Village – 1 Camera – 30 fps – 1.5 Mbps

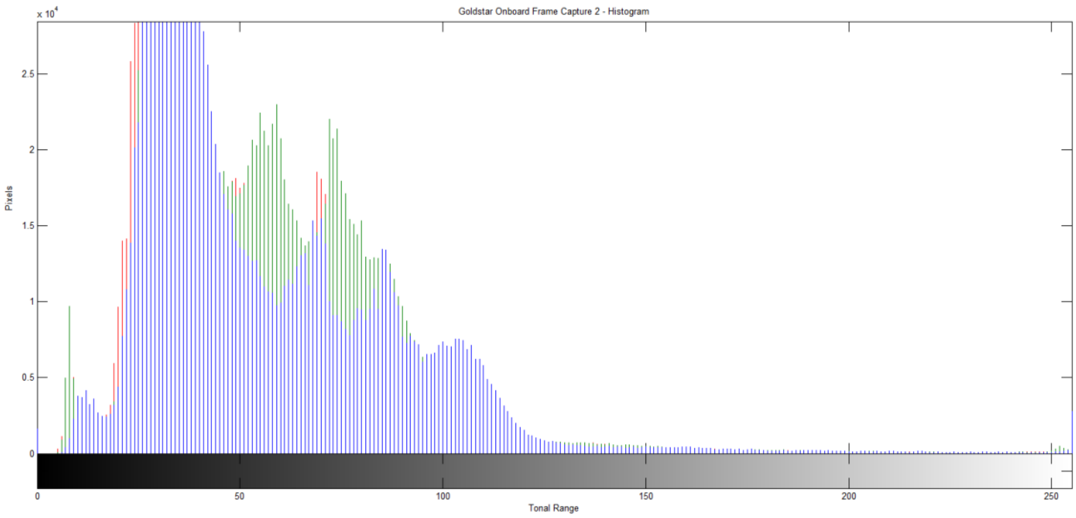

Figure 45 - Histogram of Fig. 44

Figures 40, 42 & 44 show a much busier frame in contract to the first sequence, it is expected this would increase the load on the video encoder leading to less efficient encoding, this has been chosen more to find the limits of the devices. Changing lighting conditions are much more frequent due trees and objects lining the side of the road profile.

All three captures show movement in the frame around the outside of the image, it is thought this is related to encoding efficiency is areas outside of the focal plane of the image. Initial observations indicate image distortion does not have a major effect on this area size.

The Pandaboard capture shows distinct lack of clarity, sharpness and focus within the image, it is thought this relates to the transfer rate of the video, a higher rate would allow for more information within the image to be captured. The dynamic range of colour within the image are also expected to have an affect encoding efficiency.

Histograms presented from Ez storage device show a significant change from an increase in darker regions encoded, whereas the Pandaboard shows a small change toward lighter regions though the clarity of the image is much less, it is thought this again relates to the transfer rate of the video stream. The Goldstar device tends to a similar fashion to that of the Ez storage device with both devices giving a clearer and more defined image.

Throughout the image sequence the Goldstar device also tends toward the lower thresholds of the histogram, whilst the Ez Storage and Pandaboard tend to be more consistent around the mid region supporting initial observations on image darkness characteristics.

Further tests have been undertaken with the Pandaboard at increased transfer rates. Figures 3 & 9 are recorded at 2 Mbps, this was increased for 4 & 10 Mpbs shown in figures 13 & 14.

Figure 46 – Pandaboard – Wheatley Village – 1 Camera – 30 fps - 10Mbps

Figure 47 - Pandaboard - Wheatley Village – 1 Camera – 30 fps - 4Mbps

The higher transfer rates show a much improved image quality, cropped versions of figures 7 & 8 show a clear difference in image clarity. Taking into consideration a slight change in lighting conditions for colour tone, a clear effect of image definition can be seen from the additional information captured.

Figure 48 – Pandaboard - 4 Mbps

Figure 49 – Pandaboard - 10 Mbps

4.1.2.2 Comparison of Device transfer Rates

Average capture rates for each device have been calculated. Both the Pandabaord and Ez Storage devices exhibit similar speeds, whilst they both use the same encoder it is unclear whether they use the same image sensor. This may help explain the difference in picture quality at relatively close transfer speeds. The Goldstar device exhibits a higher rate, it is thought this is down to a possible difference processor architecture and image processing method used.

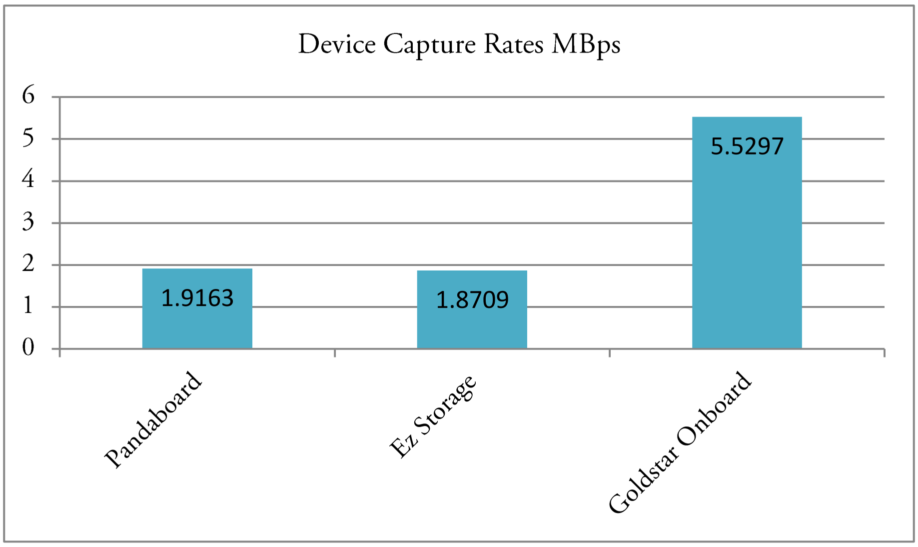

Figure 50 - Device Capture Rates

A slightly deeper analysis has been carried out to understand the relationship between image quality and data transfer rates.

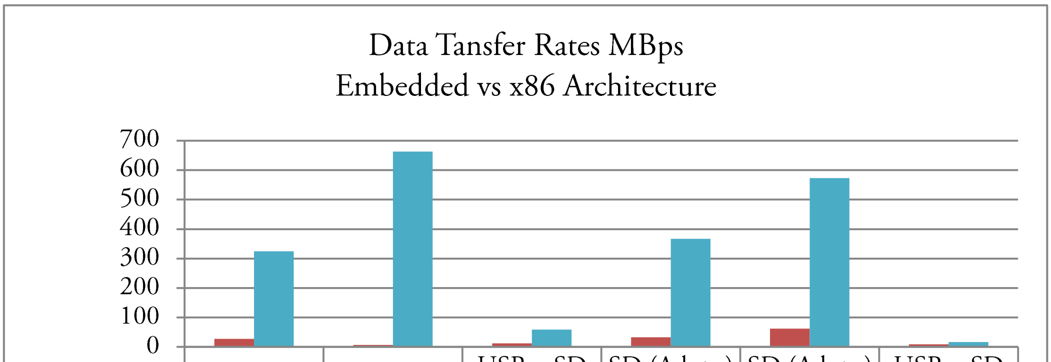

	USB > FS	FS > USB	USB > SD (Adptr.) (1)	SD (Adptr.) > USB (1)	SD (Adptr.) > USB (2)	USB > SD (Adptr.) (2)
Pandaboard	27.4	6.55	12.7	33.3	62	9.33
x86	325	663	59.2	367	573	16.4

Figure 51 - Data Transfer Rates

Bulk Transfer Protocol

A single file of 272 MB was transferred using several different methods. Embedded and x86 based architectures were compared. The file system (FS) to USB method represents most closely how the video is captured from a camera and stored. The uppers limits of USB 2.0 are 480 Mbps (60 MBps).

This test was undertaken to assess the hardware capabilities to stream data up to 10 Mbps (1.25 MBps), as previous tests show this is approximate data rate able to clearly define and capture fast moving object and backgrounds for a given capture.

The Pandaboard capture shows more frames are out of focus for the duration of the capture, the graph indicates these frames are more localised toward areas of the capture where a lot of change between frames is seen, typically areas with changing background alongside objects and vehicles within the foreground. The Goldstar device shows more consistency through the video length.

4.2 Data Acquisition Result Analysis

4.2.1 Testing Outline

A vehicle provided by the RDAC is equipped with sensors on the steering column and brake, throttle pedals. The developed camera device is also installed into the vehicle. Participants undertake the route shown in figure (52).

copyrighted map images removed

Figure 52 – Testing Driving Route

copyrighted map images removed

Figure 53 – Testing Driving Route – Close up

Data acquisition devices are situated close to the CoG of the vehicle, just behind the front seats in front of the middle rear seat.

A calibration run is undertaken before each session and Matlab scripts have been generated to normalize the run data to ensure consistent and fair testing procedures are adopted. Steering brake and throttle inputs are calibrated to full scale deflections before each run.

4.2.2 Steering

We begin by considering the steering wheel displacement data throughout the entirety of a given run. From a steering position deemed neutral, where the heading angle of the wheel direction is the same as the vehicle heading direction. 540° full scale deflection has been measured both clockwise and anti-clockwise of this position. Standard deviations for steering displacement and velocity have been calculated from data gathered for the entirety of the route, table(2).

	Standard Deviation		
Participant	**Displacement (Deg)**	**Velocity (Deg/Sec)**	**RDAC Score**
1	77.57	37.26	3
2	106.99	48.02	2
3	76.60	42.13	2
4	74.19	35.32	3
5	80.69	46.77	3
6	20.41	29.50	3
7	90.54	50.91	3
8	77.06	36.75	2
9	79.67	34.48	2
10	111.46	35.04	3
11	88.60	28.31	3
12	82.03	35.86	3
Average	80.49	38.36	2.67

Table 2 – Steering Displacement and Velocity Standard Deviation with Driving Assessor Scores

Figure (54) shows the tabulated results above graphically.

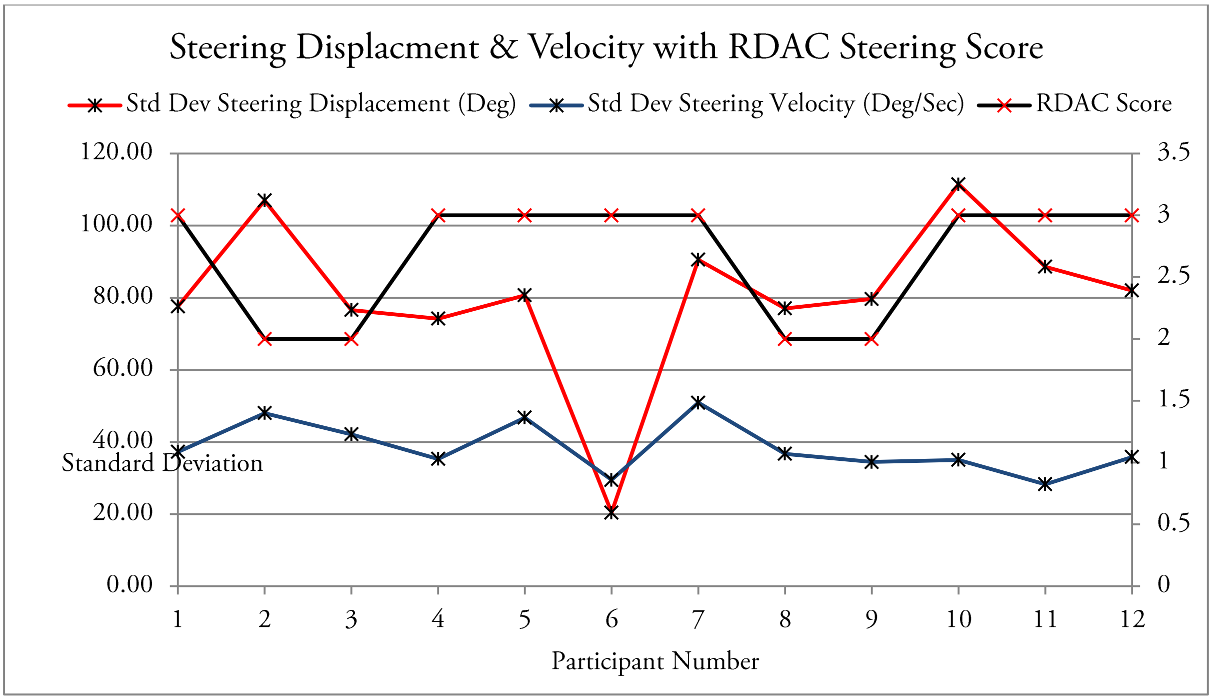

Figure 54 – Steering Displacement and Velocity with Driving Assessor Score

The standard deviation of steering displacements show the variation in the amount of steering used throughout the run, considering a participant undertaking the route without any external environmental influences such as traffic, a low variation would indicate behaviour as average or above average. Steering velocity variation is indicative of the nature of the input. A low standard deviation would be analogous to a smooth, slow rate of change. This again would be considered as average or above average behaviour.

+	1	2	3	4
Exceptionally Good	Good	Acceptable	Poor	Very Poor

Table 3 – 5 point assessment scale

Analogous to a 5 point Likert scale (Garland, 1991), the scores provided by the driving assessor relate to two results on the scale, acceptable(2), poor(3). As the difference is 1 point on the scale it is hard to conclusively say whether the behavioural difference is large or small due to the subjective nature of the scoring. For example a poor score maybe given due to one or maybe two sections of the route driven *"badly"* or the average of the drive conducted in a manner that is deemed slightly less effectively than the previous participant. Further because the assessments have taken place over a timescale in which an average of 6 investigations are conducted over 2 days, the next participants may undertake the drive typically a month later, it is hard to say if for example, a participant was to repeat their drive exactly the same with the same driving conditions whether they would receive the same score or not. Considering participants 1 and 8, exhibiting very similar displacement and velocity variations but have been given scores of poor (3) and acceptable (2) respectively. It is likely these scores may also relate to overall performance, including other factors such as the control of vehicle velocity, throttle and brake control. Assessments with scorings ranging from exceptionally good (+) to very poor (4) would give a clearer indication of behavioural range to correlate steering variation data more accurately.

As the above calculated standard deviations are calculated from the entirety of the route driven, the effects of vehicle heading velocity have not been considered. This is important as vehicle heading velocities throughout a given run range from 60 mph to < 30 mph, yielding not only different performance characteristics with the same steering behaviour but also because erratic steering inputs pose much less of a driving hazard at lower heading velocities. It is possible to normalise the steering data against heading velocity data, though because the heading velocity data is recorded from the GPS, the resolution of which is ≈ 1– 2 Hz, compared to the higher sample rate of the steering potentiometer data (≈ 40 Hz), the accuracy of normalisation yields poor results.

Typically analysis of steering behaviour would orientate around an ideal driving line, where deviations from this line would indicate how well the vehicle was handled for a given road profile/curvature. Using conventional forms of data acquisition GPS position coordinates is the most common way to define a driving line. This is more commonly used to motorsport applications.

Figure 55 – GPS Coordinates – Section F

Figure(55) shows the distribution of coordinates for the section, a point is received approximately every second. Dependant on the speed of the vehicle and its position determines the spread of points, as the speed varies whilst driving an uneven spread of points along the sector can be seen. The distance resolution of the points also maintain ± 15m accuracy for a single receiver (Survey, 2015), meaning the points received may not necessarily be on the line that was driven. To generate an ideal route, not only is this accuracy important but deviations on the driven route are likely to occur due to traffic or environmental influences and this can change for each participant. Furthermore, to perfectly replicate the profile of a given corner a sample rate close to 1 Hz doesn't allow for a high fidelity portrayal for an ideal route, it is possible to calculate the curvature over 3 data points and this could be done with the corner shown above, but if the local points to the central curve on the figure were used, not only would we get a mathematical spline fitted to only 3 –5 points over the whole corner but also, the positioning of the route shows deviation from the map due to GPS distance resolution. This means an ideal route would pass through areas that are not on the road. Interpolation of the data would allow for an increased number of points to calculate a profile from, but this does not increase the resolution of the data or overcome the errors mentioned above. Instead the route is divided into 7 sections for the resultant analysis, allowing for independent section consideration figure (56).

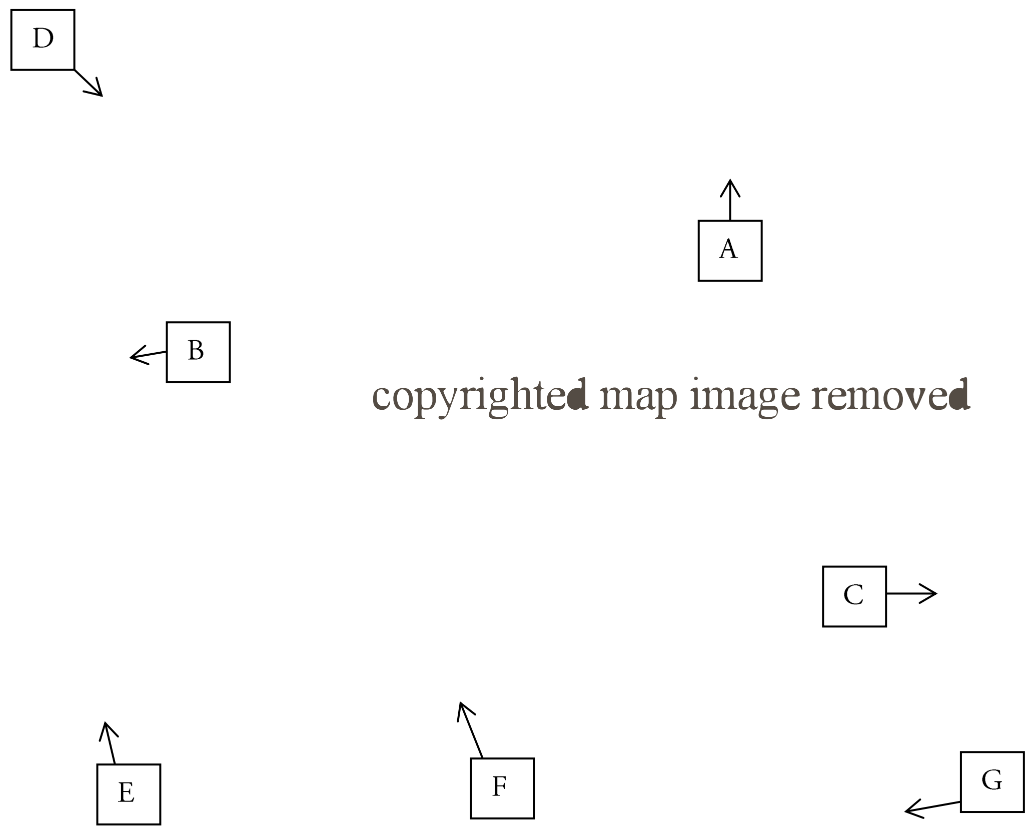

Figure 56 – Driving Route Sections

The 7 sectors have been labelled A, B, C, D, E, F and G. Sections A, B and C are used for the straighter areas of the drive where lower steering displacements are expected. The remaining sections, D, E, F and G are junctions or corners demanding steering control where higher steering inputs are expected.

Instead the sectors will used be for analysis of the data statistically, this allows for comparison of each driver fairly within the same range of longitude and latitude coordinates and this method also does not necessitate the need to rely on GPS accuracy or sample rate. The data for each sector is split into new variables using Matlab, where these new variables can be used to divide total run data such as steering and braking. Figure (57) shows the an example steering trace for the above sector F driven by a participant.

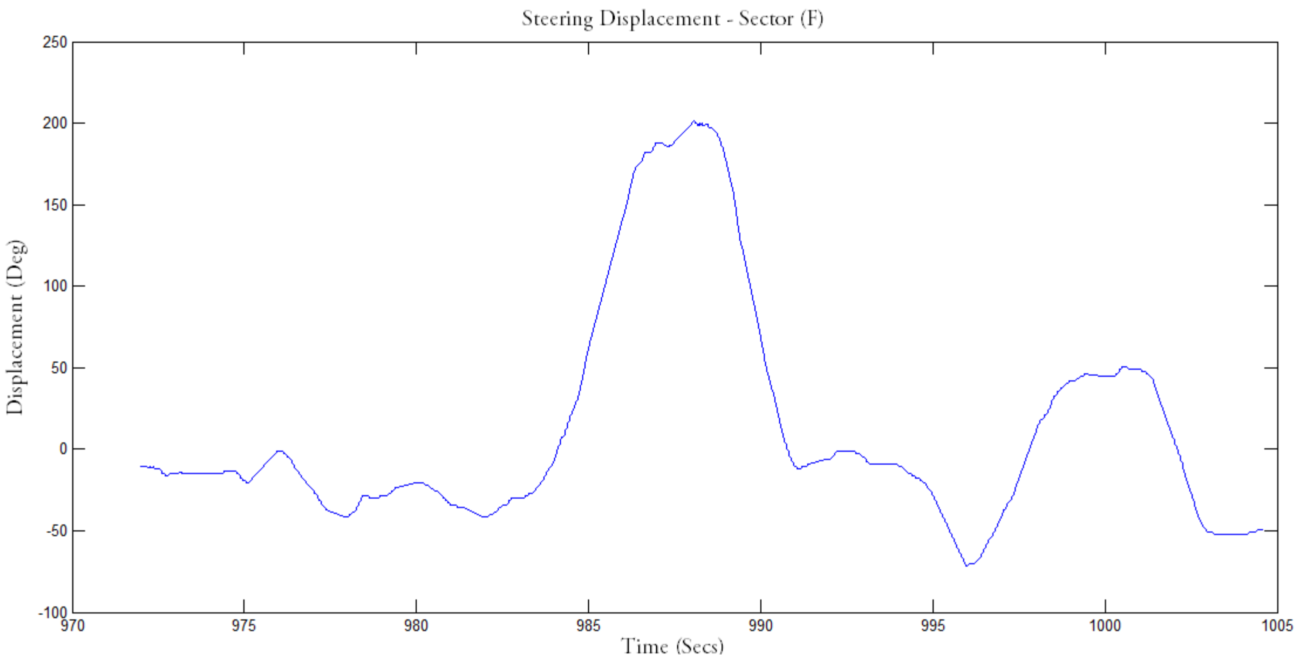

Figure 57 – Steering Displacement – Sector F

This data is then gathered for each participant and the variation of displacement used to calculate the standard deviation to find the amount of steering used. A plot of standard deviation for each participant for each section can then be made, figure (58).

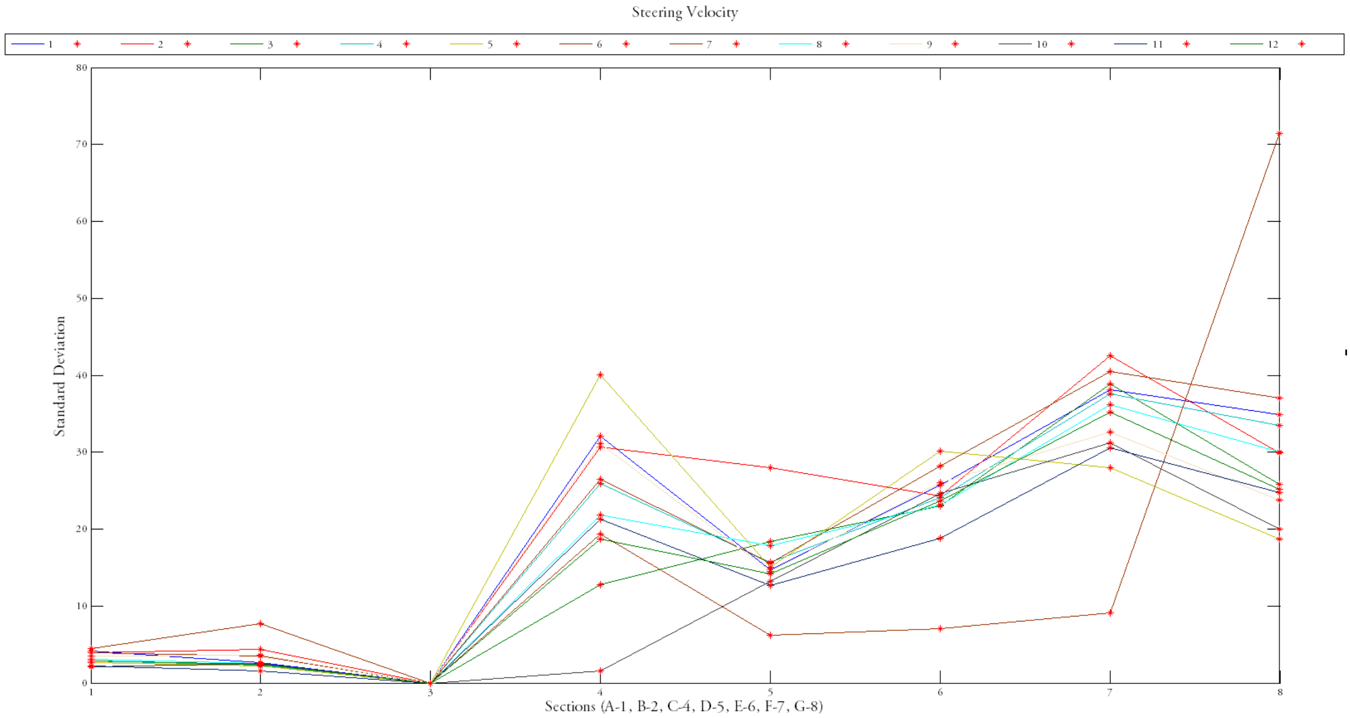

Figure 58 – Steering Velocity Section Standard Deviation

Sections 1, 2 and 4 are straighter stretches of road with 5, 6, 7 and 8 being defined cornering areas of the route. Noticeable variation can be seen throughout the sections, straighter sections of the route indicate less variation apart from section C.

Conducting the same analysis with steering velocity yields much similar data point dispersion for the driving sections. It should be noticed participants do not tend to exhibit consistent steering variation throughout the run, that is, for one participant exhibiting high standard deviation for the first section does not consistency hold this high variation relative to the rest of the group throughout the run. As there does not appear to be a strong correlation between steering behaviour for cornered and straight road sections, analysis for each section should be adopted to help further understand the characteristics for each defined section. A further section 3 shown on the graphs is where a parking manoeuvre is conducted on the route, this is to be ignored for this study. It is now reasonable to introduce scorings provided by the assessor.

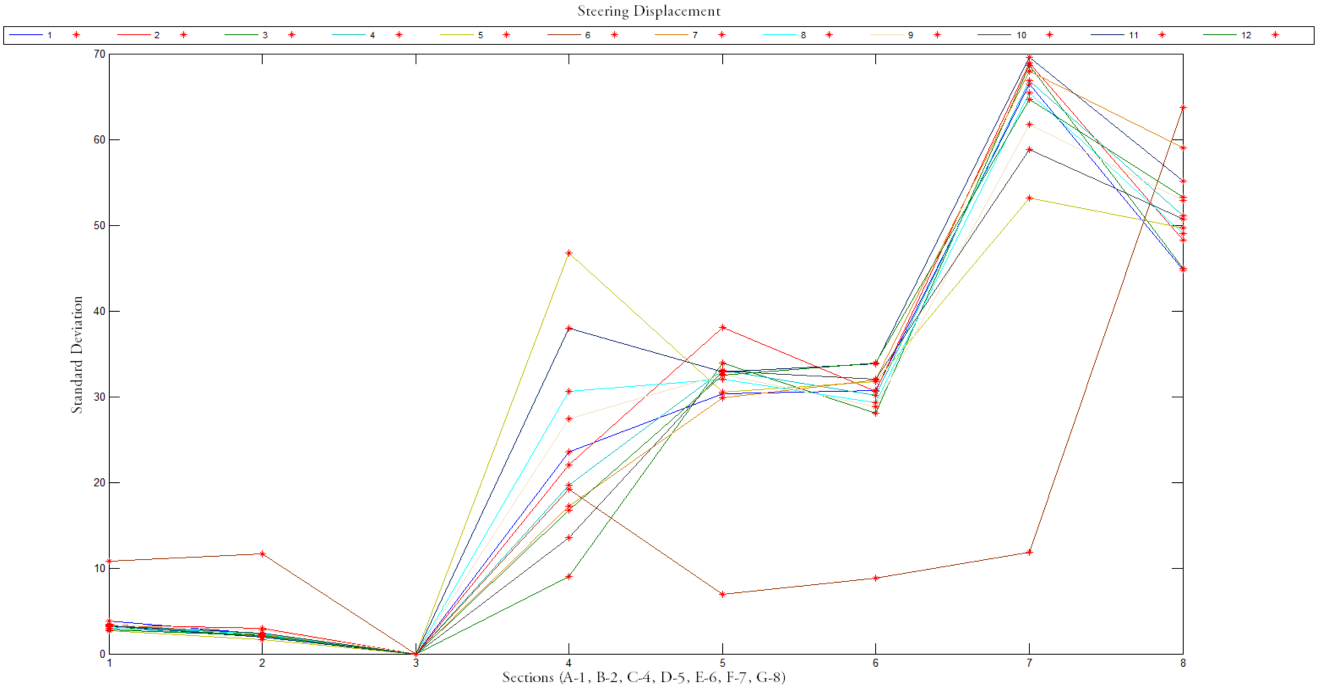

Figure 59 – Steering Displacement Section Standard Deviation

The following 7 figures show the standard deviation of each participant for the defined driving sections compared to results given by the driving assessor.

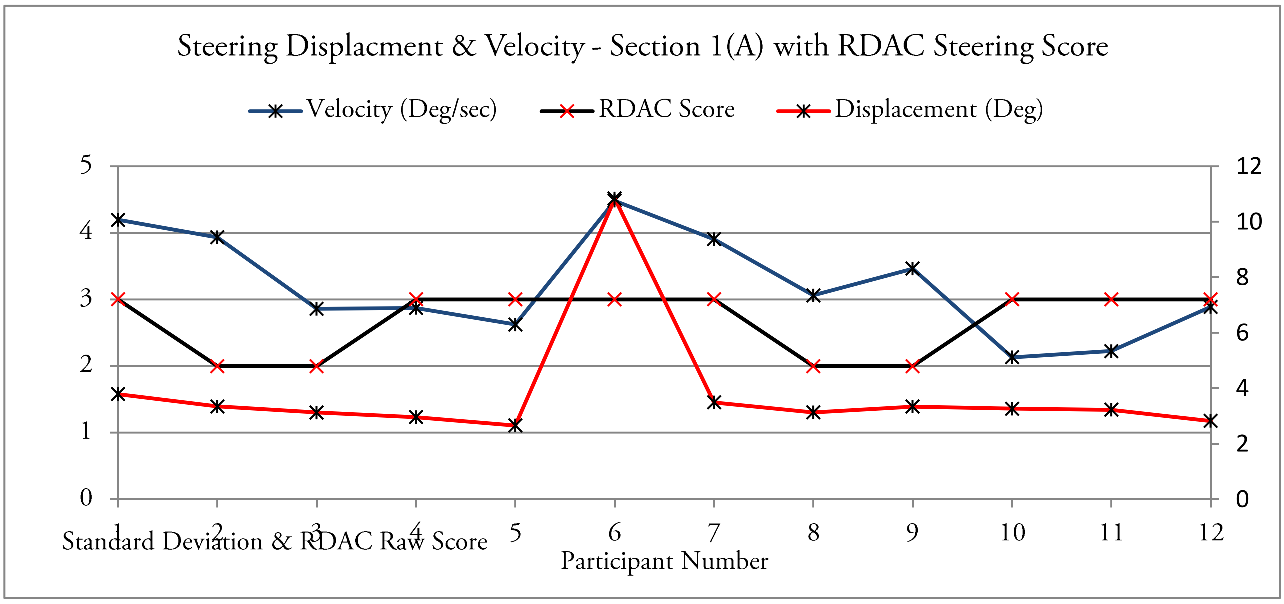

Figure 60 – Steering Displacement, Velocity and Driving Assessor Scores Section 1(A)

Section 1 Displacement			Velocity	
Average	3.8314		Average	3.2193
SD High	6.0569		SD High	3.9875
SD Low	1.6059		SD Low	2.451

Table 4 – Figure 60 Averages and Standard Deviations

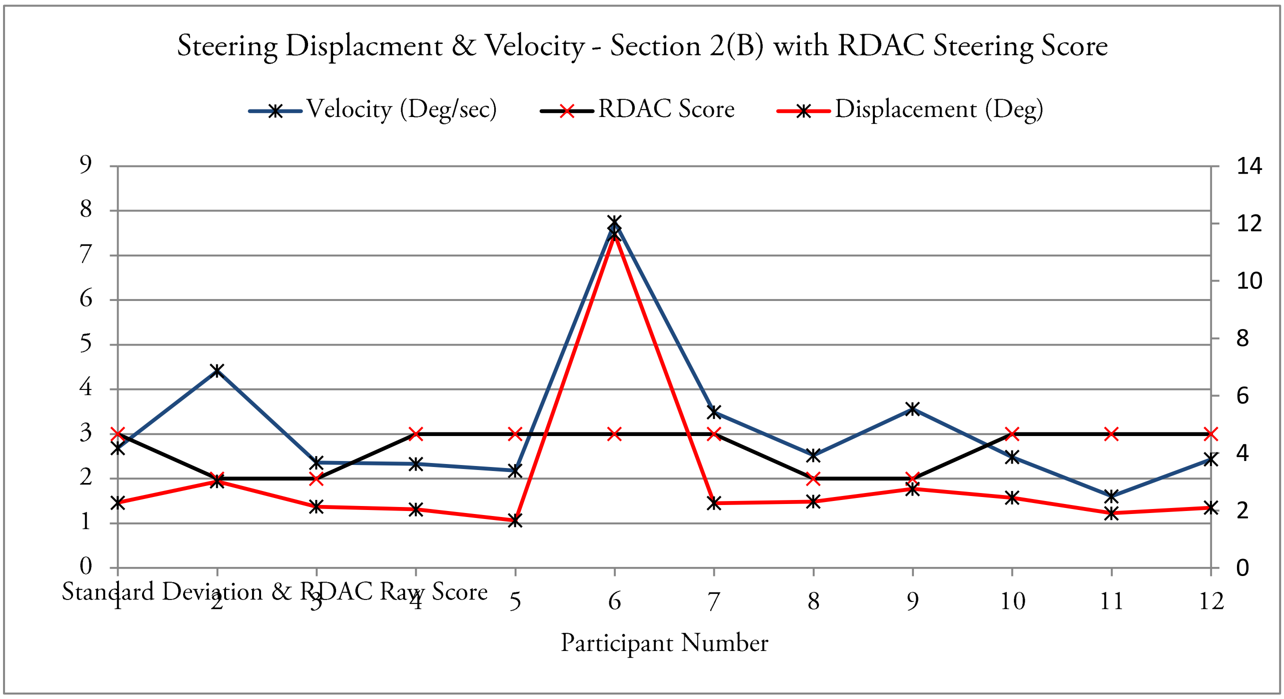

Figure 61 - Steering Displacement, Velocity and Driving Assessor Scores Section 2(B)

Section 2				
Displacement			Velocity	
Average	3.0442		Average	3.1499
SD High	5.7691		SD High	4.7785
SD Low	0.3193		SD Low	1.5214

Table 5 – Figure 61 Averages and Standard Deviations

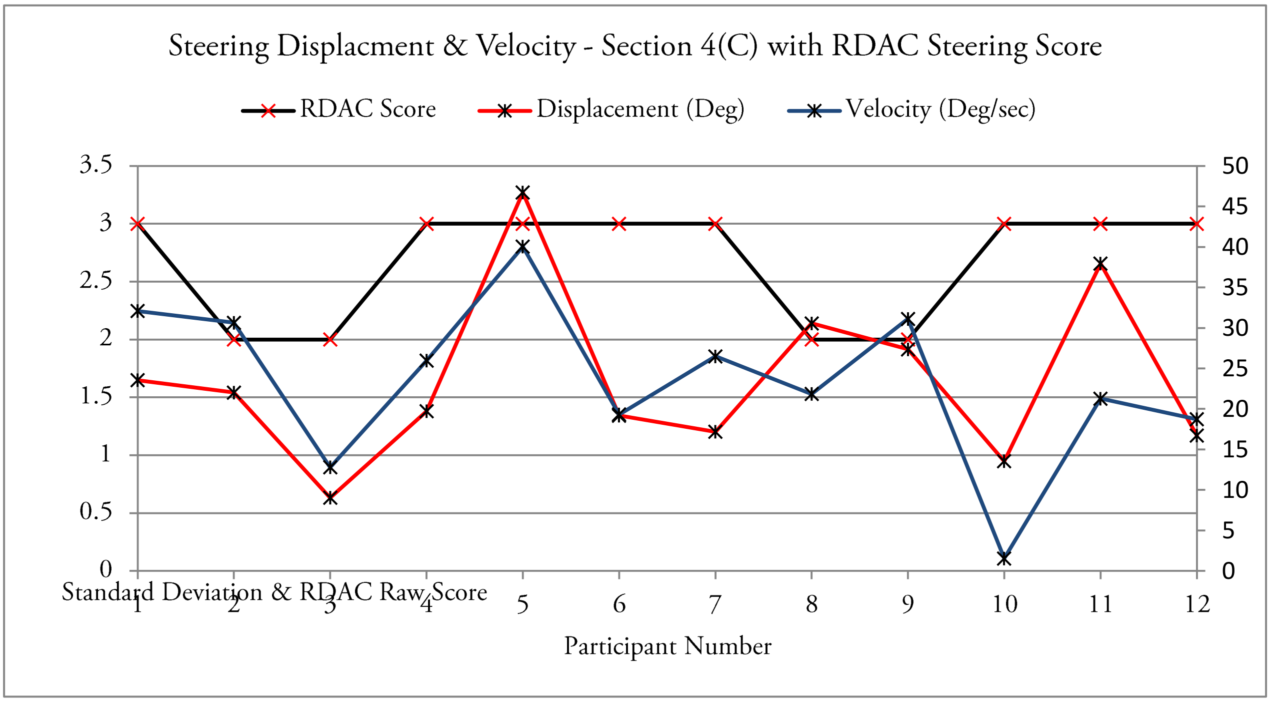

Figure 62 - Steering Displacement, Velocity and Driving Assessor Scores Section 4(C)

Section 4				
Displacement			Velocity	
Average	23.629		Average	23.49
SD High	34.249		SD High	33.559
SD Low	13.008		SD Low	13.42

Table 6 – Figure 62 Averages and Standard Deviations

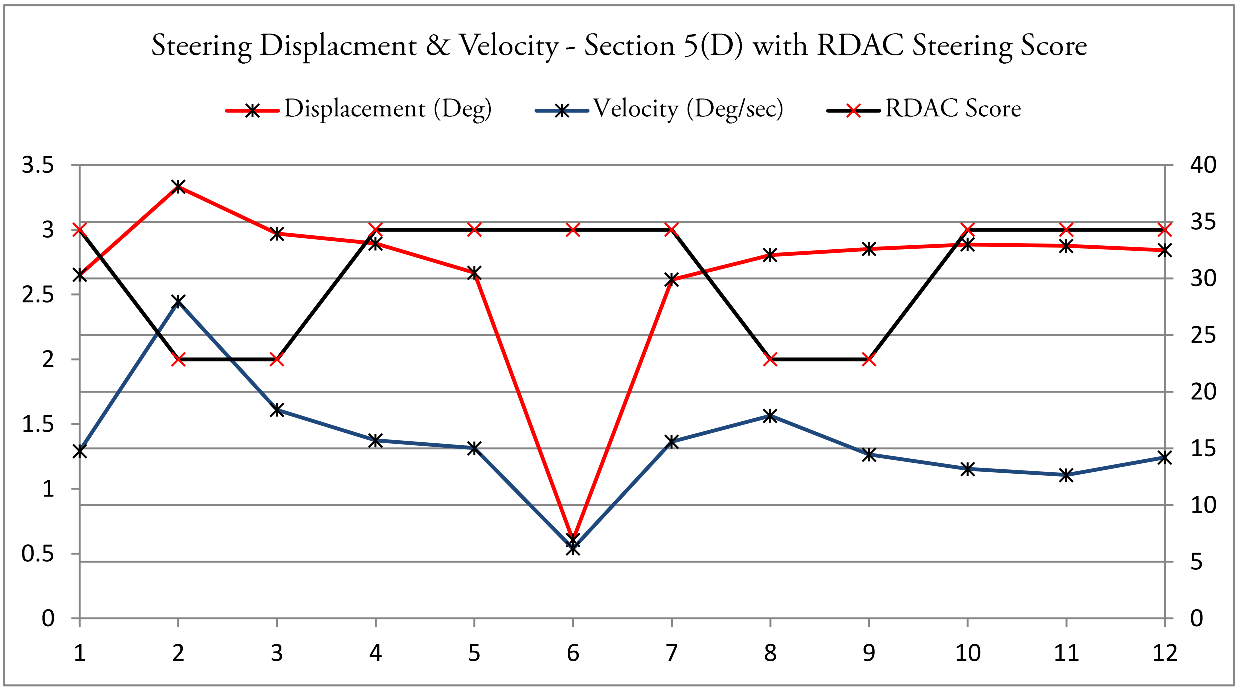

Figure 63 - Steering Displacement, Velocity and Driving Assessor Scores Section 5(D)

Section 5					
Displacement			Velocity		
	Average	30.473		Average	15.493
	SD High	38.192		SD High	20.474
	SD Low	22.755		SD Low	10.512

Table 8 – Figure 63 Averages and Standard Deviations

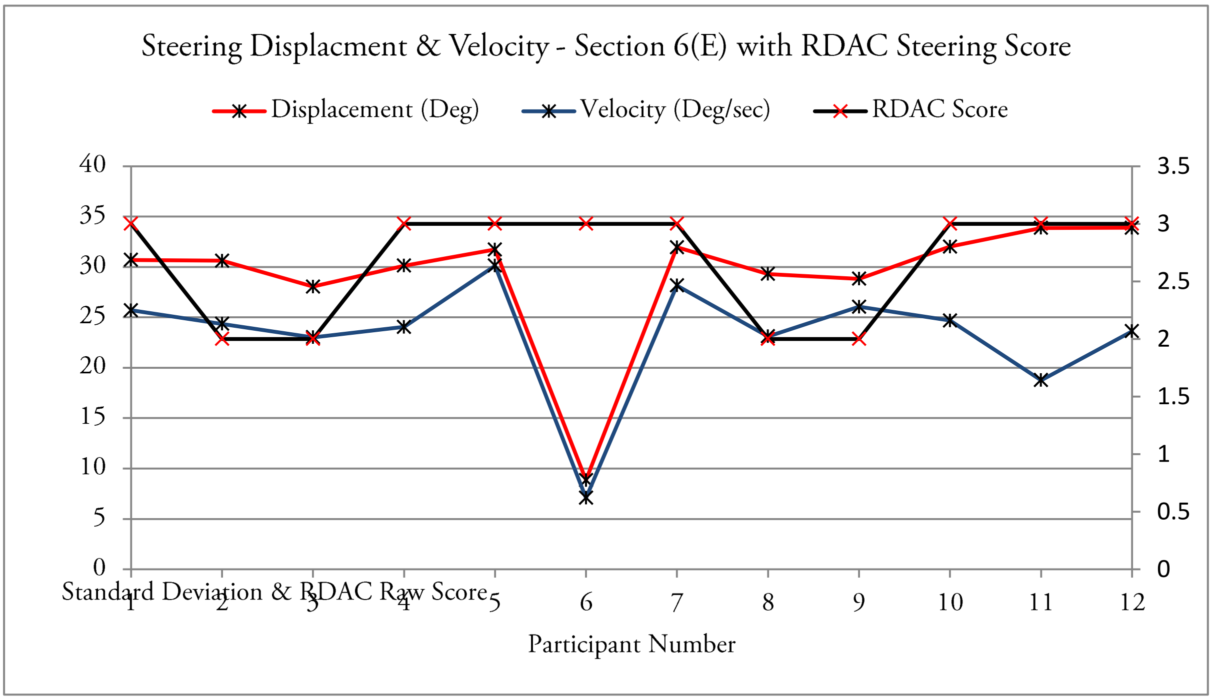

Figure 64 - Steering Displacement, Velocity and Driving Assessor Scores Section 6(E)

Section 6					
Displacement			Velocity		
	Average	29.161		Average	23.226
	SD High	35.81		SD High	29.031
	SD Low	22.513		SD Low	17.421

Table 7 – Figure 64 Averages and Standard Deviations

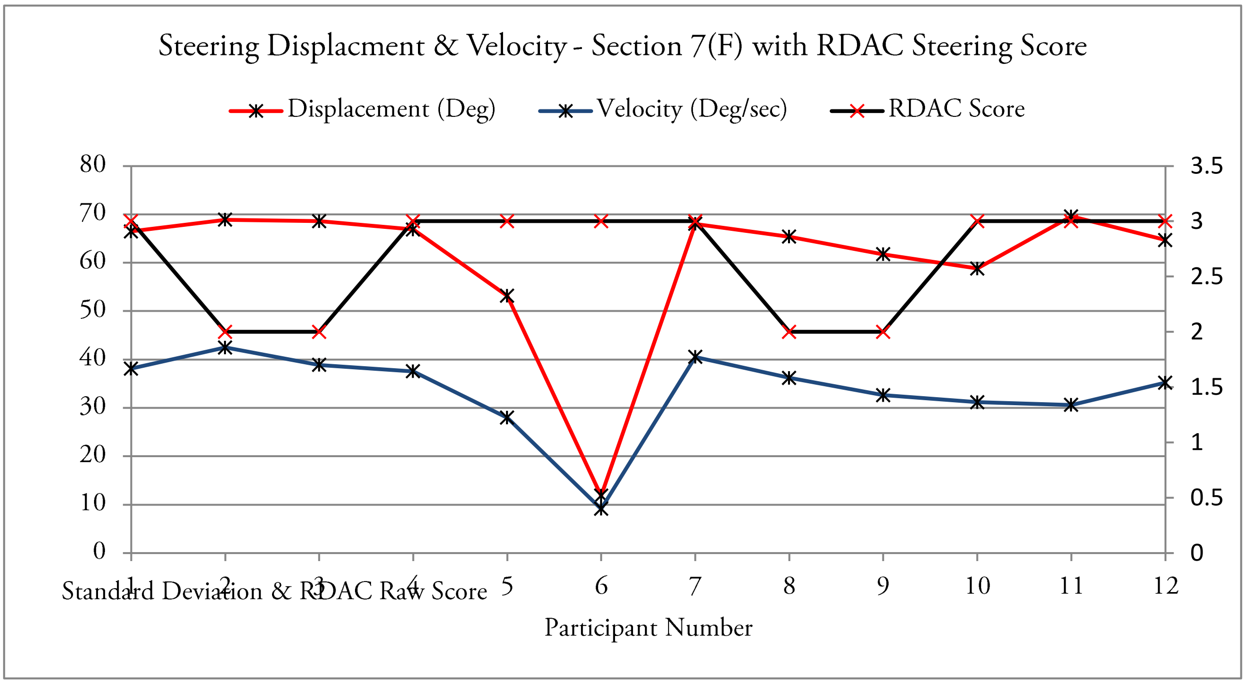

Figure 65 - Steering Displacement, Velocity and Driving Assessor Scores Section 7(F)

Section 7					
Displacement			Velocity		
	Average	60.334		Average	33.37
	SD High	76.339		SD High	42.136
	SD Low	44.328		SD Low	24.604

Table 9 – Figure 65 Averages and Standard Deviations

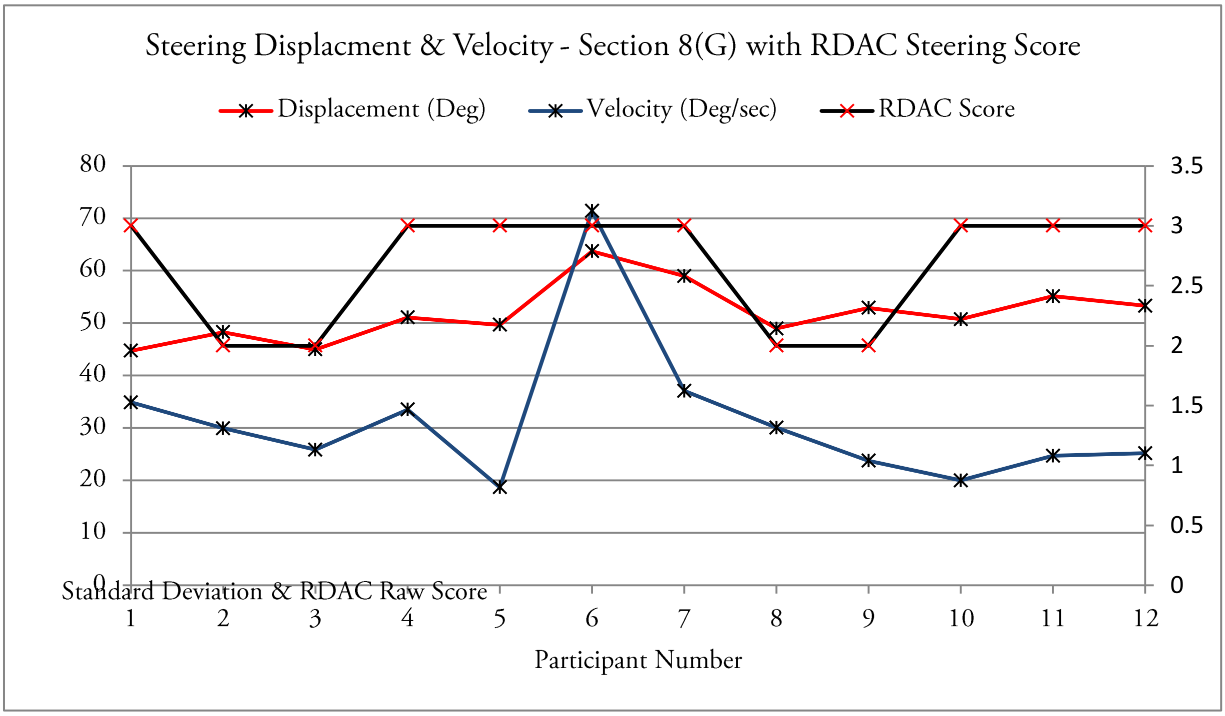

Figure 66 - Steering Displacement, Velocity and Driving Assessor Scores Section 8(G)

Section 8					
Displacement			Velocity		
	Average	51.875		Average	31.25
	SD High	57.36		SD High	45.12
	SD Low	46.389		SD Low	17.38

Table 10 – Figure 66 Averages and Standard Deviations

It is clear to notice a higher variation of data points in sections C, D, F and G. Where C is the only straight section out of the 4 sections, further inspection upon this area of the drive highlights the presence of chicanes and traffic calming measures with the addition of an increased amount of parked vehicles roadside compared to the remainder of the route. The higher usage of steering is expected at < 40 mph.

The sectioned data exhibits a low correlation with scorings provided by the RDAC. From the data recorded by the data acquisition system, participant 6 exhibits the highest variation through sections A and B with the lowest variation in section D, E and F, with variation between 5 and 20 Deg displacement and also 5 and 20 Deg/Sec steering velocity. Though this participant shows a lack of correlation with the overall group, the participant maintained the most consistent behaviour throughout. Section G the participant shows the highest deviation, observing comments from the assessor, the participant has been noted with sometimes showing high heading velocity into a corner. The variation on section G may relate to corrective steering with high velocity on the approach to the junction.

Taking into consideration the human elements and subjective nature inherent in the assessor scorings and that these scores are more likely to be relative to heavy or light traffic conditions and also weather dependant, it is hard to draw clear conclusions between strictly only steering data. The above results show for steering displacement that an average of 87.5% of the participants exhibited displacements of that below the upper standard deviation boundary with 91.7% above the lower boundary. For steering velocity the respective values are 91.7% and 89.6%. 66.7% of the participants scored poor (3) by the driving assessor. The analysis gives good confidence for characterising benchmarks for the total number of participants, though further investigation should be made for correlation with the driving assessor scores. To help further understand how the drive was conducted the remaining driver inputs, brake and throttle, should be inspected. Table (11) shows the results provided by the assessor for steering.

Participant	Score	Comments
1	3	much too close to the left hand side
2	2	n/c
3	2	n/c
4	3	choppy at corners
5	3	sharp steering action at lane changes
6	3	occasionally fast into corners and through lines of parked cars (diving in and out)
7	3	Jerky movements and difficulty maintaining a consistently straight line when distracted or focusing on other tasks.
8	2	n/c
9	2	n/c
10	3	right hand slow on the steering wheel at junctions
11	3	Wandering in lane caused by staring ahead instead of moving eyes around
12	3	harsh steering on bends caused by remaining on power as enters

Table 11 – Driving Assessor Steering Results

4.2.3 Braking

Each participant is required to undertake an emergency stop manoeuvre during the driving run. Whilst driving, the assessor will indicate when the participant can be expected to perform the manoeuvre, once deemed safe the assessor will raise his hand and ask the driver to stop in the shortest time possible. A button trigger has been created where the assessor is required to generate an input at the same time as executing the command for the driver to stop, the use of this trigger allows for the identification of the event within the data set and also the reaction time of the driver. The following table shows the reaction time taken for each participant to initiate braking.

Participant	1	2	3	4	5	6	7	8	9	10	11	12
Delta (Secs)	0.304	0.224	N/I	0.36	0.44	0.496	0.464	0.432	0.44	N/I	0.436	0.484

Table 12 – Emergency Stop Reaction Times

*N/I = No trigger input

Driver 2 exhibits the fastest reaction time of 0.24 Secs, while driver 6 shows the longest time difference, 0.496 Secs. An average time of 0.408 Seconds has been calculated with a standard deviation of 0.0863 Secs. The following graph shows the data spread with the average line (red) and the upper and lower standard deviation limit lines (blue).

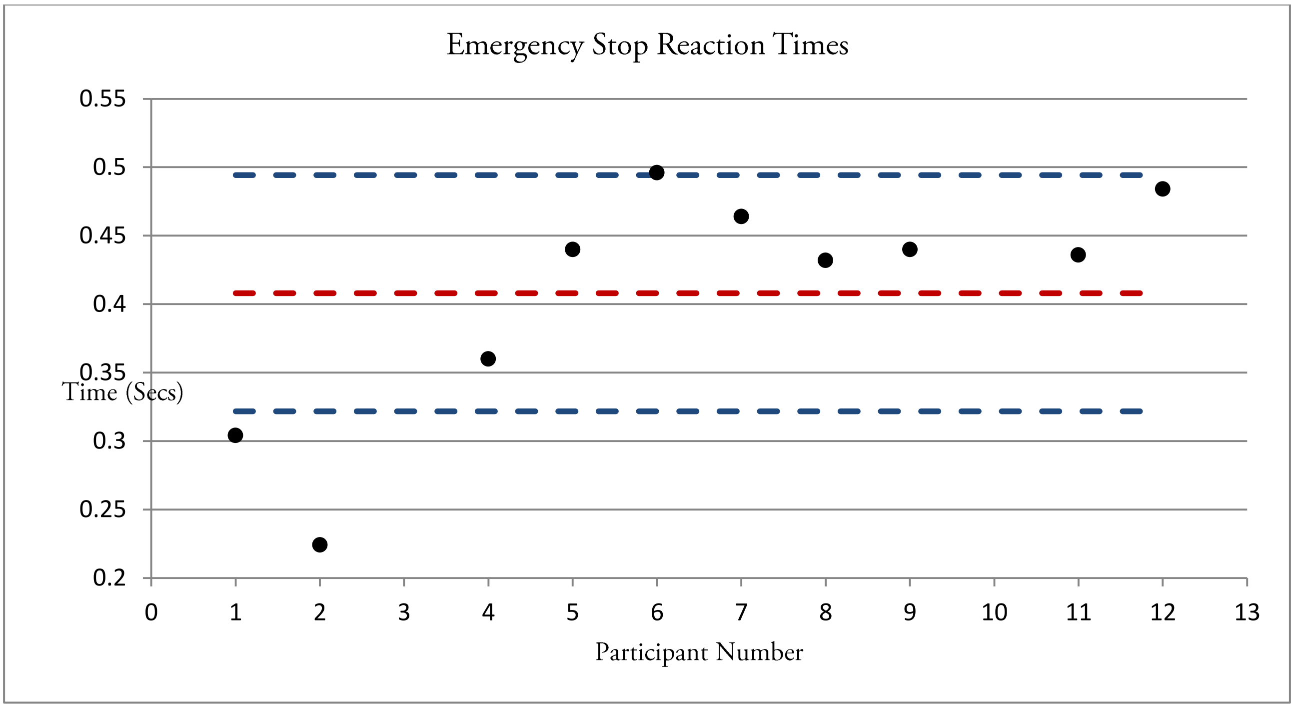

Figure 67 – Emergency Stop Reaction Times

To fully understand how effectively the event was conducted further information is required on how the brake input was used. In an emergency stop drivers should be adopting aggressive use of the brake. We can look at the time taken for each driver to reach their maximum brake input from the time it was initiated. Table (13)

Participant	1	2	3	4	5	6	7	8	9	10	11	12
Time (Secs)	0.92	3.212	N/I	0.54	1.38	0.708	1.216	1.348	0.344	N/I	0.696	0.904
Max Pressure (%)	76.7	92.7	N/I	71.2	112.6	124.4	120.3	85.6	37.2	N/I	73.7	82.6

Table 13 – Maximum Brake Input Time

Driver 2 shows the slowest time taken to reach maximum brake pressure whilst driver 9 was the fastest. Driver 6 exhibited the highest brake input with driver 9 showing the lowest. The following graph (68) shows the difference between their reaction time and the time taken to reach the maximum input displacement. Driver 2 exhibited the fastest reaction time but was by far the slowest to reach their maximum input, whilst driver 9, the fastest to reach their maximum input, had one of the slowest reaction times (0.44 Secs) but actually only took 0.344 Secs to hit their maximum.

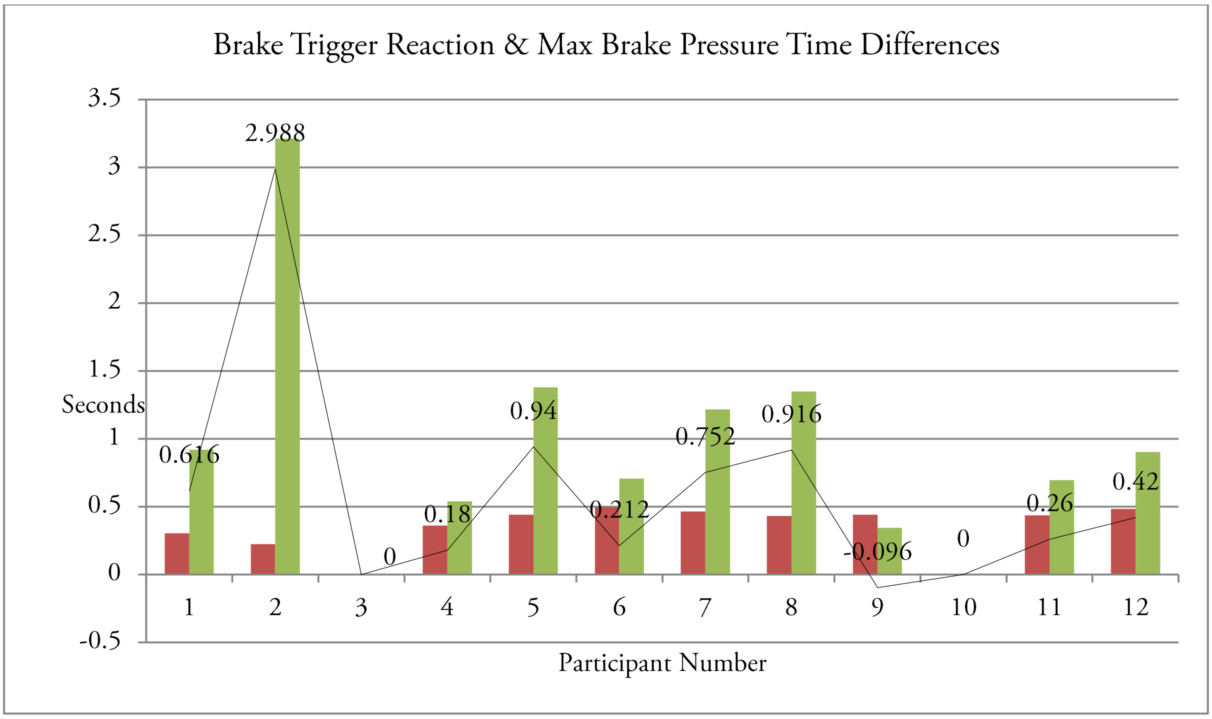

Figure 68 – Brake Reactions and Maximum Input Time Differences

Though this is starting to show an understanding of characteristic behaviour, generating benchmarks for the better and lesser limits of event effectiveness is still difficult to obtain. We do have a good amount of information now on how each driver conducted their input but due to the nature of the emergency stop the event can only be considered completed when the vehicle reaches zero velocity. The time taken from the driver to initiate the brake and the vehicle to cease moving is calculated and shown in Table (14).

Participant	1	2	3	4	5	6	7	8	9	10	11	12
Event Time (Secs)	2.148	3.12	N/I	2.872	2.088	1.864	1.732	*	*	N/I	*	*

Table 14 – Brake Response Times

*= Data Error

Due to the poor resolution of the vehicle speed, accelerometer data has been used to calculate the time taking for vehicle velocity to reach zero. Due to the inherent nature of accelerometer data being noisy, there are many application specific filtering techniques adopted. A low pass Butterworth filter has been used in this study. Unfortunately data from participant numbers 8,9,11 and 12 has been deemed erroneous due to high signal to noise ratios and sufficient calculation of resting accelerations and velocities would affect results.

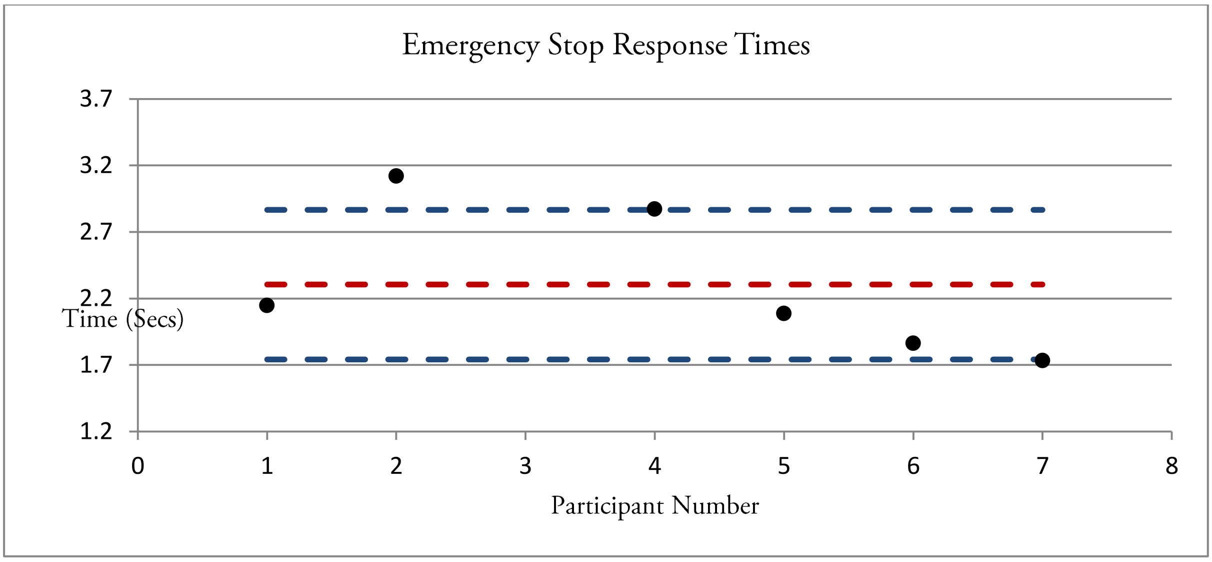

Figure 69 – Brake Response Times

Driver 7 exhibited the fastest event time of 1.732 Secs where driver 2 took the longest, 3.12 Seconds. Driver 2 also showed the slowest time to reach maximum brake pressure but was the fastest to react to the event trigger. Though again due to the vehicle velocity results the heading velocity at which braking begun is not known the time taken for a given driver to stop at 20 mph would be faster than at say 40 mph. The driving assessor's comments relate more to the time taken to begin braking and nature of the input, i.e aggressive or mild. The input percentage has been calculated, 3 participants show percentiles above the deemed 100% from calibration. Calibration errors have been investigated, though because the calibration routines were undertaken with the vehicle stationary at idle engine speed after the engine has not been running for at least 20 minutes, compliance within the braking system may exhibit higher impedance compared to when the emergency event, where the brake has been used more constantly over the previous 20 minutes with higher engine speeds. The highest percentile recorded is 124.4%, the calibration displacement recorded for each calibration routine was 45mm. The maximum input seen relates to a displacement increase of 10.98mm yielding 55.98mm. This has been deemed acceptable as measurement of variation in parameters such as braking fluid viscosity and material expansion within the system are currently out of the scope of this study.

It is reasonable now to compare the results against the ones provided by the assessor, table(15) shows the RDAC provided results.

Participant	Score	Comment
1	3	Sometimes Sharp
2	3	leaves braking late
3	2	n/c
4	3	need to brake sooner
5	3	Sometimes hard due to following too close and lack of forward planning
6	3	very slightly late on approaching hazards
7	2	n/c
8	2	n/c
9	2	n/c
10	2	n/c
11	2	n/c
12	3	Late braking caused by rushing and poor planning

Table 15 – Braking Driving Assessor Results

+	1	2	3	4
Exceptionally Good	Good	Acceptable	Poor	Very Poor

n/c = No Comment Provided

Comments have only been provided for participants where a rating of (3) poor has been awarded, the data from these poor scoring runs is to be considered against the remaining participants. Initial consideration uses the reaction times with the calculated average and standard deviations.

Average – 0.408 Secs

Standard Deviation – 0.0863 Secs

Participant	1	2	3	4	5	6	7	8	9	10	11	12
Delta (Secs)	0.304	0.224	N/I	0.36	0.44	0.496	0.464	0.432	0.44	N/I	0.436	0.484

Table 16 – Brake Reaction Times

From the comments provided by the driving assessor all participants excluding 1 and 5 have been considered exhibiting late brake behaviour, where 1 and 5 have been noted as having sharp braking inputs. Using the calculated average it can be seen that participants 2 and 4 exhibit a reaction input faster than that of the average. Though observing table(16) drivers 2 and 4 do have the slowest time taken for the vehicle to reach zero velocity.

This shows that the calculated average has some relative consistency with observations made by the assessor and can be used as an initial benchmark for an acceptable reaction time. The average total event time taken is 2.304 Secs with 2 and 4 being the only drivers to take longer than the average. It is reasonable now to suggest observations made by the assessor reflect the total emergency stop performance and both reaction time and response time data highlight a good correlation that can be used for benchmarking the event.

4.2.4 Throttle

Compared with investigating brake behaviour there isn't a specific event or manoeuvre defined to assess effectiveness of use as in the case of braking. Instead throttle behaviour must be assessed for the entirety of the run, more specifically each section. Considering the nature of driving on the road a smooth and controlled approach to vehicle control is ideal, this relates heavily the heading velocity control which inherently relates to the nature of the throttle input.

Initially we will look at section A, the A 40. Due to the long constant speed nature of the section, smooth throttle nature is ideal negating external influences, the maximum throttle pedal input velocities for each participant are shown below.

Average – 0.001289 (%/Sec)

Standard Deviation – 0.000693 (%/Sec)

Participant	1	2	3	4	5	6	7
Pedal Vel (%/Sec)	0.001205	0.000579	0.002202	0.000752	0.00113	0.001783	0.002329

	8	9	10	11	12
	0.001769	0.000525	0.00032	0.001939	0.000942

Table 17 – Throttle Pedal Velocity

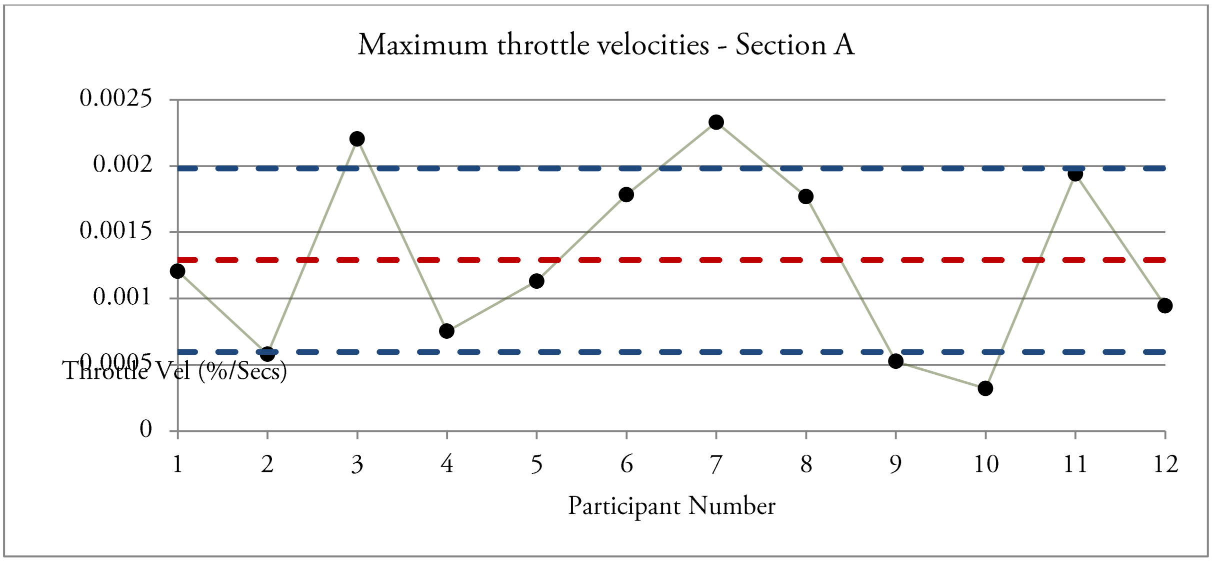

Figure 70 – Maximum Throttle Velocities

As with the braking analysis the average and standard deviation upper and lower boundaries have been calculated. Participants 3 and 7 show to have exhibited high velocities indicative of aggressive or sharp behaviour, as the smoothest velocity yields better control the lower boundary is not as of such importance compared to the upper boundary but it should be noted participants 9 and 10 show to have the lowest velocities, indicative of smooth usage. The remaining sections have also been considered and are shown below. Figure(71) shows throttle pedal velocities for the longer, straighter sections where smooth usage is more desirable than other areas of the route. Figure (73) shows the remaining areas of the route where higher steering inputs are required, meaning increased throttle usage is likely, though in all of the sections of the route smoother the pedal usage is more ideal.

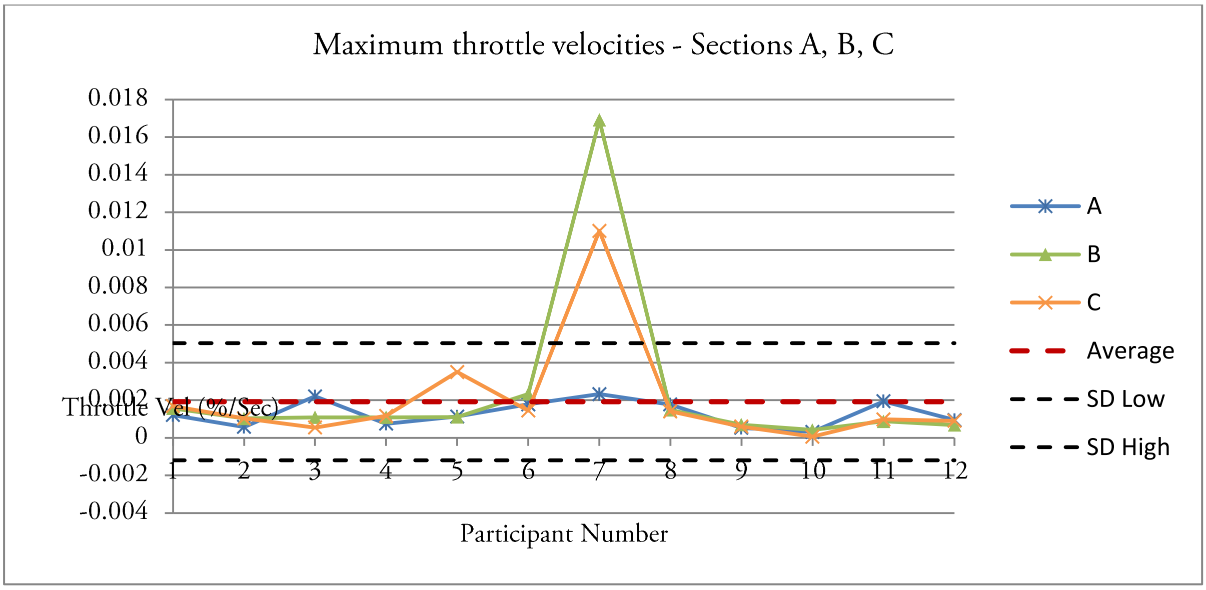

Figure 71 – Maximum Throttle Velocities Sections A, B and C

Throughout the sections shown in the above figure(71) participant 7 exhibits quite aggressive throttle inputs, is it unlikely that these results are due to an external influence on one part of the drive due to repetitive high variation through sections B and C. Most participants show quite low variations about the average where most tend to exhibit smoother usage closer to the average than the standard deviations boundaries.

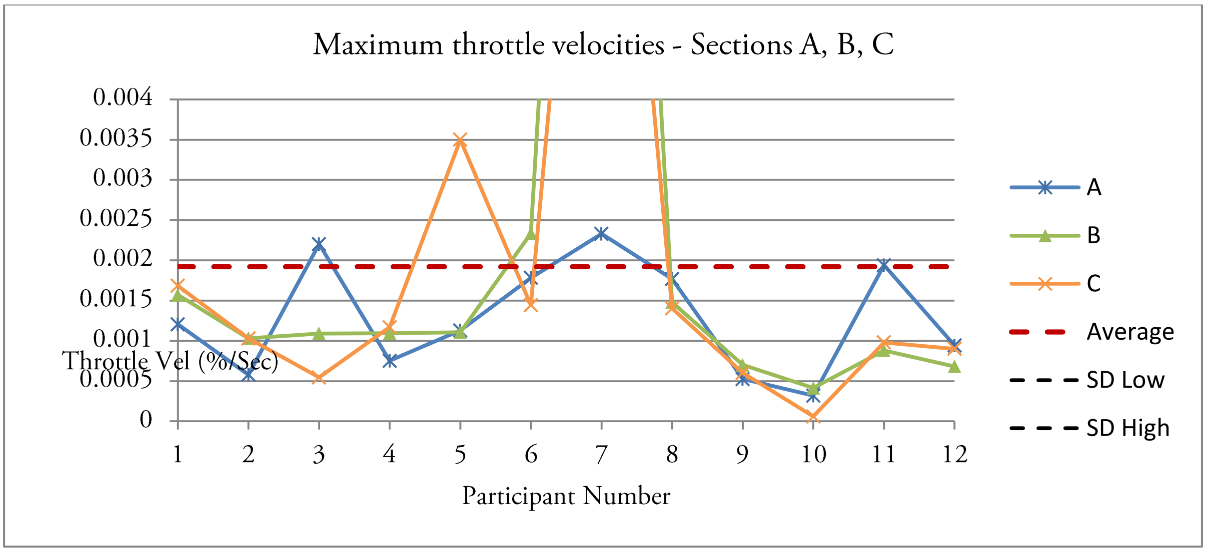

Figure 72 - Maximum Throttle Velocities Sections A, B and C

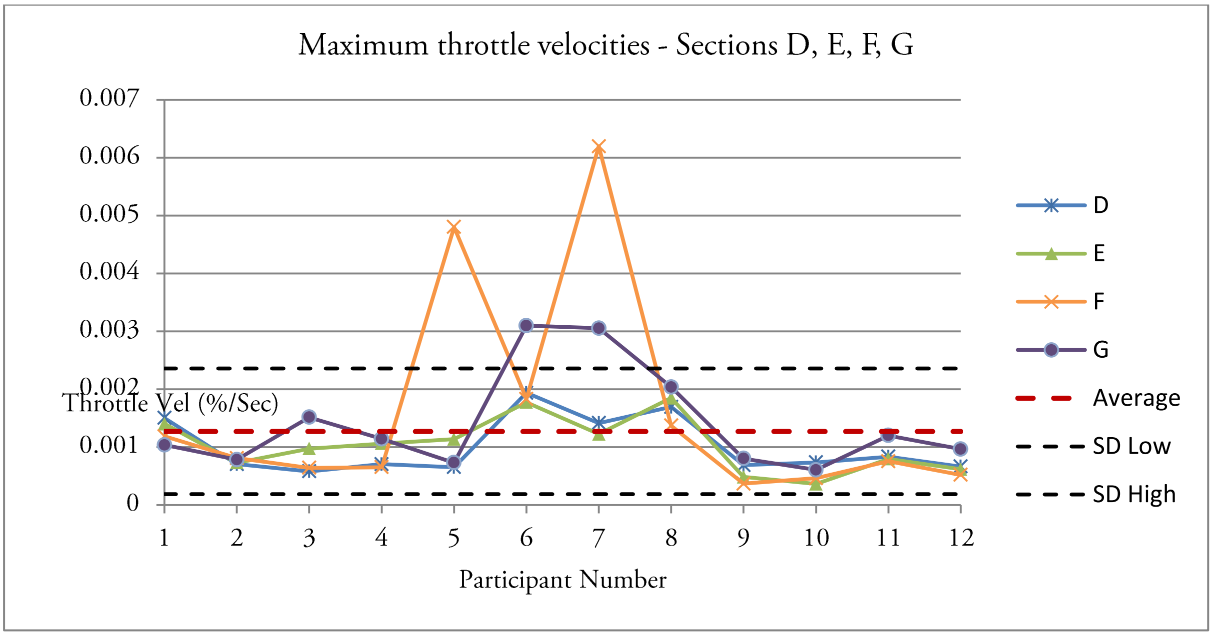

Figure 73 - Maximum Throttle Velocities Sections D, E, F and G

Figure(73) above shows the sections of the drive where higher steering inputs are expected, giving the increased likelihood of less stable vehicle heading velocity being present. The general trend of most participants are still consistent with having low variations between the sections, these values are also comparable to the ones seen in the straight, longer sections on the drive. Drivers 5 and 7 indicate higher variations, though driver 5 shows consistent low variation through all other sections other than F, outside of the standard deviation upper boundary. This could be due to an external influence on the given section. To help show whether this is the case the mean pedal velocities are found.

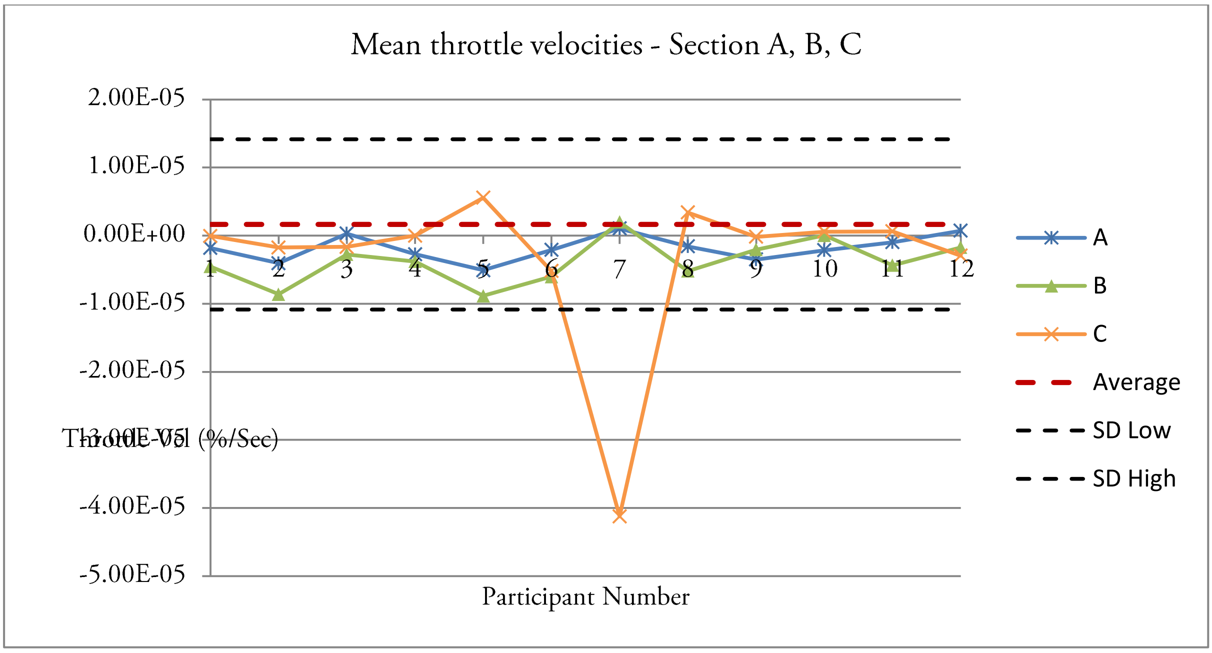

Figure 74 – Mean Throttle Pedal Velocities Sections A, B and C

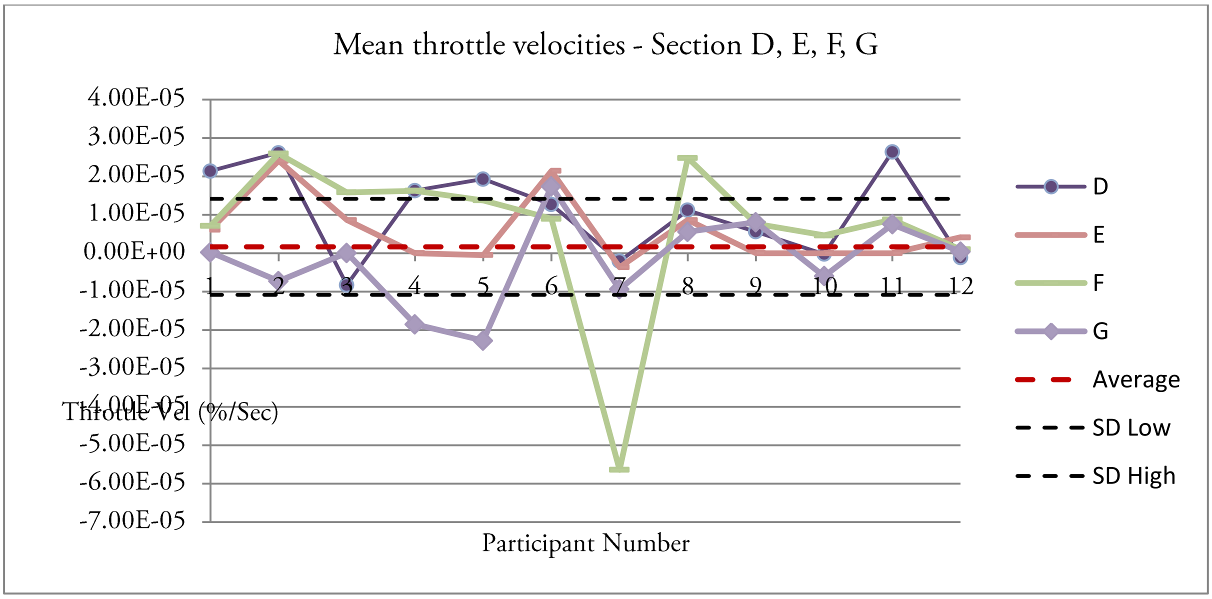

Figure 75 – Mean Throttle Pedal Velocities Section D, E, F and G

Though driver 7 does show the highest maximum throttle velocity, the driver showed to have a much smoother average usage throughout, this indicates they perhaps were fast initially to reach their desired pedal position but maintained fairly constant control of the position.

Table (18) shows the driving assessor results and comments for throttle usage and vehicle velocity control for both fast and slow conditions. The first thing to note is no participant scored a higher result in the velocity related observations than has been rewarded in throttle/accelerator usage. Drivers 1, 3, 4, 7 and 12 have resulted with a scoring of 3 (poor) by the assessor. To see if there's any clear difference between these 5 drivers, the difference is calculated for mean and maximum usage shown in the previous figures, Figures (74) and (75)

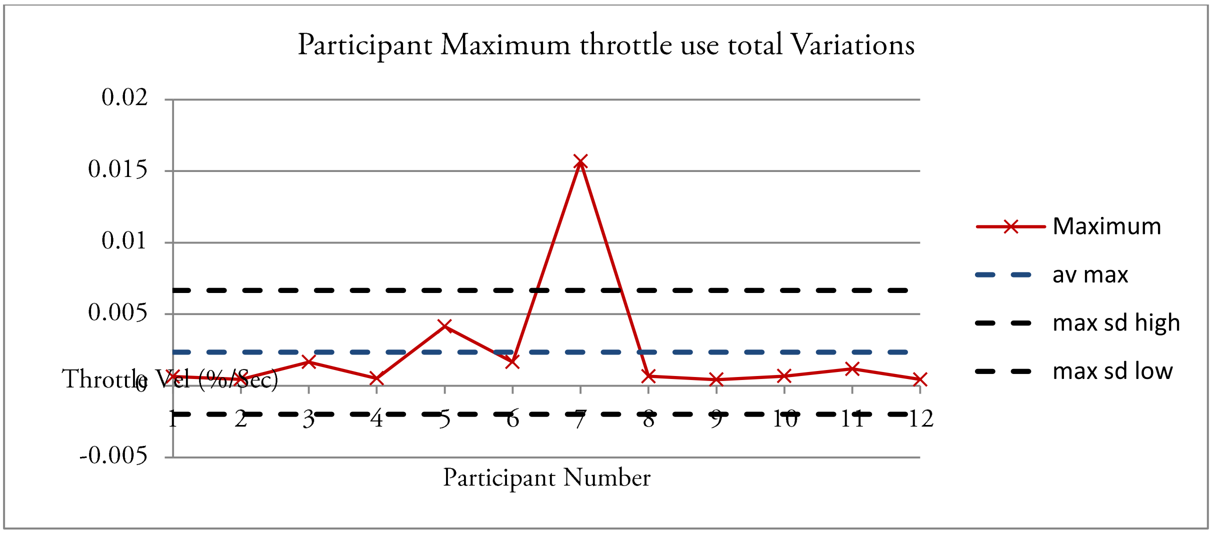

Figure 76 – Maximum Thortle use Variations

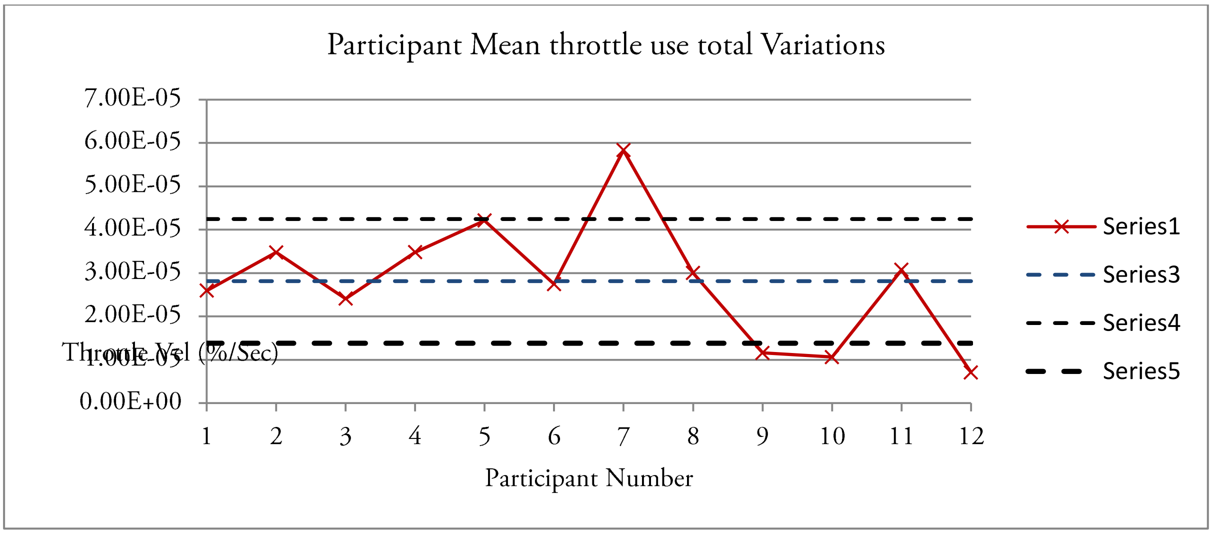

Figure 77 – Mean Throttle use Variations

Driver 7show the highest variation with both maximum and average throttle use, the assessor has provided the following comments for this participant *"acceleration sometimes jerky on take up and not in correlation to level of steering input"*. The remaining drivers 1, 3, 4, and 12 have also received similar comments related to the sharpness of acceleration from a stationary position, though all have shown to exhibit usage between the calculated average and the lower standard deviation boundary. As scorings for speed fast and slow have been awarded either lower to equal to that of accelerator/throttle usage it is more likely the case that the consideration of overall vehicle positioning, speed and control may play a role in the score provided. Driver 12 showed to have one of the lowest throttle use, but has been noted by the assessor as exhibiting harsh acceleration and inappropriate speeds for situation, rushing. Though the driver has shown to have one of the lowest maximum and mean throttle velocities showing smooth usage, this doesn't take into consideration the steering and vehicle velocity observations that the assessor has. To fully quantify throttle usage, further aspects should be considered for correlation.

Participant	Observation	Score	Comments
1	Accelerator	3	Occasionally sharp when moving off
	Speed Fast	3	n/c
	Speed Slow	3	n/c
2	Accelerator	2	n/c
	Speed Fast	3	n/c
	Speed Slow	3	n/c
3	Accelerator	3	could have balanced steering and accelerator better
	Speed Fast	4	excess in 30's
	Speed Slow	3	n/c
4	Accelerator	3	sharp moving off
	Speed Fast	3	n/c
	Speed Slow	3	n/c
5	Accelerator	2	n/c
	Speed Fast	4	n/c
	Speed Slow	4	n/c
6	Accelerator	2	overall good use, some instances of harsh acceleration on moving off
	Speed Fast	3	n/c
	Speed Slow	4	could have made better progress on national limits
7	Accelerator	3	acceleration sometimes jerky on take up and not in correlation to level of steering input
	Speed Fast	3	n/c
	Speed Slow	3	n/c
8	Accelerator	2	n/c
	Speed Fast	//	//
	Speed Slow	//	//
9	Accelerator	2	n/c
	Speed Fast	3	n/c
	Speed Slow	3	n/c
10	Accelerator	2	n/c
	Speed Fast	2	n/c
	Speed Slow	2	n/c
11	Accelerator	2	n/c
	Speed Fast	3	n/c
	Speed Slow	3	n/c
12	Accelerator	3	harsh acceleration on moving off
	Speed Fast	3	often, inappropriate speed for situation- rushing
	Speed Slow	3	n/c

Table 18 – Driving Assessor Throttle use Scores

// = Section not provided

n/c = No Comment Provided

The same scoring index from + to 4 remains as shown for the braking case.

Chapter 5

Application of Computer Vision

5.1 Definition

As shown in chapter 4 the use of data acquisition in the on road driving task allows for the characterisation of driver behaviour for a given number of drivers, this has become more of a statistical challenge for defining an ideal or typical average driver where accuracy of behavioural characteristics inevitably relies on the measurement of an increased number of drivers. Supporting this method of data acquisition and analysis with computer vision allows for observations and measurements to be made that aren't necessarily captured and understood with conventional methods of data acquisition, i.e. why a driver showed heavy braking or exhibited high steering velocity to avoid an object in the road. Vision allows for these influences to be recorded.

This chapter will investigate techniques of computer vision useful for increasing portrayal fidelity and understanding of the driver and driving event. The application of computer vision uses Python and OpenCV.

The video capture used for analysis is taken from participant 6.

5.2 Lane Detection

When analysing steering behaviour for a given driver investigating the nature of their input in comparison to other drivers has allowed us to identify relative average usage. This average is expected to move as more drivers are assessed. A method that allows for each driver to be assessed independently of statistics from a group of drivers gives a much more objective approach that isn't reliant on benchmarks generated from previous tests. The use of lane detection will allow for identification of driving events supporting analysis conducted in Chapter 4.

A forward facing camera is used to detect lanes driven by the vehicle. Captured video is divided into the same sections created for the data acquisition analysis.

5.2.1 Colour Space and Region of Interest

It is necessary to initially convert the image sequence to a grayscale colour format, this allows for ease of distinction between high and low brightness areas of the image (Yasui, et al., 1998).

Each frame is then cropped into a region of interest for further analysis, this restricts areas of the image having an effect on the features detected within the image, increases processing time and also helps reduce the computation power required.

Figure 78 – Original Capture – Section 8 - Frame 0

Figure 79 – Capture after grayscale conversion and image crop – Section 8 – Frame 0

The region of interest has been cropped to the following coordinates (200:350, 240:590), (y1:y2,x1,x2). The zero datum of the image is found at the top left corner of the image.

5.2.2 Detecting Edges

The Canny edge detection method is applied to the cropped image for identification of road lines of interest, the central lane separation lines and the road boundary lines.

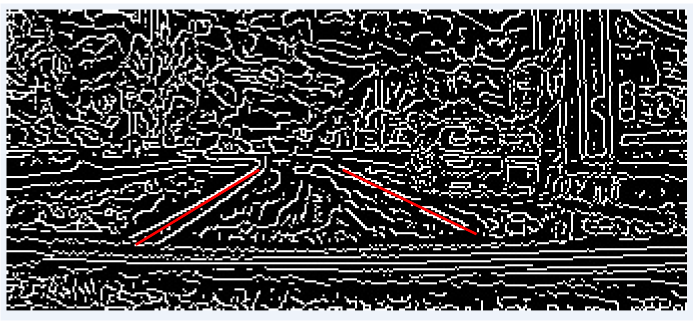

Figure 80 – Edges detected within the image – Section 1 – Frame 6508

Two red lines have been added to the figure through the edges of the road lines to highlight the edges of interest. Even though the image is cropped to the region on interest to identify lanes, the edge detection method results edges for features found in the region at all angles. Configuration parameters of the edge detector are as follows:-

- Threshold 1 = 30
- Threshold 2 = 150
- Aperture Size = 7

5.2.3 Probabilistic Hough Transforms

The probabilistic Hough Transform (PHT) differs from the standard Hough Transform as an optimization to use less computation and uses fewer points for results comparable to the original method (Mordvintsev & K, 2014). The PHT is applied to the detected edges.

Figure 81 – Probabilistic Hough Transform

As the lanes of interest within the image are close to vertical a filter has been applied to the transform to only show lines within a specific angle range, that is angles less than equal to – 20 Deg and angles more than or equal to 20 Deg. The probabilistic Hough Transform configuration parameters are as follows:-

- Minimum line length = 10
- Maximum line Gap = 10

Each detected line has the coordinates (x1,y1) and (x2,y2), the angle in degrees of each detected line can be found by the following equations:-

$$dy = y2 - y1$$

$$dx = x2 - x1$$

$$Angle = (\tan^{-1}\frac{dy}{dx}) * \frac{180}{\pi}$$

5.3 Combined DAQ and Video Data Analysis

Section 5 will be considered for this analysis Figure (82)

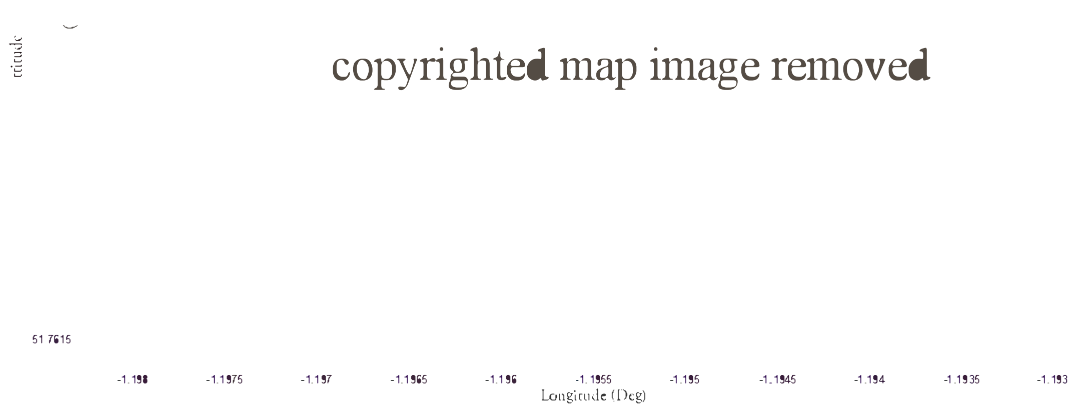

Figure 82 – GPS Coordinates – Section 5 – Participant 6

From the statistical analysis performed in chapter 4 the participant exhibited average steering displacement and velocity results throughout the section of 6.91 Deg and 6.16 Deg/Sec respectively. These were far below the averages of 30.47 Deg with standard deviations of 38.92 Deg for the upper boundary and 22.755 Deg for the lower boundary and 15.493 Deg/Sec with standard deviations of 20.474 Deg/Sec for the upper boundary and 10.512 Deg/Sec for the lower boundary.

Using the synchronised data from the data acquisition device and the video capture device, this section has been isolated from the remaining data gathered from the run.

On approach to the roundabout a slip round must be used for the driver to take the first exit off of London road, the driver then must merge back onto the Eastern Bypass after the roundabout. Observing the steering data gathered from the section we can identify at which point on the section maximum steering displacements and velocities occur. It should be noted at this point the average steering displacement throughout the section is 1.92 Deg. Figure (83) shows the steering trace for the section.

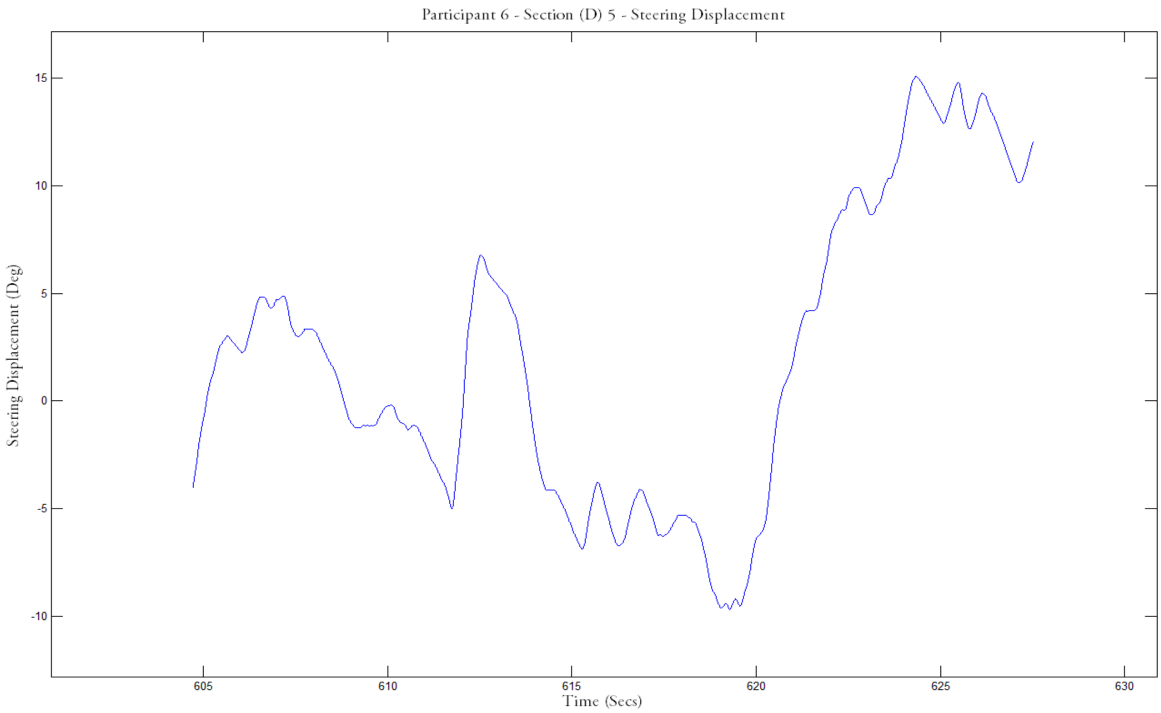

Figure 83 – Section 5 Steering Trace Participant 6

It should be noted the maximum and minimum steering inputs throughout the section are 15.09 Deg and -9.697 Deg, further to this the decreasing nature of the graph relates to steering inputs on the left direction from the perspective the driver position. Lanes have been detected to show when the vehicle begins to merge onto the entrance lane.

Figure 84 – Section 5- Frame 33

This allows for computational identification for when the vehicle changed lane into the slip road, as the data acquisition device and the video capture are synchronised, this frame can be cross referenced to the time in seconds with the steering data. Figure is replicated below with the events indicated with red crosses based on the lanes detected from a given frame.

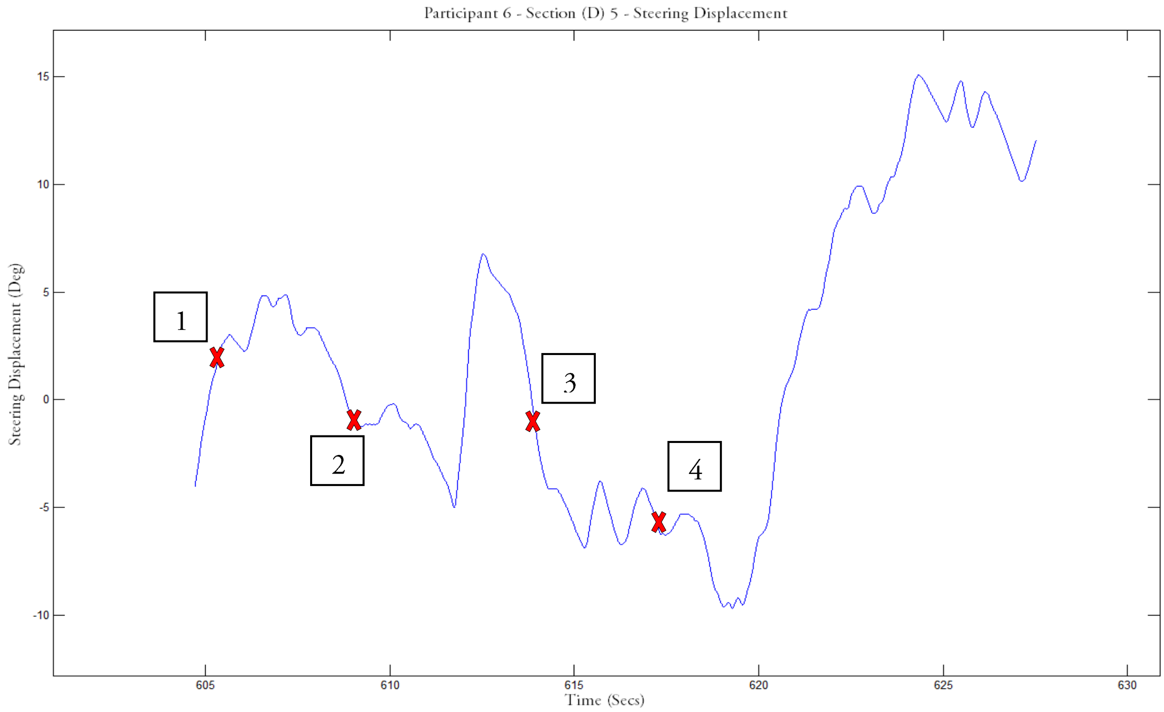

Figure 85 – Section 5 Steering Trace with Markers

The following list shows the events observed from the markers:-

1. First lane detected to show start of the merge onto the slip road
2. Indication of vehicle successfully in the slip road
3. Last lane detected before occlusion
4. First detected lane after the occlusion

Figure (86) shows the detection of the first events, the following figures show the detection of the remaining 3 events.

Figure 86 – frame 128 – Section 5

Figure 87 – frame 281 – Section 5

Figure 88 – frame 377 – Section 5

As the driver continues along the lane, an obstruction can be noticed along the driving path, the heading velocity of the vehicle is adjusted to compensate. The driver is then has to make a decision whether they feel the vehicle has enough room to negotiate around the obstruction or to stop the vehicle and wait for the lane to clear. The driver decides to negotiate around the obstruction figure (88)

We now have an objective method using vision to identify obstructions or external events that may cause drivers to drive in a manner that wouldn't be necessary or expected without the external influence, in this case a traffic obstruction. This allows for the analysis of steering behaviour to be conclusively explained and analysed justified by evidence from the event. Though the obstruction or occluding feature on the slip road doesn't directly explain why the driver exhibited such low steering displacement but due to the driver slowing the vehicle down and taking more care around the sections it suggests the driver may have taken a more cautious approach throughout the remainder of the run, especially while considering they were being assessed. The remaining sections of the route also showed the driver exhibited steering behaviour far lower than the average.

The percentage of frames for each section with lanes detected are shown in the below table (19)

	s1	s2	s4	s5	s6	s7	s8
Total	6689	7013	4337	829	230	584	191
Detected	1607	1709	996	166	46	152	50
Percentage	24.02452	24.36903	22.96518	20.02413	20	26.0274	26.17801

Table 19 – Frames with lanes detected percentages

The average number of frames where lanes have been successfully detected throughout the complete drive has been calculated as 23.4%. Although sufficient lanes have been detected to allow for the identification to support the analysis in this study consistency of detection should be greatly improved for a reliable method of computationally measuring lane and steering behaviour. The main cause of this average relates to the recovery of lost frames for a given capture. The video device uses the h.264 video encoding protocol, this protocol has increased efficiency over others such as mpeg4 as it recognises features between frames which can reduce transfer bandwidth required. Though frames can be dropped due to the inherent nature of digital video capture and the transfer protocols used, a range of frames can be specified for image recovery, though the clarity of the image is affected.

Figure (89) shows a frame where the previous frame has been dropped.

Figure 89 – Frame 1492 – Section 1

Figure (89) results in the following edge detection shown in the below figure (90). As seen in the video capture the lanes become almost un recognisable and the edge detection method identifies the pixilation in the image rather than the useful features. This can results from a number of aspects such as sudden changed in lighting conditions and has been found the be the result of video captures with moving foreground and backgrounds where the encoding efficiency is low due to feature recognition between frames during encoding.

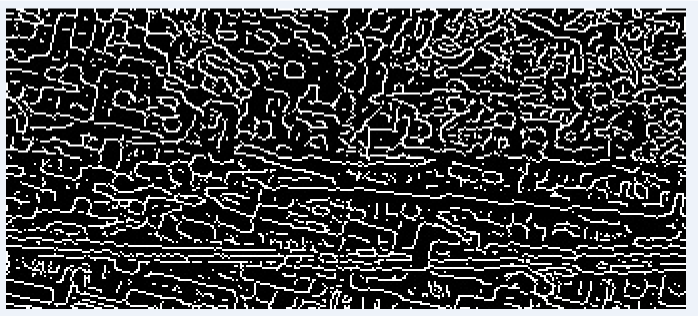

Figure 90 – Frame 1492 – Section 1 – Edge Detection Results

The analysis of section 5 has allowed for the identification of an external influence, on this occasion a traffic obstruction to begin explaining the reasoning behind the influences on driving characteristics. The use of lane detection now allows for computational recognition of the lateral movement of the vehicle with respect to the road. Though the use of data acquisition has allowed for a clear objective identification of steering nature and behaviour where vision would fail, the use of vision allows for this nature to be explained. To fully understand a driving event computer vision should still be supported with conventional data acquisition methods and the use of a synchronised device allows for events to be observed and analysed objectively.

Chapter 6

Conclusions

A method to evaluate driver performance has been generated using data acquisition and video capture devices developed. Experimental work has been undertaken for both device development and validation of driver behaviour incorporating a technique to identify influences factors for on-road driving with the addition of computer vision.

Chapter 3 highlighted the required hardware and software performance parameters necessary to record real world events in the driving task. The data acquisition device has been developed in correlation with analysis scripts generated with Matlab. Files are generated on the device that allow for direct transition into the analysis shown in chapter 4. A video capture system has been developed in collaboration with Goldstar Onboard Ltd as a result of a number of generated and tested concepts before being scrutinised using a matrix selection based on key performance parameters.

In Chapter 4 results provided by a professional driving assessor and captured from the data acquisition device have been analysed using a statistical approach to characterise driving behaviour for steering, braking and throttle usage. Due to the objective nature of the recorded data and the subjective nature of the driving assessment results, direct correlations have proven further information on the event and driving task is required. Event benchmarks have been indicated as a result of the analysis.

Chapter 5 has shown how the addition on computer vision can be used to uncover key events that occur during the on-road driving task that help explain the nature of steering inputs conducted.

Synchronisation of video and data acquisition has allowed for these events to be cross referenced between both devices and the application of lane detection techniques have provided a method to identify key events during the driven event. Though the approach taken has been subjective in assessing the nature of events, the method offers an objective computational approach to relate the necessary parameters required for analysis of the event.

Results from the analysis process have highlighted the complexity in quantifying the on-road driving task and that to fully understand and characterise it both objective and subjective techniques should be employed. This study has shown how statistical analysis and applications of computer vision techniques can begin to portray on-road driving with great accuracy.

Further Work

While this study has resulted with some conclusions useful for characterisations and analysis for the on-road driving task, there are further recommendations that would help greatly improve the accuracy in the methods conducted.

The results analysis in Chapter 4 has highlighted some key elements that should be addressed for further improvement. The addition of a method to measure vehicle speed with increased sampling resolution should be investigated, this would allow parameters such as steering to be normalised against vehicle heading velocity to help further understand the nature in high and low variations of steering displacements and velocities. Though the data acquisition device has yielded results with sample rate resolutions stable enough for this analysis, increased rates with further stability would help develop a more detailed portrayal for a given driving task and also aid in providing accelerometer data with higher signal to noise ratios.

Further investigations should be made into the method of detecting features using computer vision when frames are dropped and features can become hard to detect, a matching technique could be adopted to help identify features throughout frames based on the characteristics of the feature.

Lane detection techniques should be exploited for the generation of an ideal path in a real time manner. This would help bridge the divide between subjective and objective approaches, it is hoped this will further support statistical analysis in steering behaviour and also begin to clearly show whether a drive has been undertaken in a hazardous or safe manner taking into consideration other road users and external influences. Real time methods to assess this alongside the use of data acquisition should be employed.

Development of a scoring method for correlation with that provided by the driving assessor, this would help identify detailed areas resulting in low correlation and how they can be improved based methods used by the driving assessor.

Benchmarking of driving scenarios and events, this would be advantageous for example, to the emergency brake event where ideal reaction and response times are defined. This would allow for clear identification a comparison for a given driver.

References

Allen Wade, R., Rosenthal, T. J. & T., S. H., 1987. *Steady State and Transient Analysis of Ground Vehicle Handling,* s.l.: Society of Automotive Engineers, Inc..

Association, S. C., 2010. *SD Specifications Part A1,* s.l.: SD Card Association.

Balkwill, J., 2013. *Advanced Chassis Engineering - Student Handbook - Version 8,* s.l.: Oxford Brooked University .

Bennett, L. J., 2012. *Ride and Handling Assessment of Vehicles Using Four-post Rig Testing and Simulation,* s.l.: s.n.

Bennett, L. J., 2012. *Ride and Handlng Assessment of Vehicles Using Four-post Rig Testing and Simulation,* s.l.: s.n.

Blundell, M. & Harty, D., 2004. *The Multibody Systems Approach to Vehicle Dynamics.* s.l.:Elsevier Butterworth-Heinemann.

Canny, J., 1986. A Computational Approach to Edge Detection. *IEEE Transactions on pattern analyssi and machine intelligence.*

Carsten, O., 2007. From Driver Models to Modelling the Driver: What Do We Really Need to Know about the Driver?. In: P. Cacciabue, ed. *Modelling Driver Behaviour in Automotive Envrionments.* s.l.:Springer-Verlag London Limited, pp. 105 - 134.

Crolla, D. A., 1992. *An Introduction to Vehicle Dynamics.* s.l.:University of Leeds.

Daniello, A., Kusano, K. & Gabler, H., 2013. *Validation of a Driver Recovery Model Using Real-World Departure Cases,* s.l.: Society of Automotive Engineers, Inc..

Davis, E. J., 2006. *Vehicle Dynamcs Measurement System for Evaluating Older Driver Performance,* University of Florida: s.n.

Dyas-Catton, H., 2011. *Tyre Modelling Using Easy to Measure Data,* s.l.: s.n.

Elliott, F. R. & Louttit, C. M., 1937. *Auto Braking Reacion Times to Visual vs. Auditory Warning Signals,* s.l.: Proceedings of Indiana Academy of Science.

Forsyth, D. A. & Ponce, J., 2012. *Computer Vision, A Modern Approach.* s.l.:Pearson.

Garland, R., 1991. *The Mid-Point on a Rating Sacle: Is it Desirable,* s.l.: Marketing Bulletin.

Gillespie, T. D., 1992. *Fundamentals of Vehicle Dynamics,* s.l.: Society of Automotive Engineers.

Gonzalez, R. C. & Woods, R. E., 2008. *Digital Image Processing.* s.l.:Pearson.

Grauman, K. & Leibe, B., 2011. *Visual Object Recognition.* s.l.:s.n.

Hodkin, D., 1965. *The Status of Vehicle Handling in Great Britain,* N.Y.: Society of Automotive Engineers, Inc..

Hoiem, D. & Forsyth, D., n.d. *Computer Vision (Presentation).* s.l.:University of Illinois.

Larminie, J. & Martin, K., 2009. *Data Acquisition Systems: Issues of Use and Interpretation of Data,* s.l.: SAE International.

Lee, H. C., Cameron, D. & Lee, A. H., 2003. Assessing the driving performance of older adult drivers: on-road versus simulated driving. *Accident Analysis and Prevention,* Volume 35, pp. 797-803.

Lee, H. C., Lee, A. H., Cameron, D. & Li-Tsang, C., 2003. Using a driving simulator to identify older drivers at inflated risk of motor vehicle crashes. *Journal of Safety Research,* Volume 34, pp. 453-459.

Ludwig, C. J. H., Davies, R. & Eckstein, M. P., 2013. *Foveal analysis and peripheral selection during active vidual sampling,* s.l.: Proceedings of the National Academy of Sciences of the United States of America.

Massachusetts Institute of Technology, 2014. *agelab.mit.edu.* [Online]
Available at: http://agelab.mit.edu/assessing-methods-enhancing-older-driver-performance

Milliken, W. F. & Milliken, D. L., 1995. *Race Car Vehicle Dynamics.* s.l.:Society of Automotive Engineers, Inc.

Mordvintsev, A. & K, A., 2014. *Opencv-python-tutorials.* [Online]
Available at: http://opencv-python-tutroals.readthedocs.org/en/latest/py_tutorials/py_imgproc/py_houghlines/py_houghlines.html
[Accessed 2014].

Oppenheim, I., 2010. *Critical State of the art and unified models of driver behaviour,* s.l.: European Commission DG Research - Sustainable Surface Transport.

Ovren, H., Nilsson, E. & Nordberg, K., 2013. *Online Calibration of Camera Roll Angle,* s.l.: Department of Electrical Engineering, Linkopings University.

RACFoundation, 2013. [Online]
Available at: racfoundation.wordpress.com/2013/04/12/number-of-vehicles-in-uk-hits-new-high/
[Accessed February 2014].

Schlipsing, M. S. J. S., 2011. *Video-Based Roll Angle Estimation for Two-Wheeled Vehicles,* s.l.: s.n.

Segel, L., 1956. Theoretical Prediction and Experimental Substantiation of the Response of the Automobile to Steering Control. *Institution of Mechanical Engineers,* 10(1).

Snowden, R., Thompson, P. & Troscianki, T., 2012. *Basic Vision: An Introduction to Visual Perception.* s.l.:s.n.

Survey, O., 2015. *Ordnance Suvery.* [Online]
Available at: http://www.ordnancesurvey.co.uk/business-and-government/help-and-support/navigation-technology/gps-beginners-guide.html

Szeliski, R., 2010. *Computer Vision: Algorithms and Applications.* s.l.:Springer.

Texas Instruments Incorporated, 1994. *Principles of Data Acquisition and Conversion,* s.l.: Burr-Brown Corporation.

Vicon, 2013. *http://www.vicon.com/.* [Online]
Available at: http://www.vicon.com/

Yasui, N., Lisaka, A. & Nomura, N., 1998. *White Road Line Recognition Using Lane Region Extraction and Line Edge Detection,* s.l.: SAE.

Zogg, J.-M., 2007. *GPS Basics.* s.l.:s.n.

Appendix A – Capture Data Tables

The following data tables show file information after decoding and the frames lost during capture, average frame rates have also been calculated. (Section 4.1.2 Video System Analysis)

Goldstar Onboard Dual Camera

Goldstar	Cam 1	RT = 1
File	8000	4
Size (MB)	645	923
Size (mins)	15.48	22.36
Decoded	28432	40643
Displayed	28422	40616
Lost	1	17
toal expected frames	27864	40248
frames per loss approx.	27864	2367.529

start	0	0
stop	15.48	22.36

size (Mb)	5160	7384
size (secs)	928.8	1341.6
Mb/s	5.555556	5.503876

Pandaboard

Pb	Cam 1	RT = 1
File	1	2
Size (MB)	185	271
Size (mins)	13.08	18.56
Decoded	22374	32750
Displayed	22901	33292
Lost	26	26
total expected frames	23544	33408
frames per loss approx.	905.5385	1284.923

start	0	0
stop	13.08	18.56

size (Mb)	1480	2168
size (secs)	784.8	1113.6
Mb/s	1.885831	1.946839

Ez Storage Device

Ez	Cam 1	RT = 0							
File	1	2	3	4	5	6	7	8	9
Size (MB)	59.2	56.4	35.4	59.8	57.7	56.2	28.6	37.1	15.7
Size (mins	5	4.86	3.03	5.08	4.91	4.86	3.22	3.09	1.64
Decoded	3117	2937	1850	3176	2994	2917	1488	1927	863
Displayed	3108	2926	1842	3168	2985	2908	1641	1919	854
Lost	0	1	0	0	0	0	0	0	0
start (RTC)	28.56	33.57	38.43	42.21	47.31	52.23	57.1	61.08	64.51
stop (RTC)	33.56	38.43	41.46	47.29	52.22	57.09	60.32	64.17	66.15
delta	0.01	0	0.75	0.02	0.01	0.01	0.76	0.34	
size (Mb)	473.6	451.2	283.2	478.4	461.6	449.6	228.8	296.8	125.6
size (secs)	300	291.6	181.8	304.8	294.6	291.6	193.2	185.4	98.4
Mb/s	1.578667	1.547325	1.557756	1.569554	1.56687	1.541838	1.184265	1.600863	1.276423

	Cam 2	RT = 0				
File	1	2	3	4	5	6
Size (MB)	112	109	109	54.9	72.7	31.6
Size (mins)	4.98	4.88	4.88	2.95	3.13	1.65
Decoded	3045	2916	2936	1460	1954	861
Displayed	3037	2908	2928	1452	1946	853
Lost	0	0	0	0	0	0
start	42.58	47.57	52.47	57.37	61.04	64.5
stop	47.56	52.45	57.35	60.32	64.17	66.15
delta	0.01	0.02	0.02	0.72	0.33	
size (Mb)	896	872	872	439.2	581.6	252.8
size (secs)	298.8	292.8	292.8	177	187.8	99
Mb/s	2.998661	2.978142	2.978142	2.481356	3.096912	2.553535

	Cam 3	RT = 1		
File	1	2	3	4
Size (MB)	45.5	48.3	47.5	24
Size (mins)	4.3	4.92	4.9	2.96
Decoded	8377	8996	8871	4554
Displayed	8369	8988	8862	4546
Lost	0	0	0	0

start	43.24	47.54	52.46	57.36
stop	47.54	52.46	57.36	60.32
delta	0	0	0	

size (Mb)	364	386.4	380	192
size (secs)	258	295.2	294	177.6
Mb/s	1.410853	1.308943	1.292517	1.081081

Appendix B – Video Capture Device Procedure

The device will activate and initiate a start await condition once powered up. Please allow up to 30 seconds from power injection.

Please connect cameras and storage medium before connecting power.

The cameras will indicate a green light for around 1-2 seconds to show a state of availability. Once this has been seen, the green start button can be pressed to begin recording.

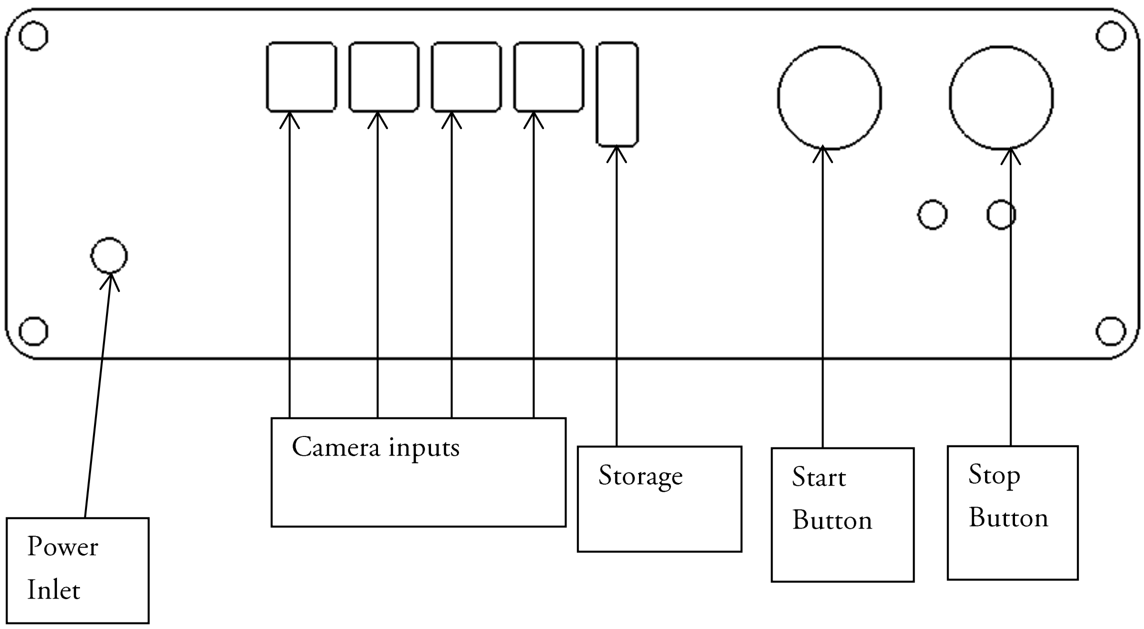

The device allows for captures with the following specification:-

- Resolution – 1920 X 720
- Frame Rate – 30 fps
- Transfer Bandwidth – 1.5 to 10 Mbps
- Start/Stop Trigger Functionality
- Storage of multiple streams to a single storage device
- Power inlets – 5v to 12V 5A

This final device specification is in line with required hardware functionality outlined by Goldstar Onboard Ltd.

END OF DOCUMENT